Extratropical Precursors to the Onset of Madden-Julian Oscillation Deep Convection over the Western Indian Ocean

Jennifer Gahtan

Yuk Yung Lunch Seminar 12-4-2019

Work done at SUNY-Albany with Paul Roundy

Current Affiliation: Jet Propulsion Laboratory, California Institute of Technology

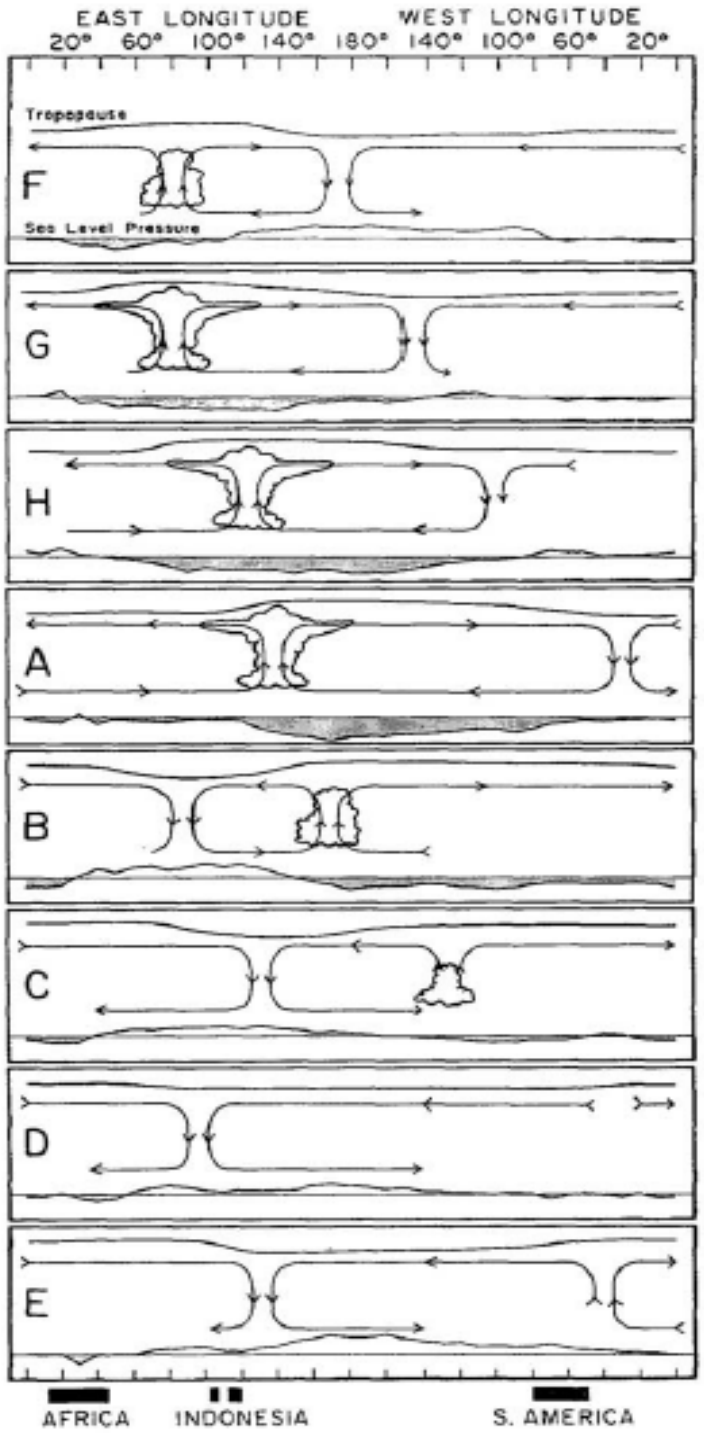

The Madden-Julian Oscillation

- Large-scale enhanced and suppressed deep convection over the tropical Indian and west Pacific Oceans
- Planetary scale circulation
- 30-90 day timescales
- Eastward propagation at globally averaged speeds of 5m/s

From Madden and Julian (1972), reproduced in Zhang (2005)

Deep Convection often initially forms over the western Indian Ocean

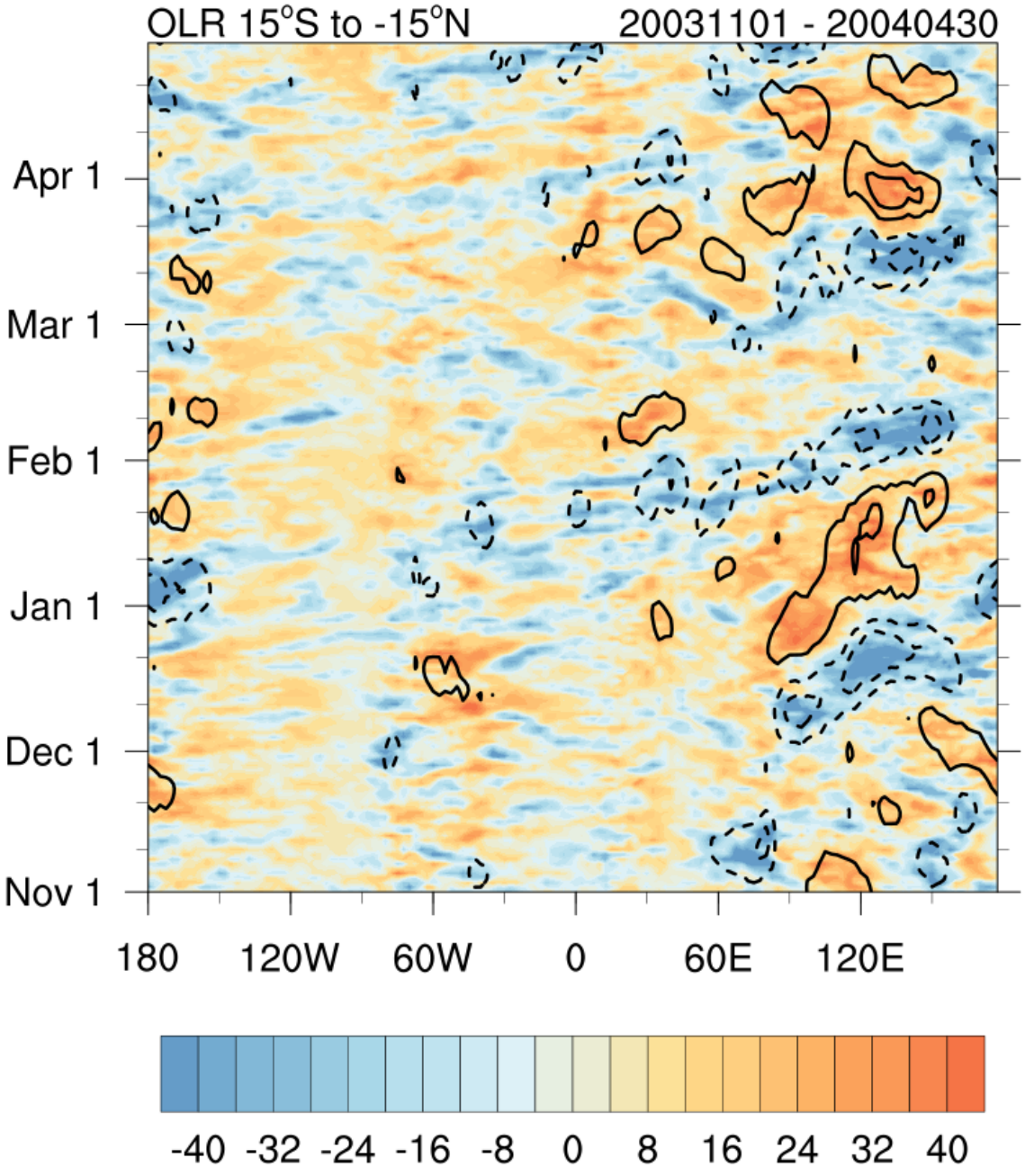

Observed precursors in the subtropics

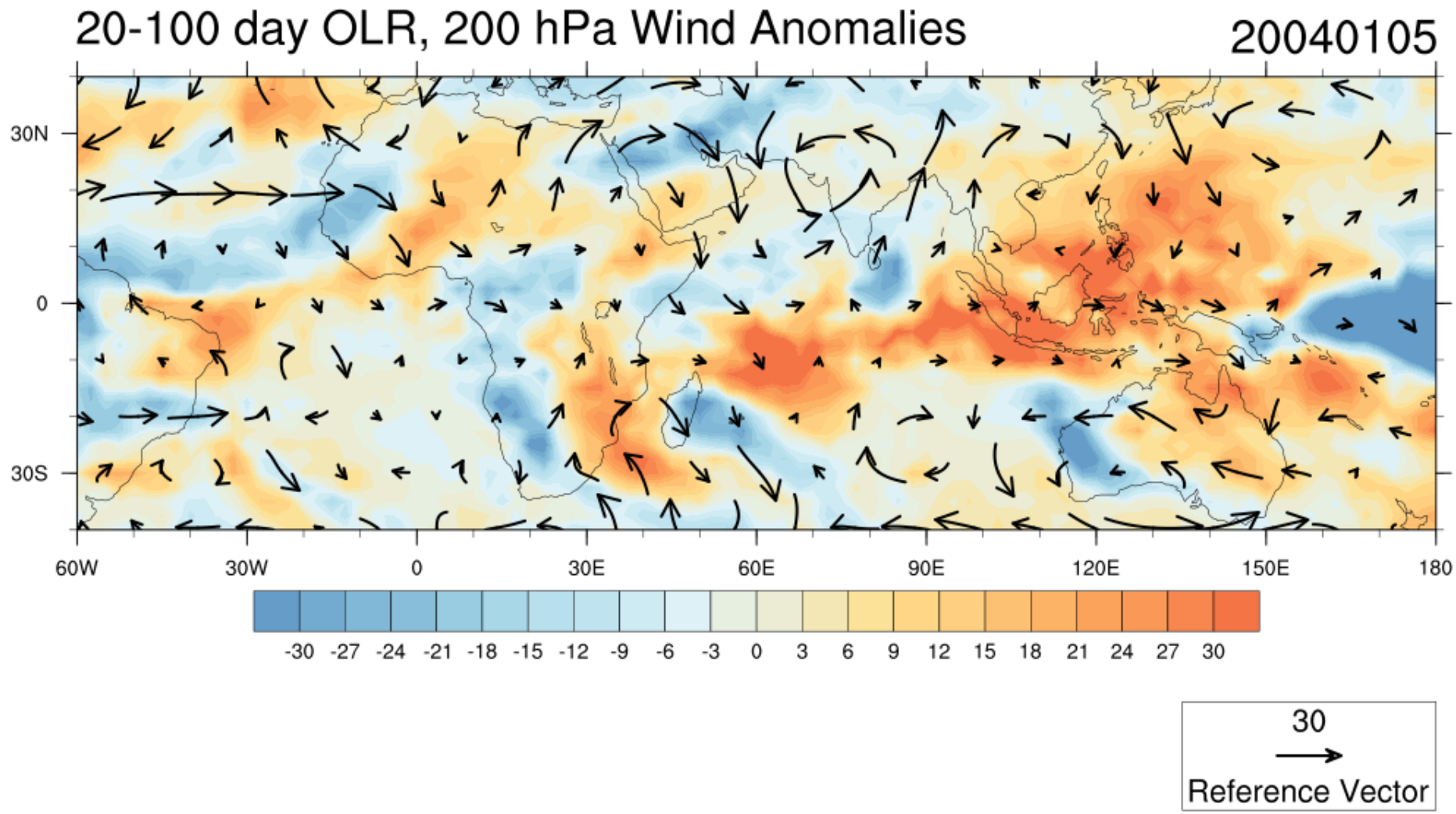

Observed precursors in the subtropics

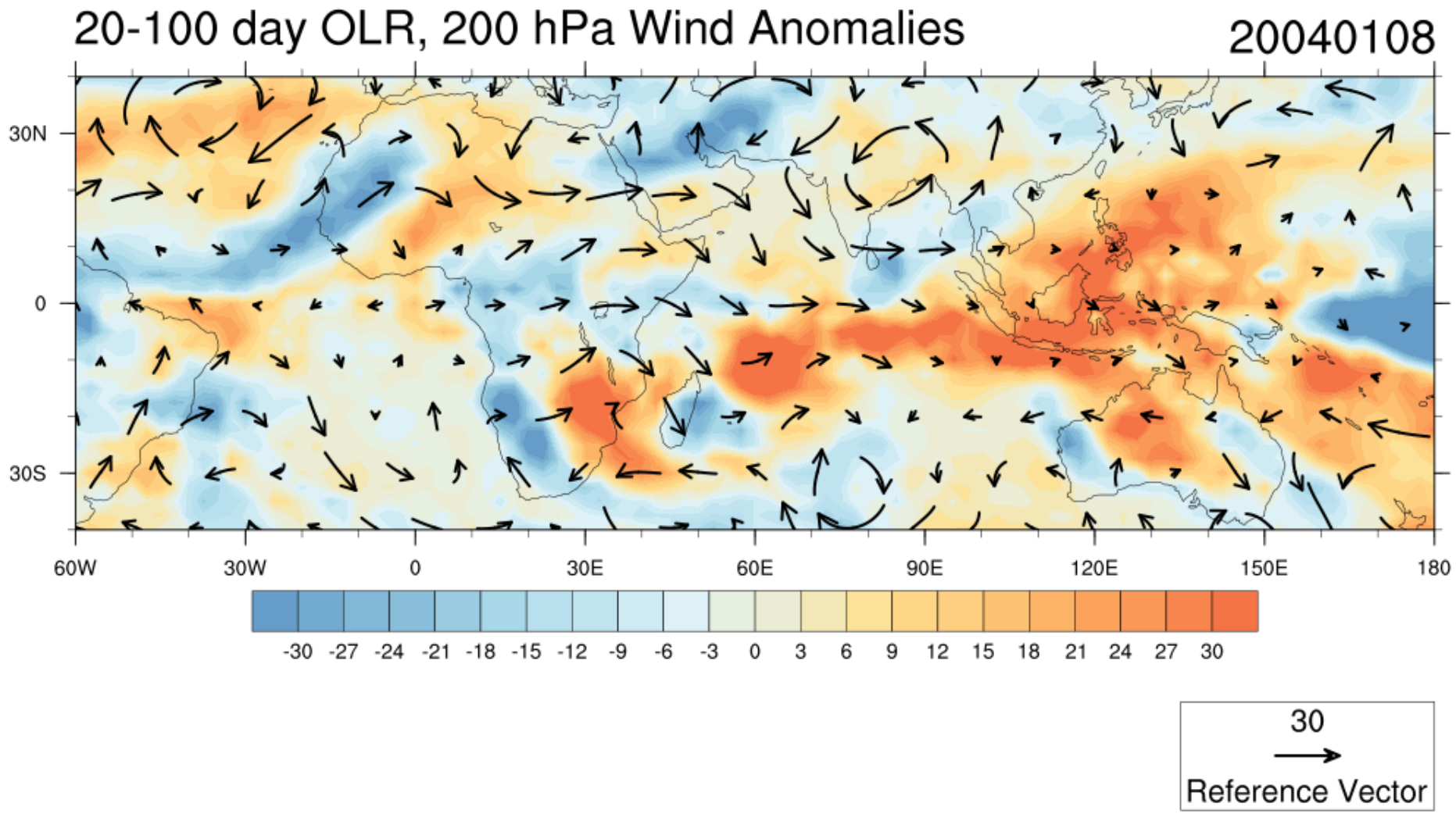

Observed precursors in the subtropics

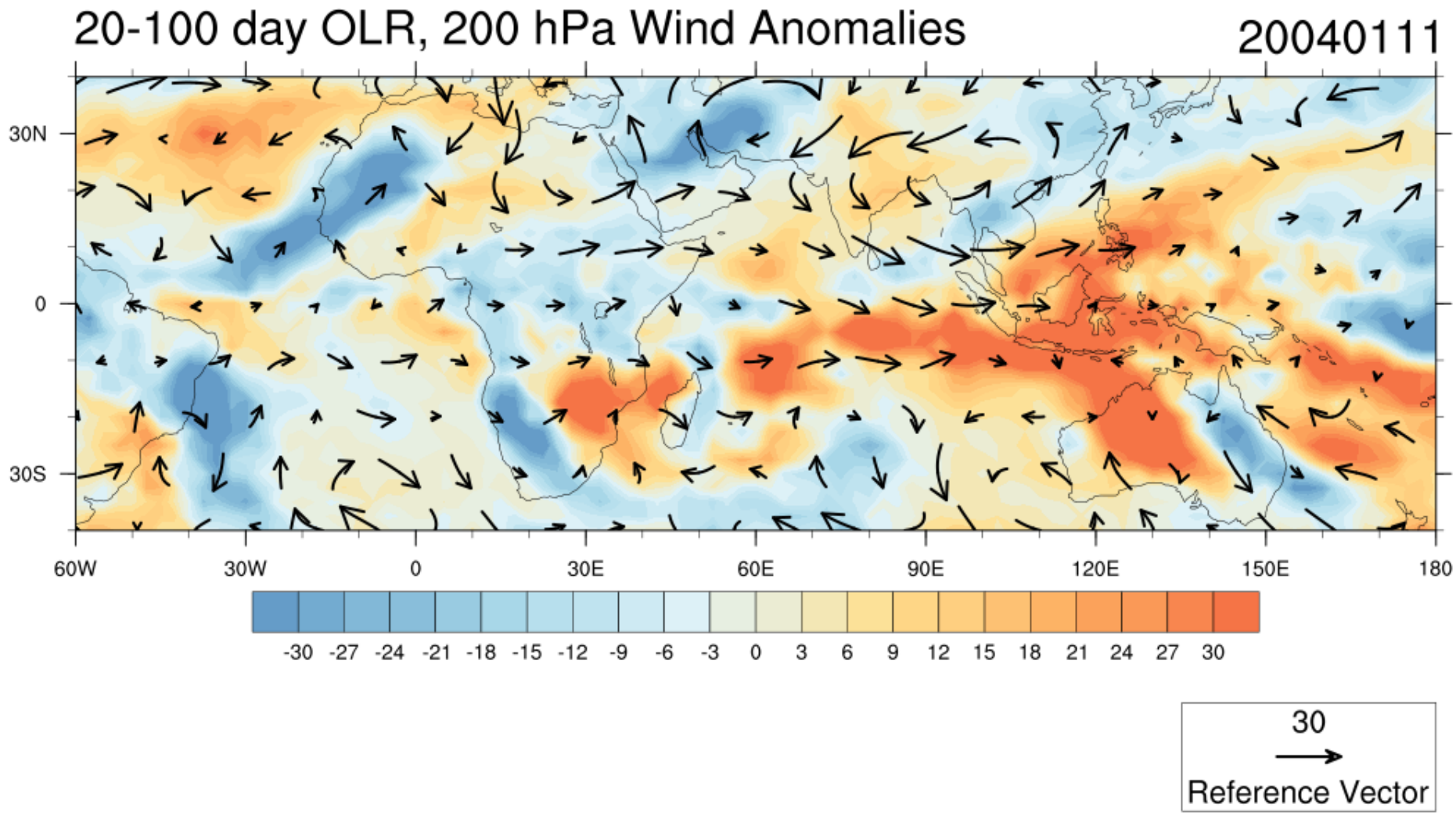

Observed precursors in the subtropics

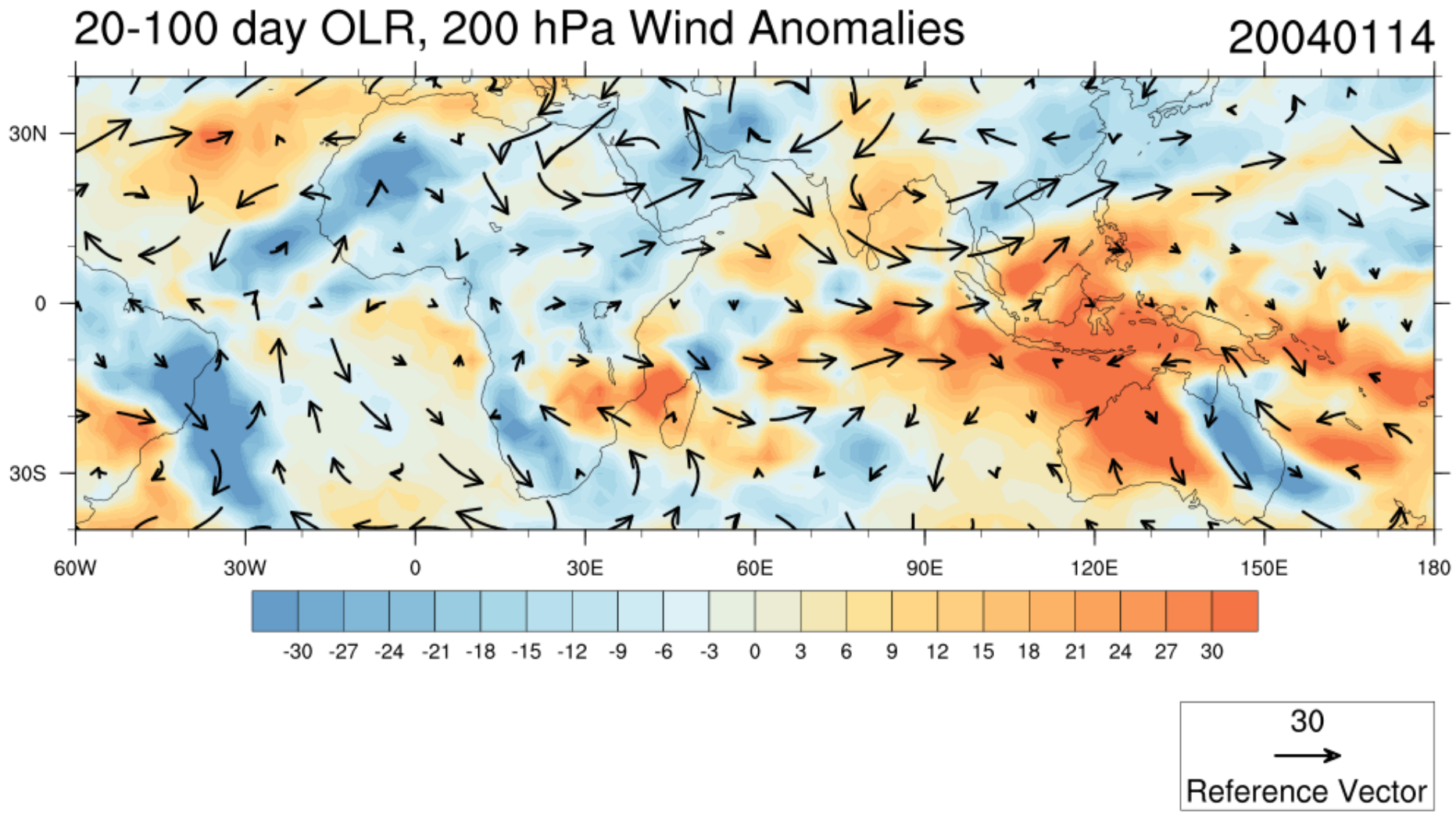

Observed precursors in the subtropics

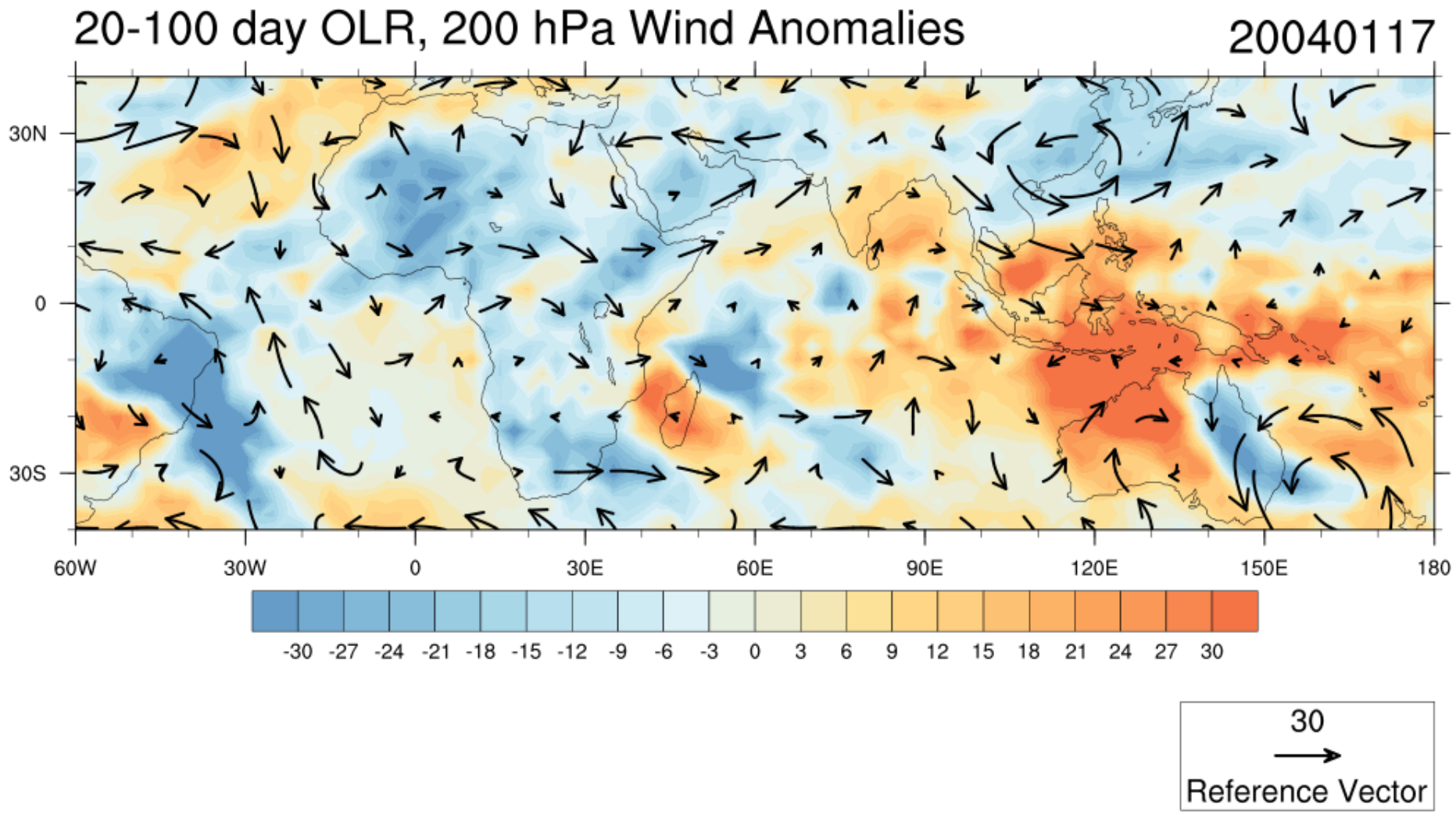

Observed precursors in the subtropics

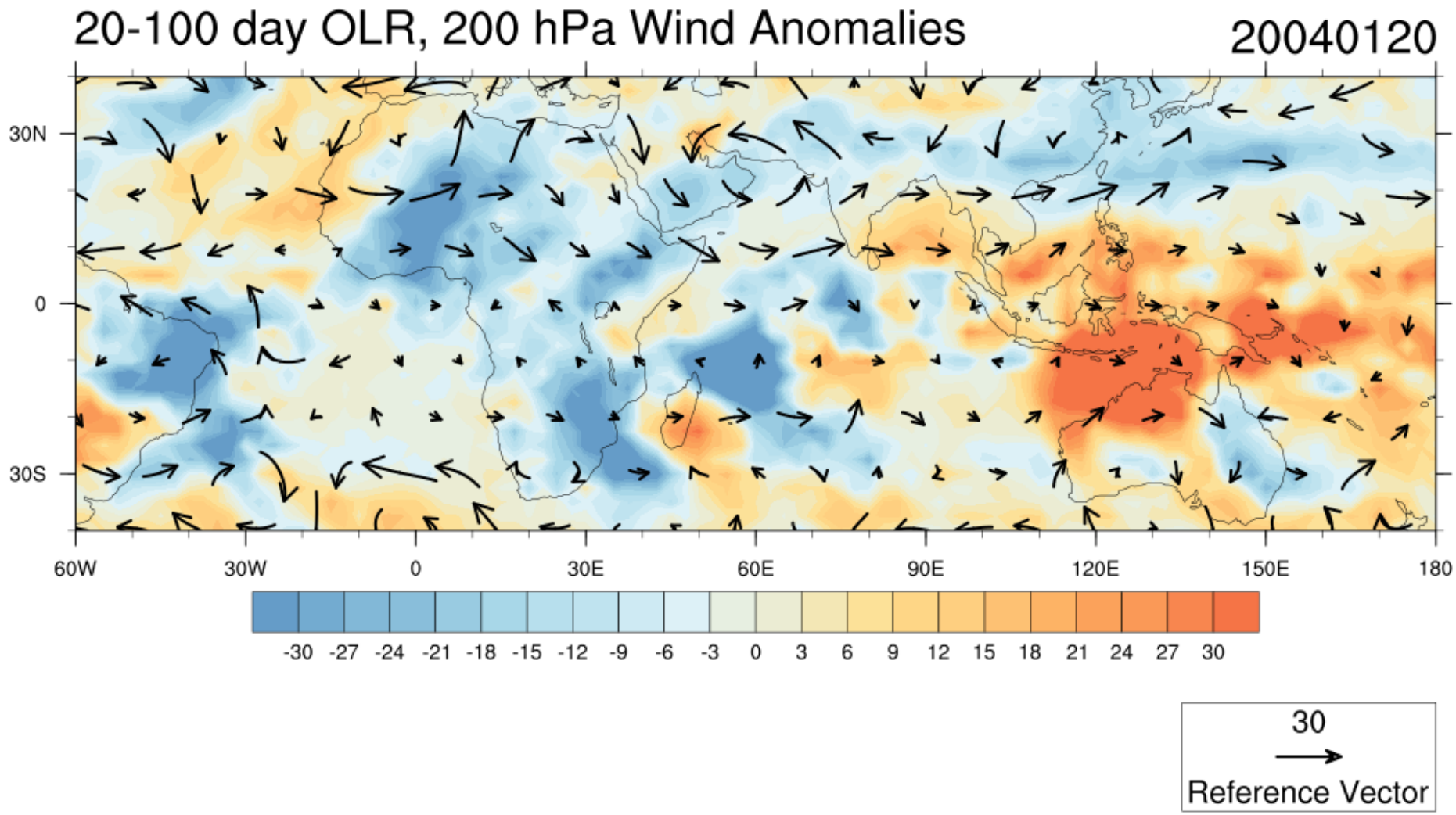

Observed precursors in the subtropics

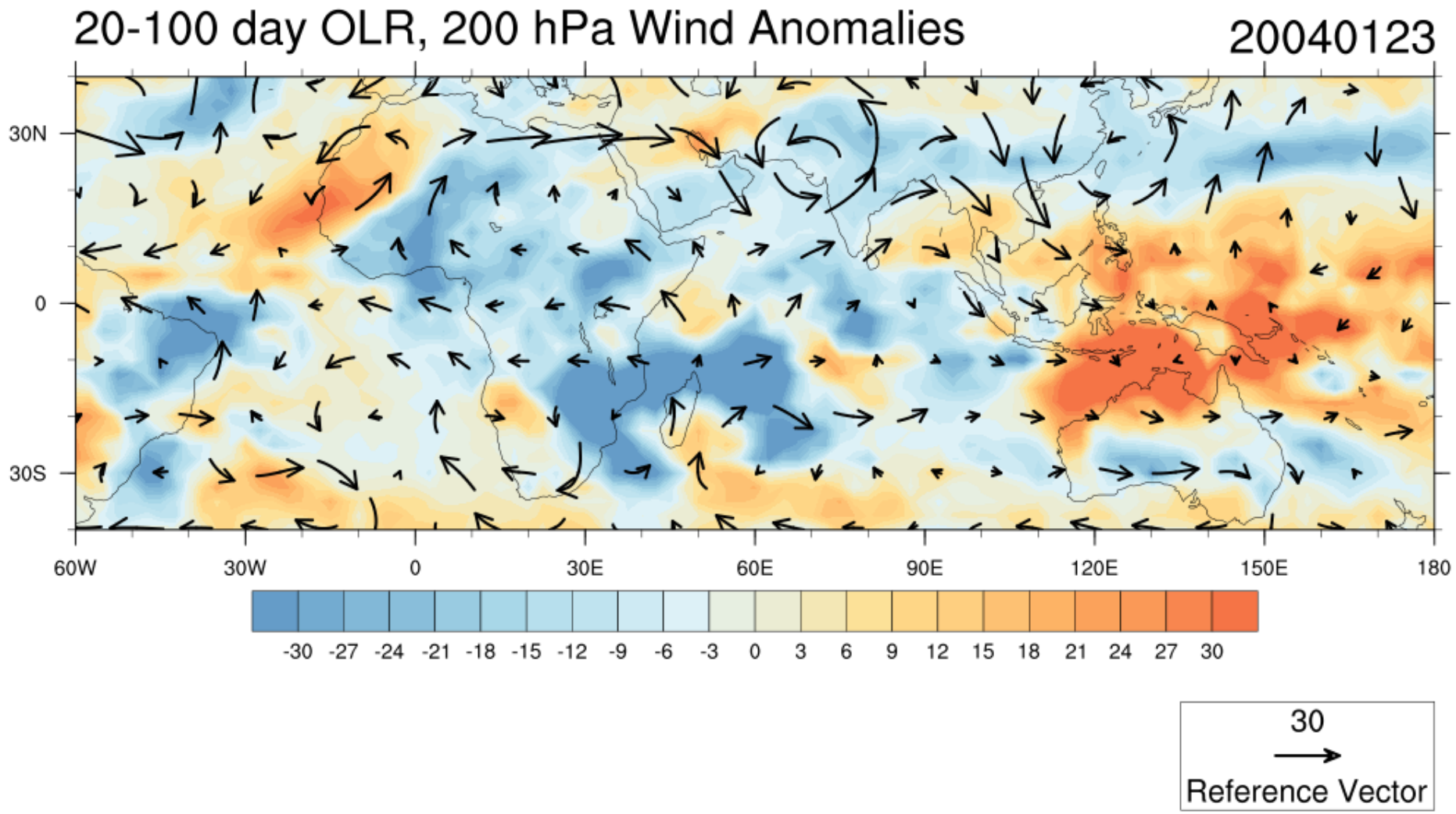

Observed precursors in the subtropics

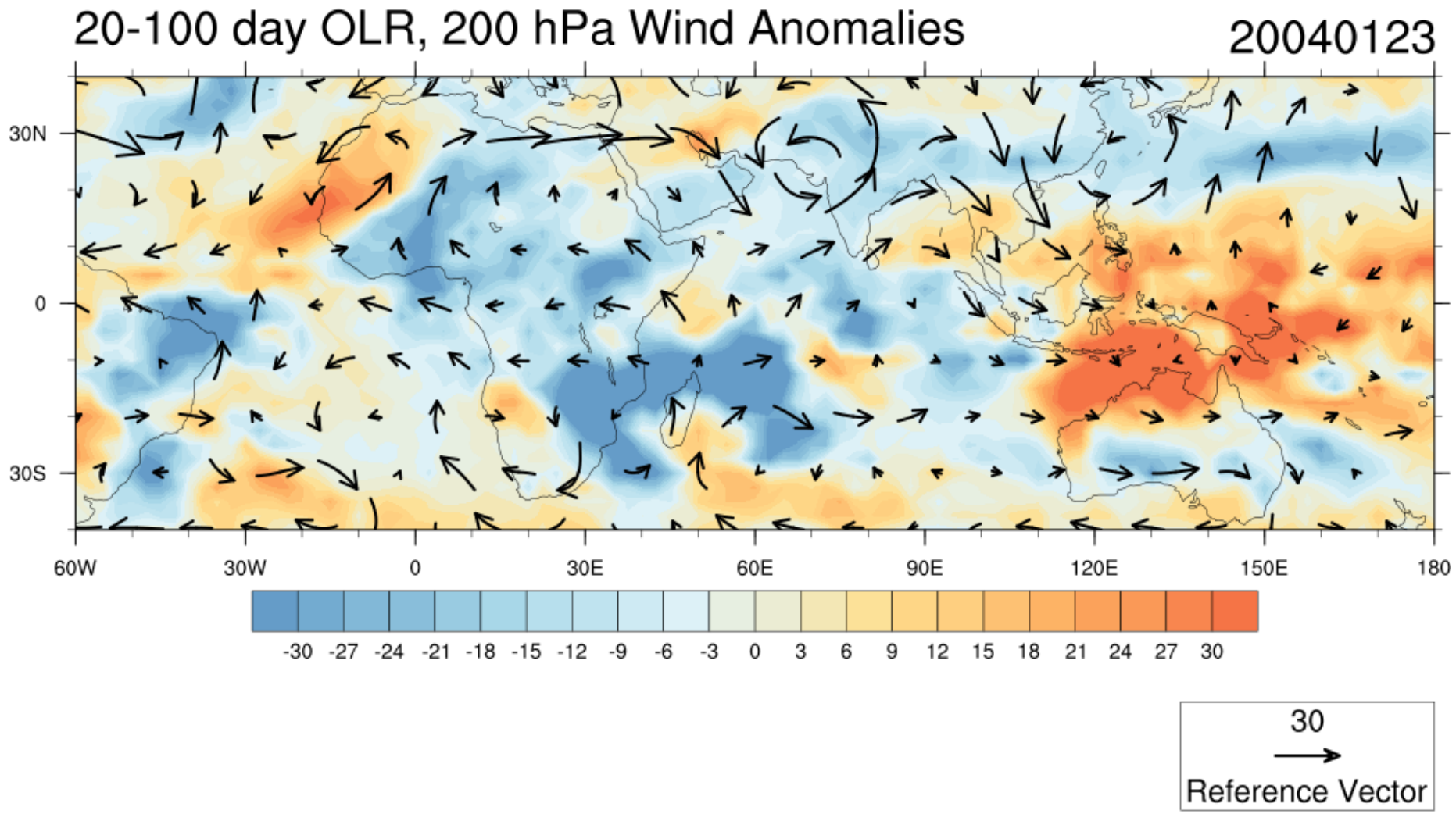

Observed precursors in the subtropics

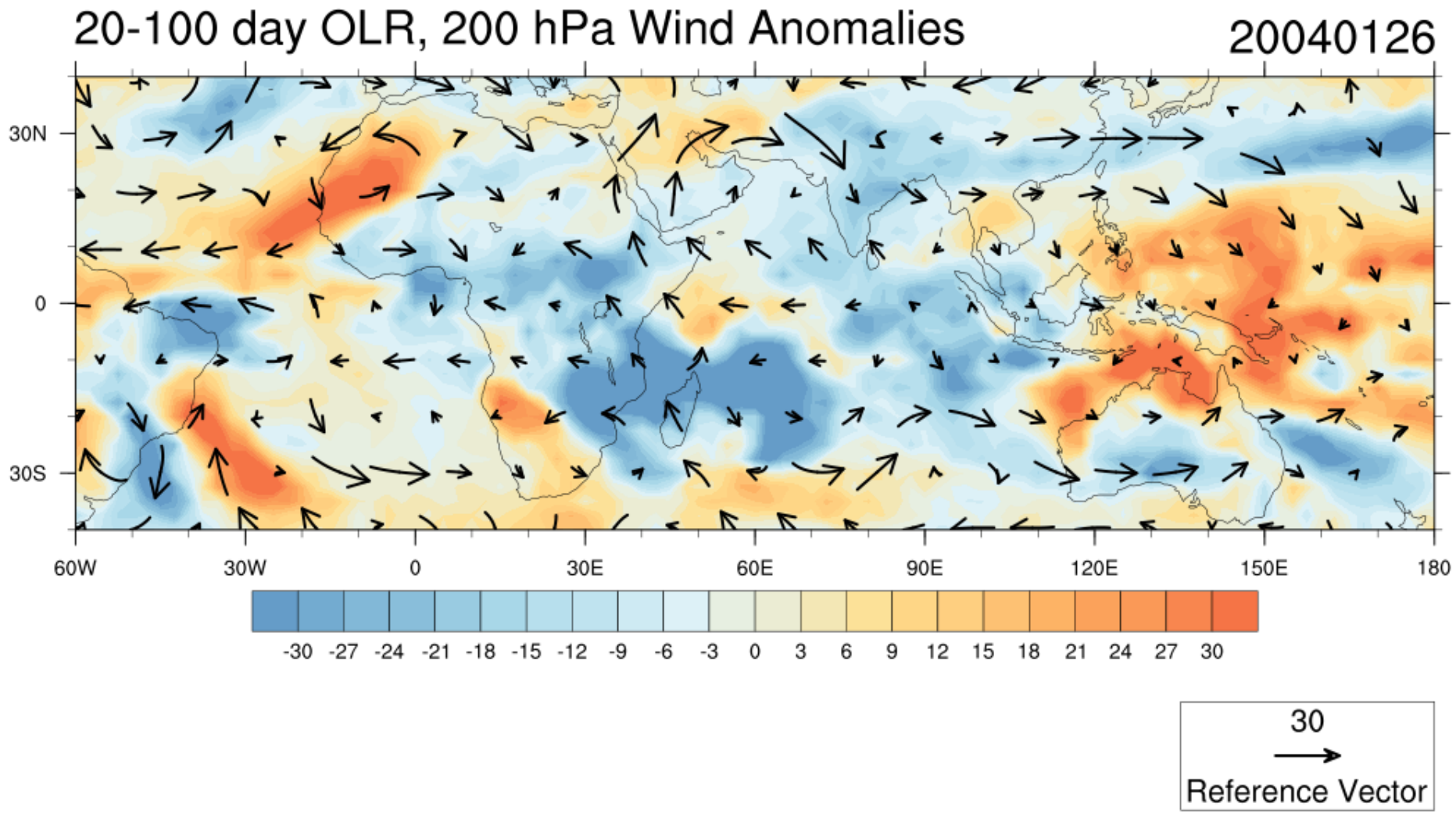

Observed precursors in the subtropics

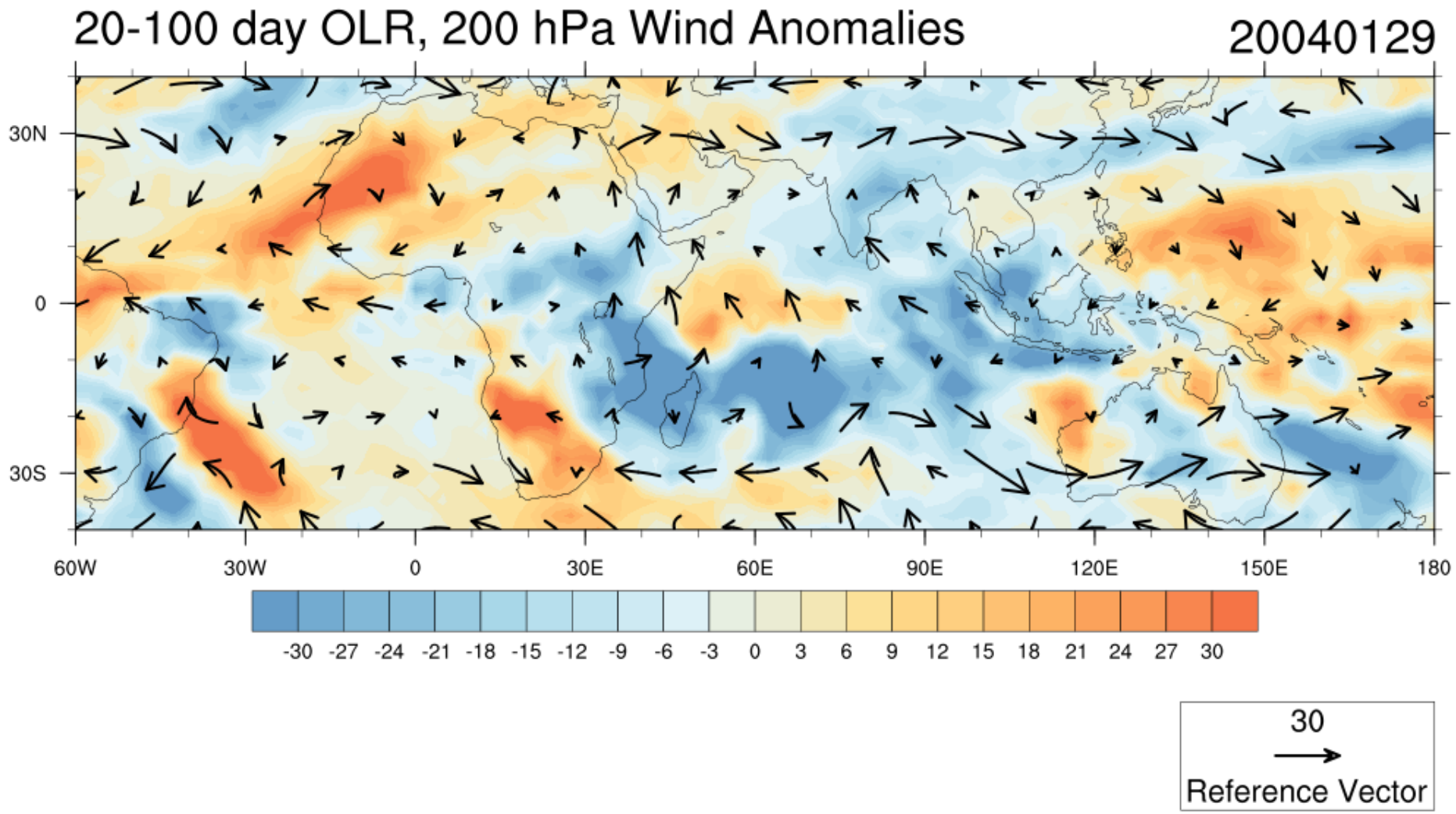

Observed precursors in the subtropics

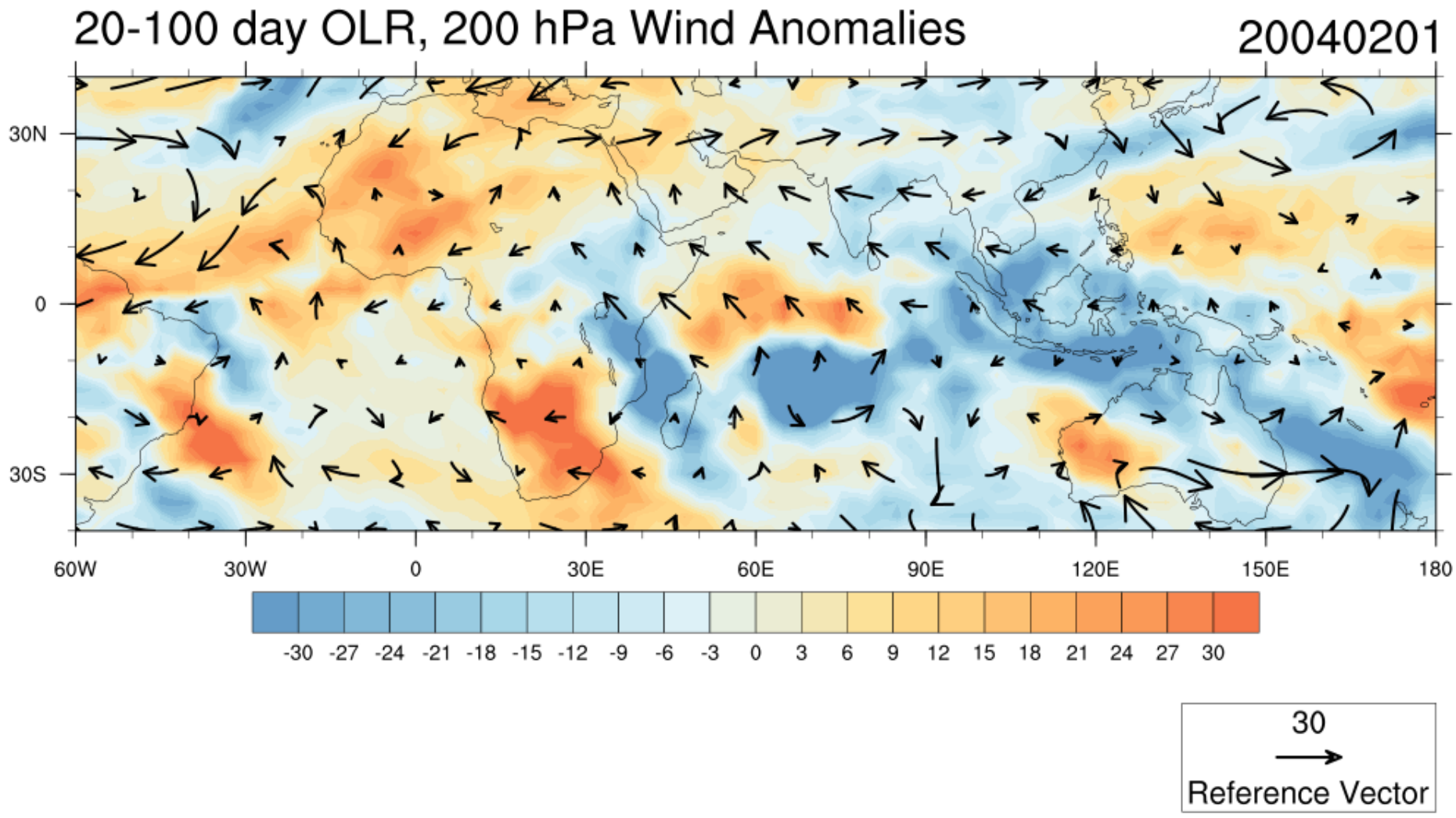

Observed precursors in the subtropics

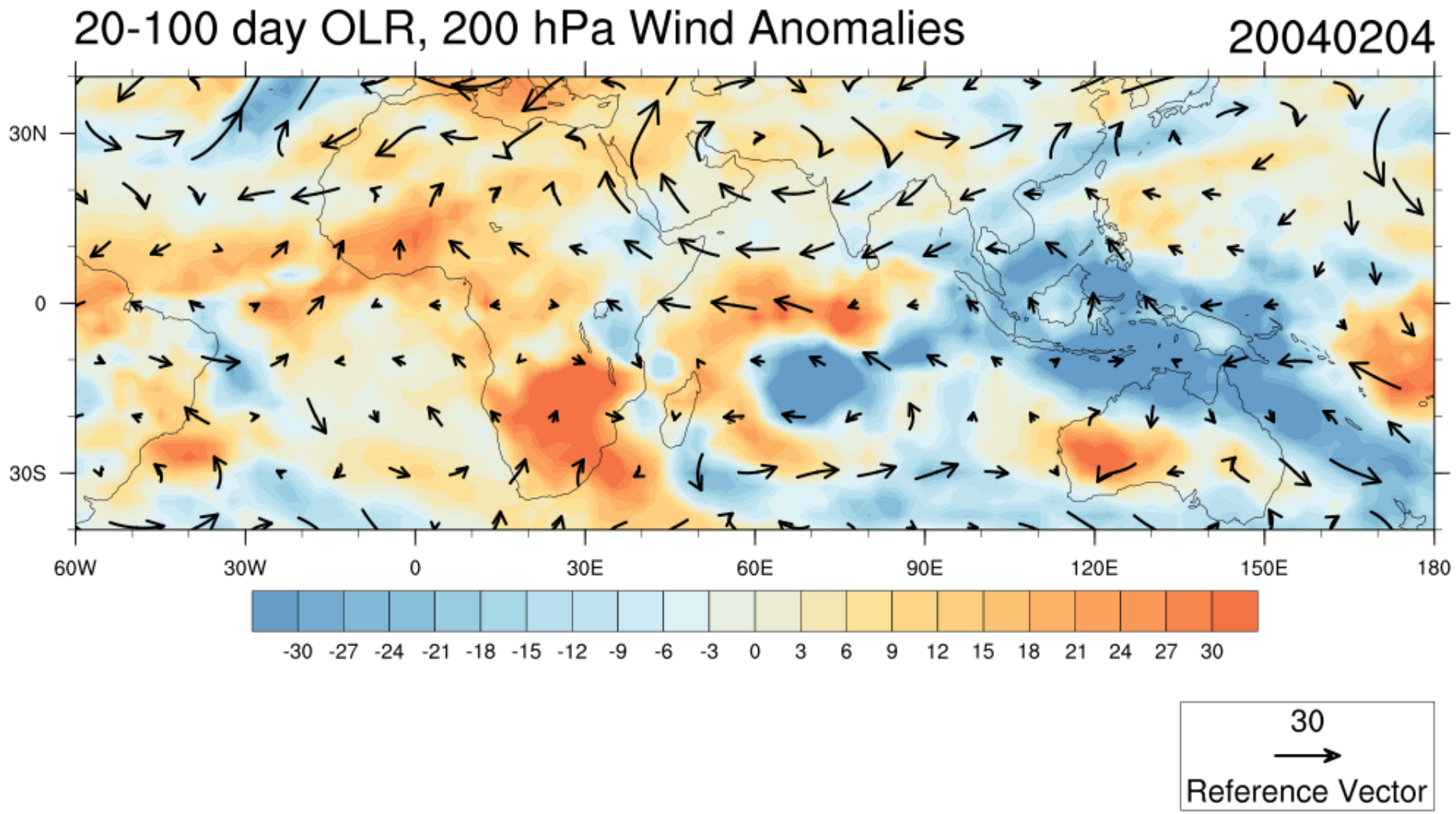

Literature suggest these subtropical signals are a response to heating anomalies from MJO convection

e. g. Gill 1980, Barlow et al. 2005, 2007

Yet to what extent are they related to the subsequent onset of MJO convection?

What causes MJO convection to initiate?

Internal versus External Processes

- Moist processes (Internal)
- Outside forcings (External)
  - Tropical
  - Extratropical

Moist processes include

- Discharge-recharge mechanism (Blade and Hartmann 1993, Benedict and Randall 2007)
- Frictional convergence (Maloney and Hartmann 1998)
- Moisture mode (e. g. Raymond and Fuchs 2009)

Results from

- DYNAMO (Powell and Houze 2013, 2015)
- Convection in general (Hohenegger and Stevens 2012)

Suggest large-scale dynamics must be favorable for convection to form

Large-scale reduction in subsidence may trigger convection

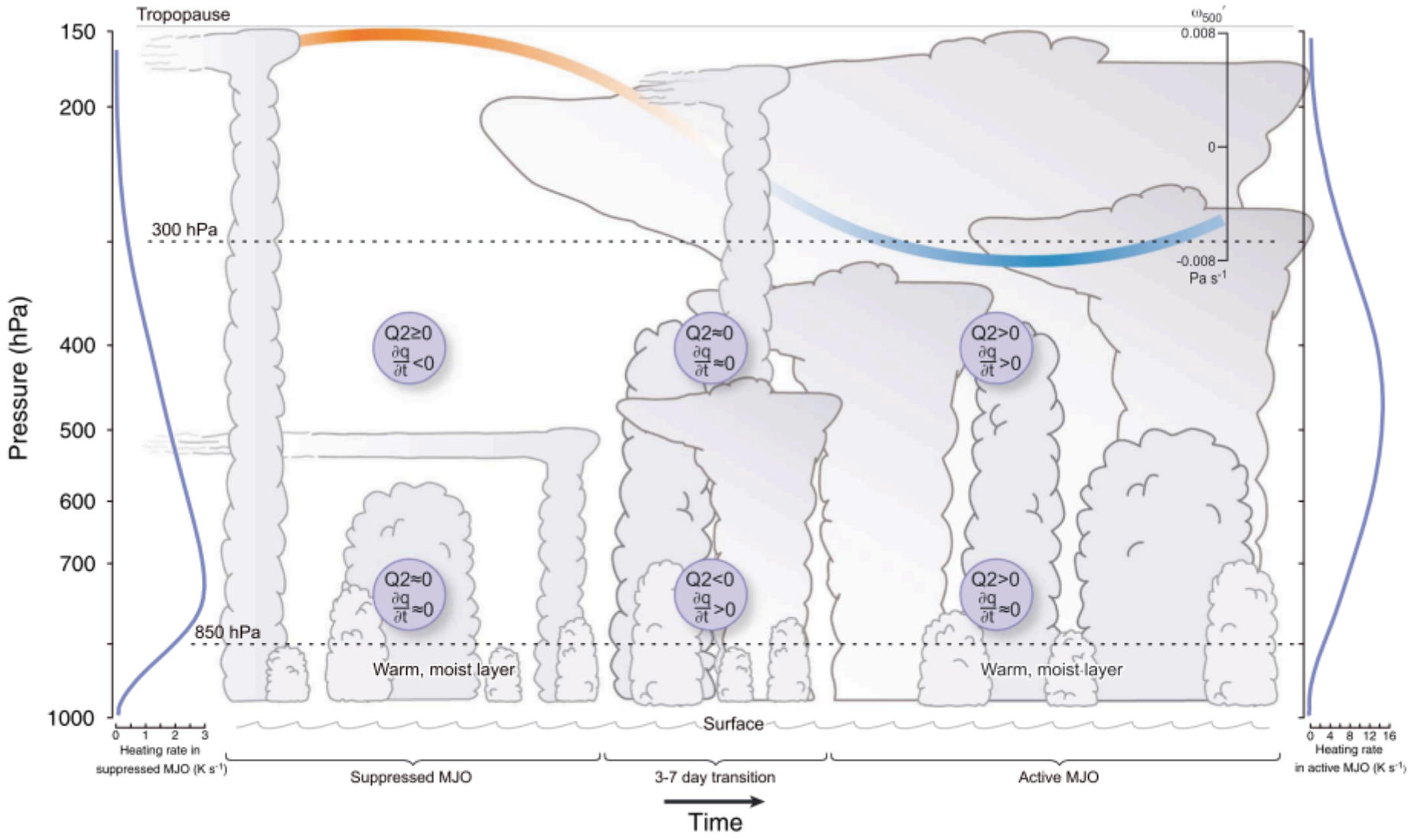

Powell and Houze (2015)

Tropical Triggers

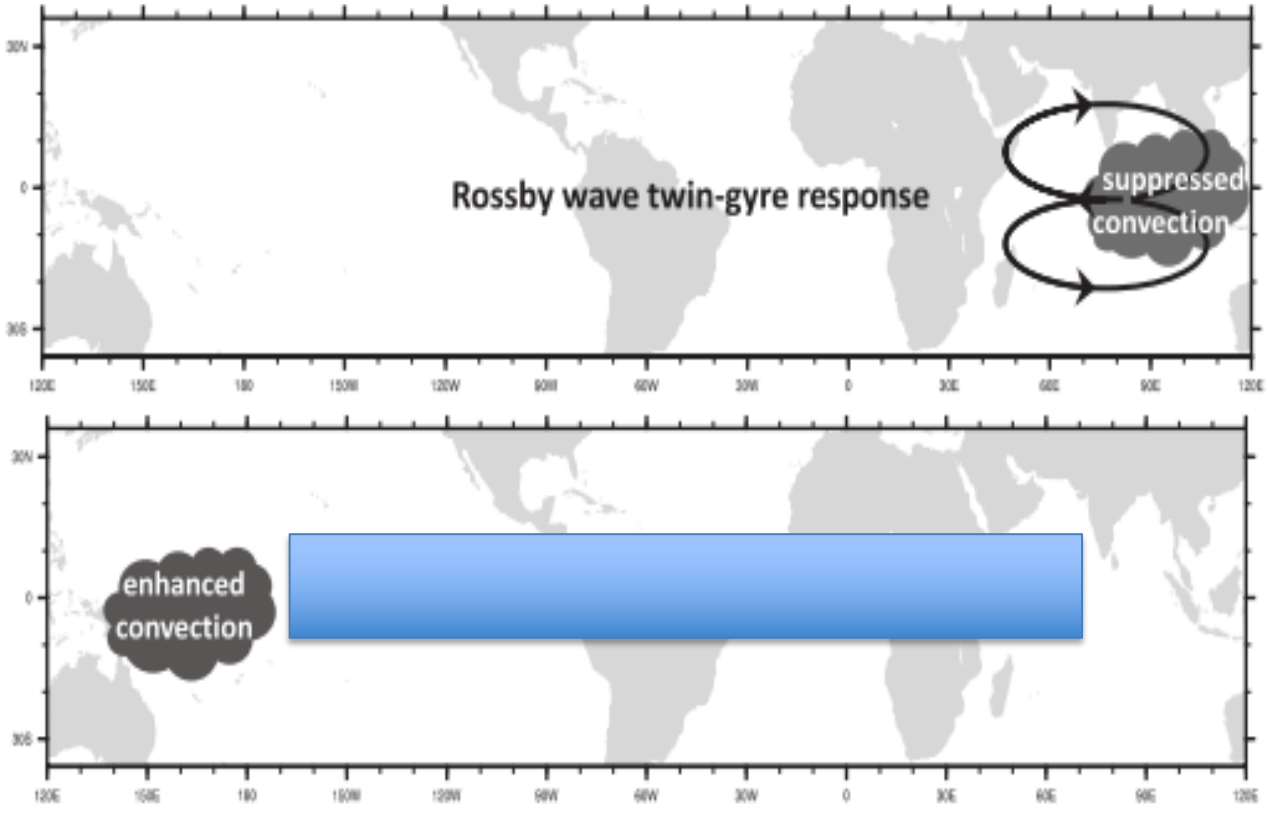

Downstream response to MJO suppressed convection

Upstream response to previous MJO convective event

Adapted from Zhao et al. 2013

Tropical Triggers

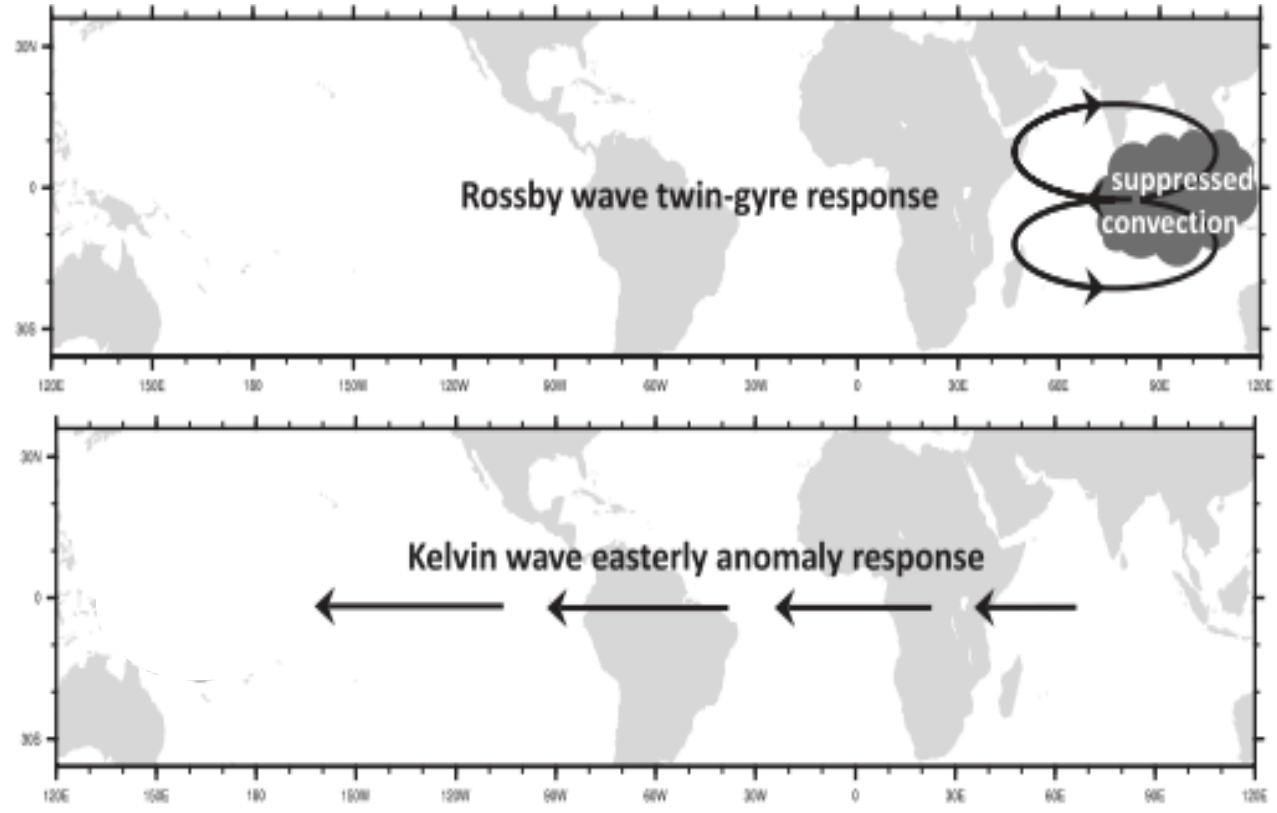

Downstream response to MJO suppressed convection

Upstream response to previous MJO convective event

Adapted from Zhao et al. 2013

Most MJO convective onset events are preceded by Western Hemispheric upper level easterlies (Straub 2013)

Events preceded by easterlies tend to be stronger than those preceded by westerlies (Roundy 2014, Sakaeda and Roundy 2015)

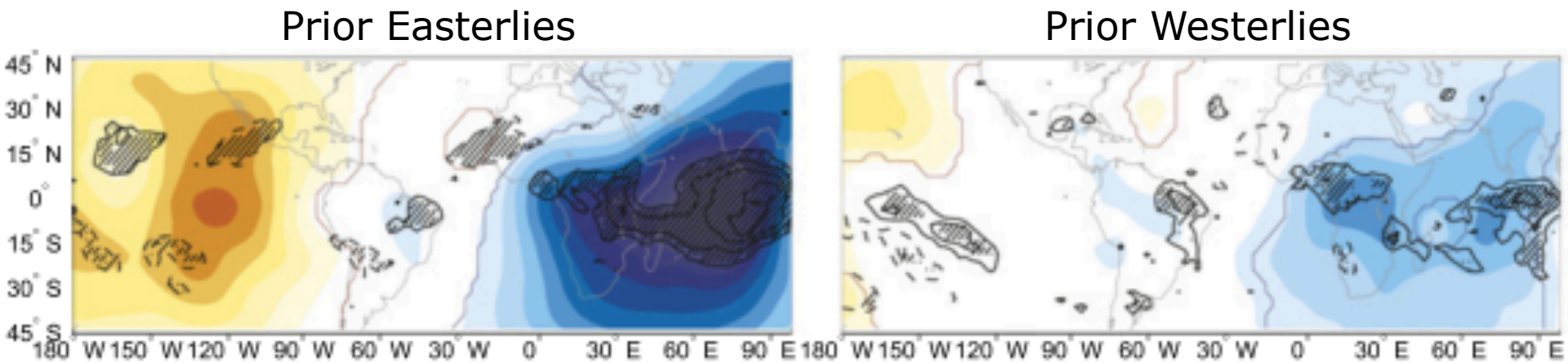

6 days After Phase 1

Velocity Potential (shading)
OLR (contours)

Adapted from Sakaeda and Roundy 2015

Circumnavigating signals are not just CCKW but are also forced by a combination of intraseasonal midlatitude Rossby wavetrains and equatorial Rossby waves over the Western Hemisphere

(Sakaeda and Roundy 2015)

Extratropical Triggers

- Increased high frequency transient wave activity moves into the Indian Ocean as MJO convection builds up (Matthews and Kiladis 1999)
- Case study (1985-86) shows incoming wavepattern (Hsu et al. 1990)

Extratropical Triggers

Models were able to trigger MJO-like disturbances by introducing extratropical forcings (Lin et al. 2007, Pan and Li 2008)

Modeling experiments block forcings from

Extratropics

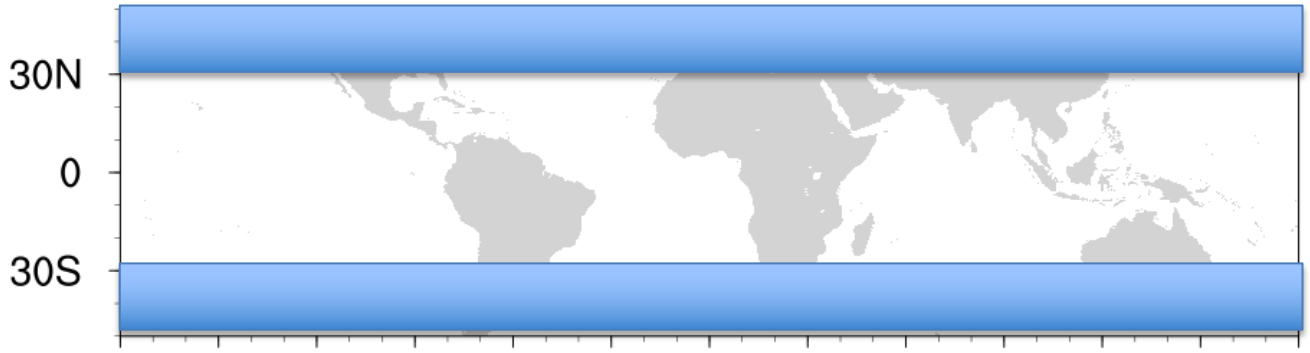

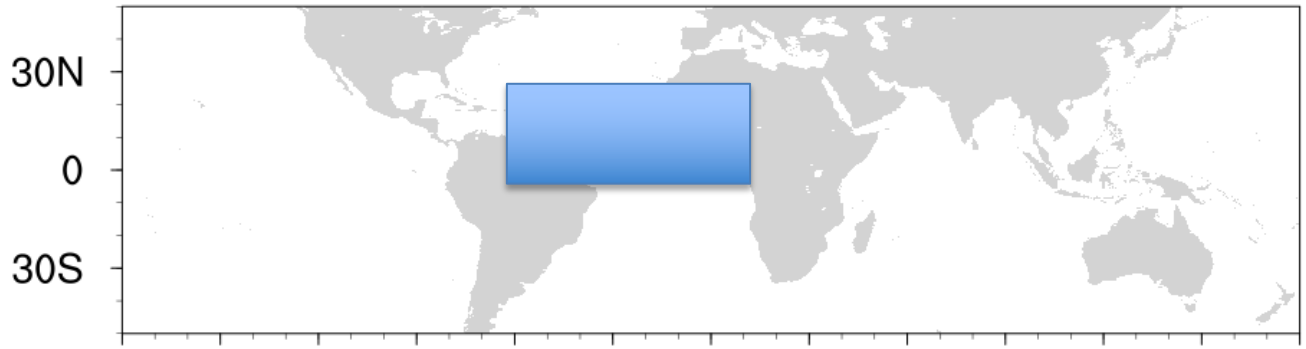

Circumnavigating from the Atlantic Ocean

to determine which has more impact on MJO convection

MJO influenced more by barriers in:

Extratropics	Atlantic Ocean	No influence
Ray and Zhang 2010; Ray et al. 2011; Zhao et al. 2013; Ray and Li 2013; Hall et al. 2017	Maloney and Wolding 2015; Zhang et al. 2017	Ma and Kuang 2016

MJO commonly identified by indices based on leading pairs of spatial structures (EOFs) in the tropics

- RMM (Wheeler and Hendon 2004)
  - Global focus
- OMI (Kiladis et al. 2014)
  - Warm pool focus

However, these indices may not capture signals near eastern Africa well…

A regional index focuses on precursors proximate to Africa

- 20-100 day OLR
- Averaged 20-70°E (black box in figure)
- Create time-extended latitudinal EOF

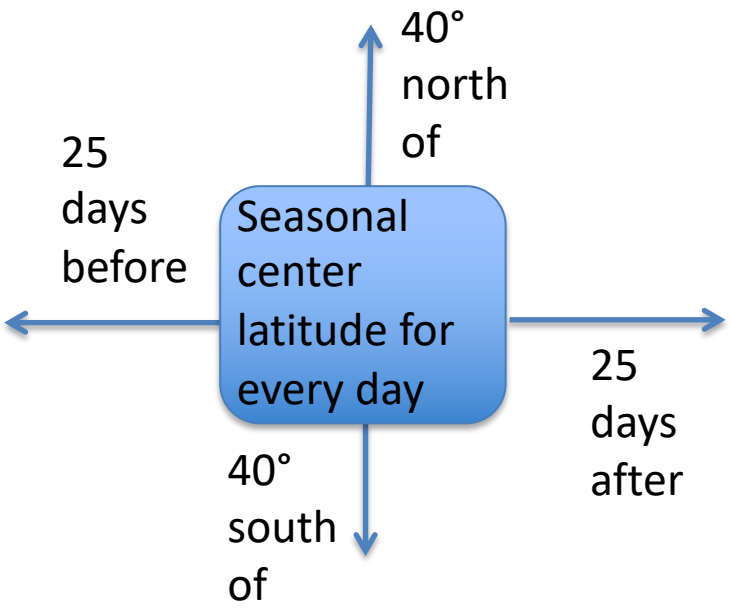

Region of Interest

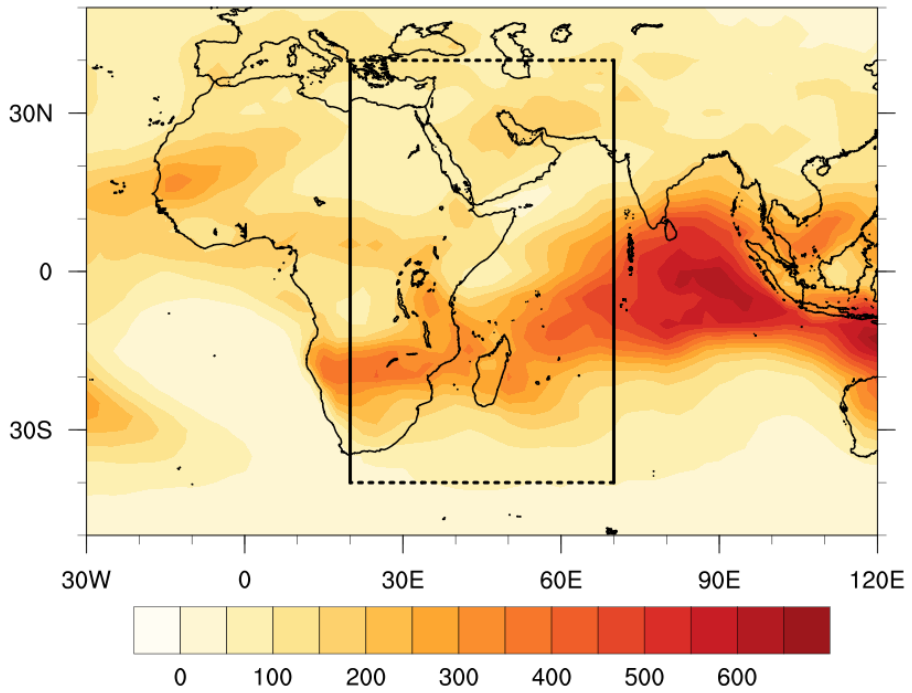

This index will later be referred to as IMMI (Intraseasonal Meridional Mode Index)

The leading two EOFs are representative of a propagating pattern

PCs 1 and 2

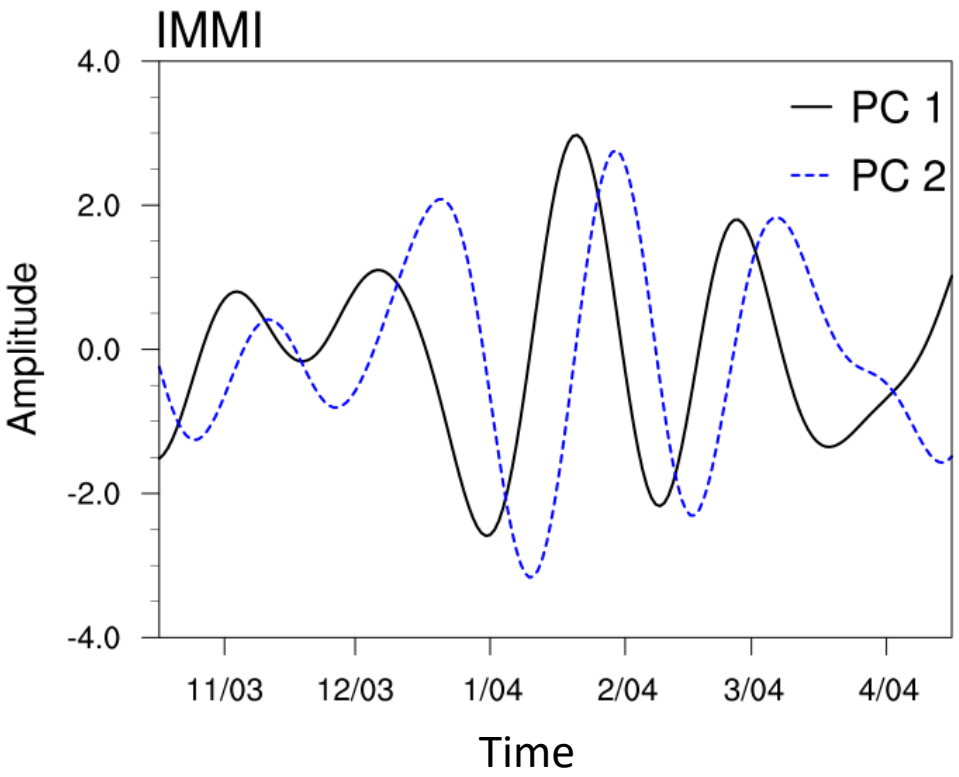

Latitude-Lag EOFs

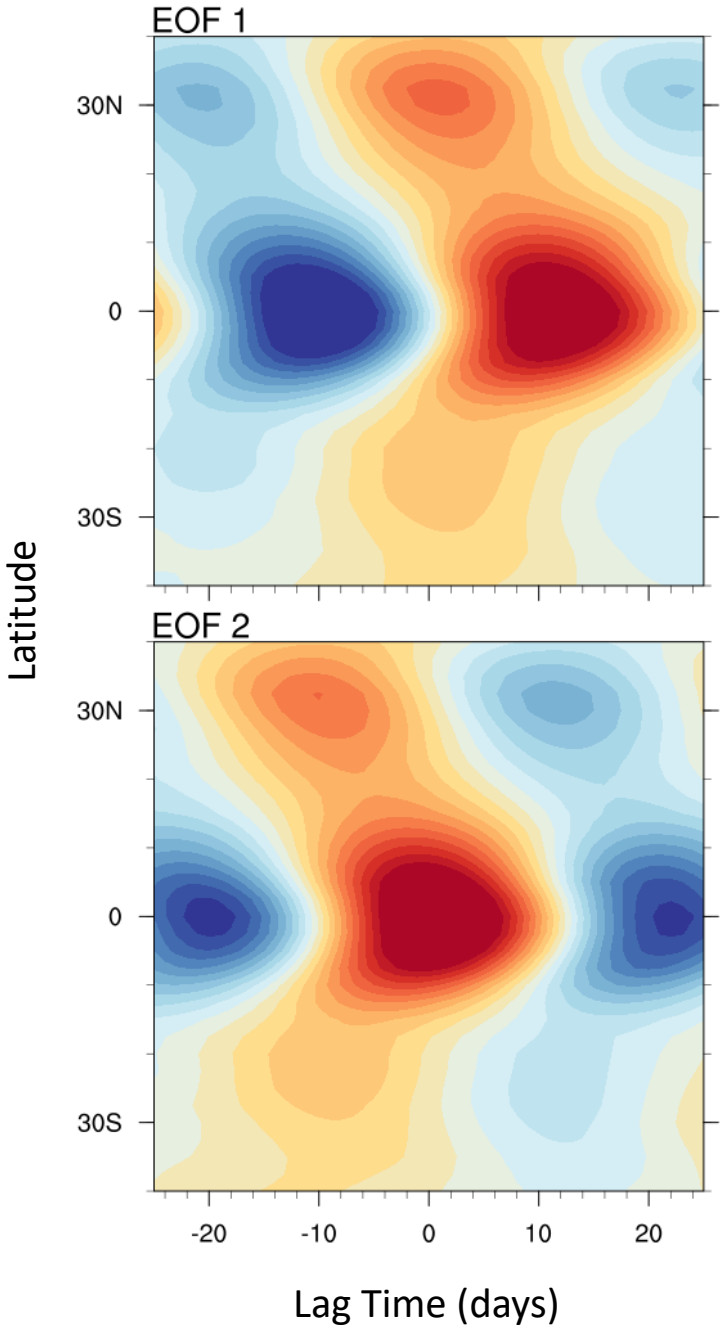

- EOFs and PCs are rotated for maximum correspondence to RMM (Wheeler and Kiladis 2004)
- Though index is regional, phasing generally agrees with RMM

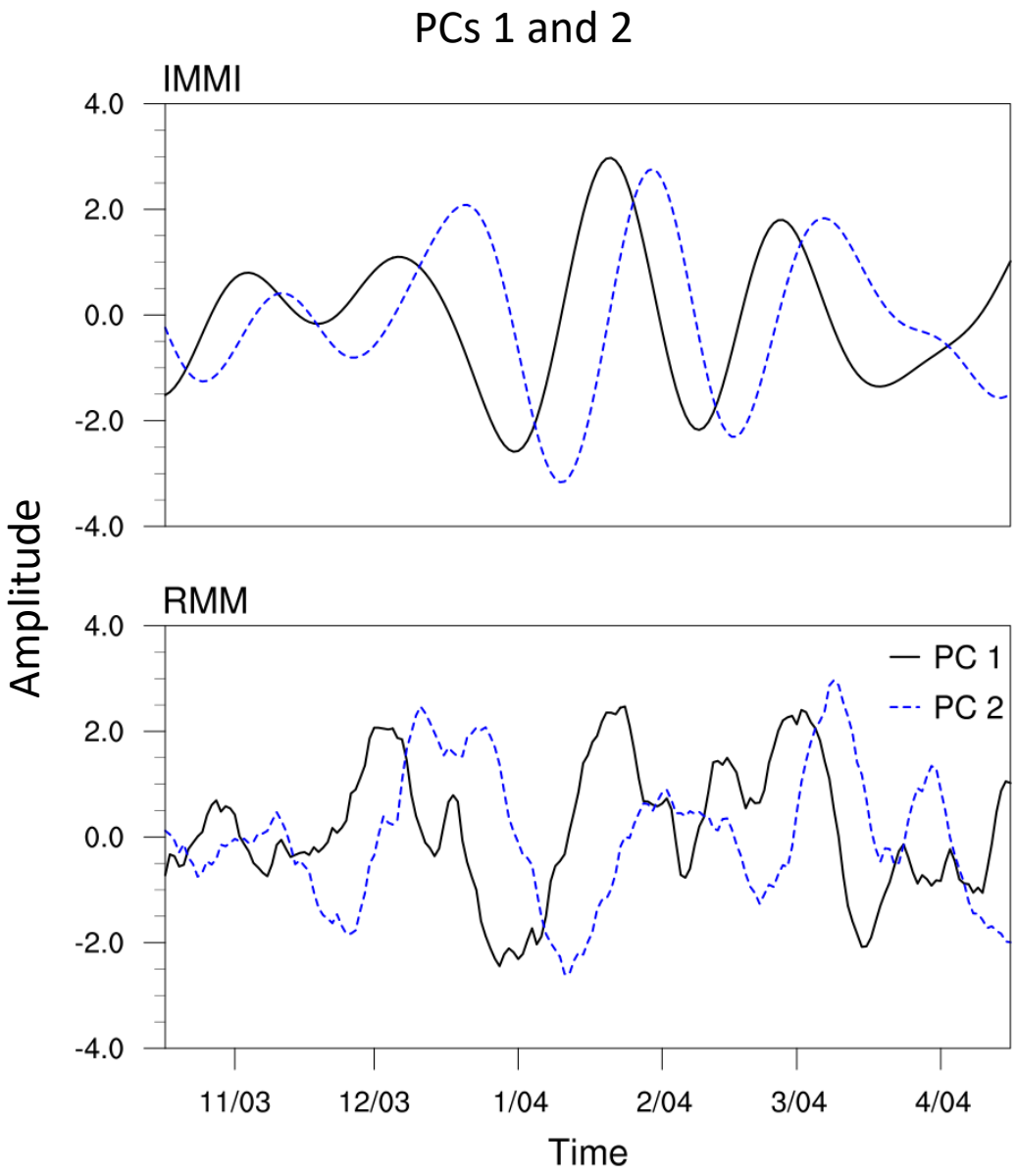

Data:
NOAA OLR and ERA-Interim

Event Identification:
regional index based on the time evolution of the meridional structure in

20-100 day OLR

20-70° E (IMMI)

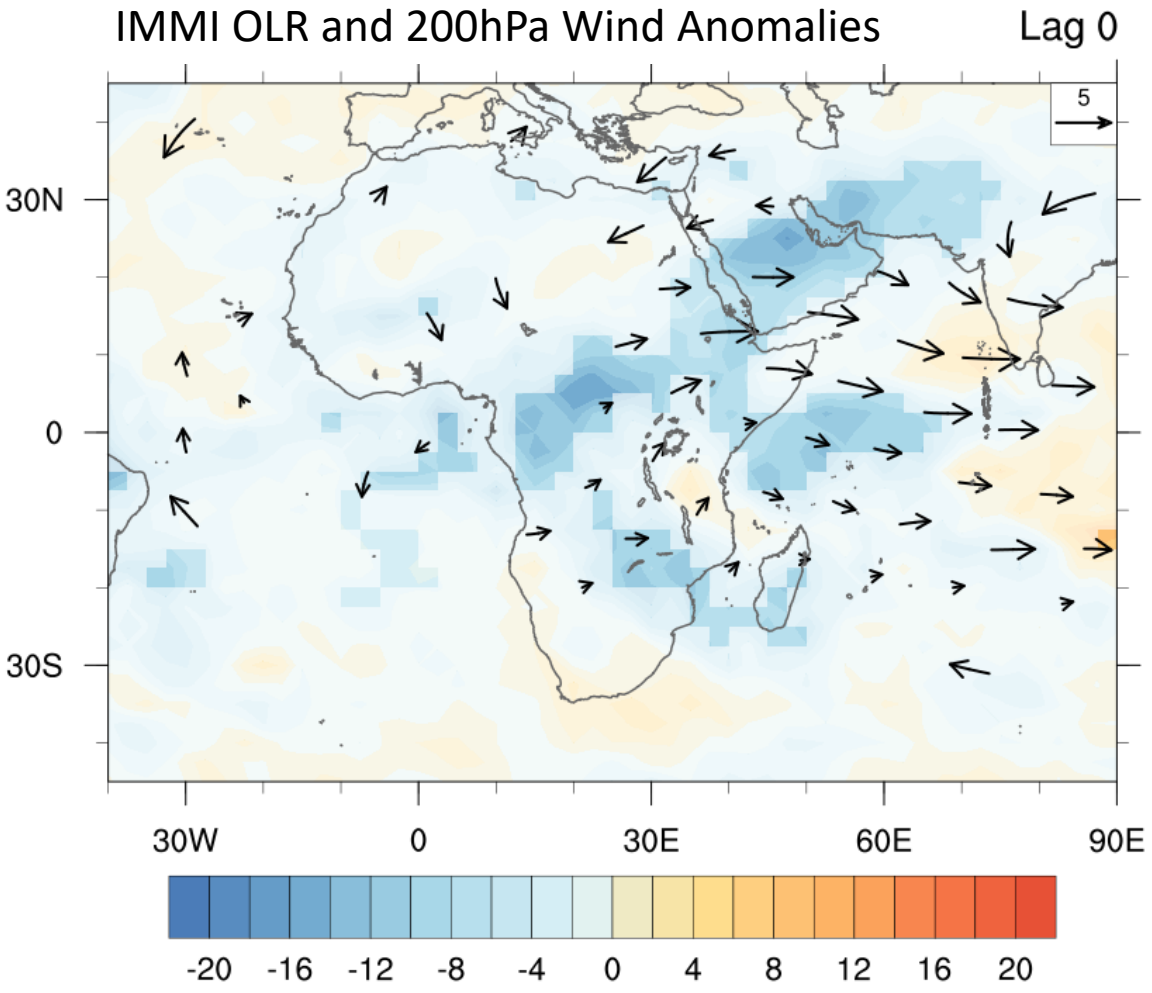

Lag zero: MJO enhanced convection begins to form over the western Indian Ocean

To better understand circulation precursors, evaluate the intraseasonal zonal momentum budget over the western Indian Ocean

Time Tendency is balanced by Advection PGF Coriolis Residual

$$\frac{\partial u}{\partial t} = -\mathbf{v} \cdot \nabla u - \frac{\partial \phi}{\partial x} + fv + X$$

Budget filtered for intraseasonal timescales (20-100 days) and taken at 200hPa

200hPa easterly acceleration (shading) is in phase with the 500hPa upward motion (contours)

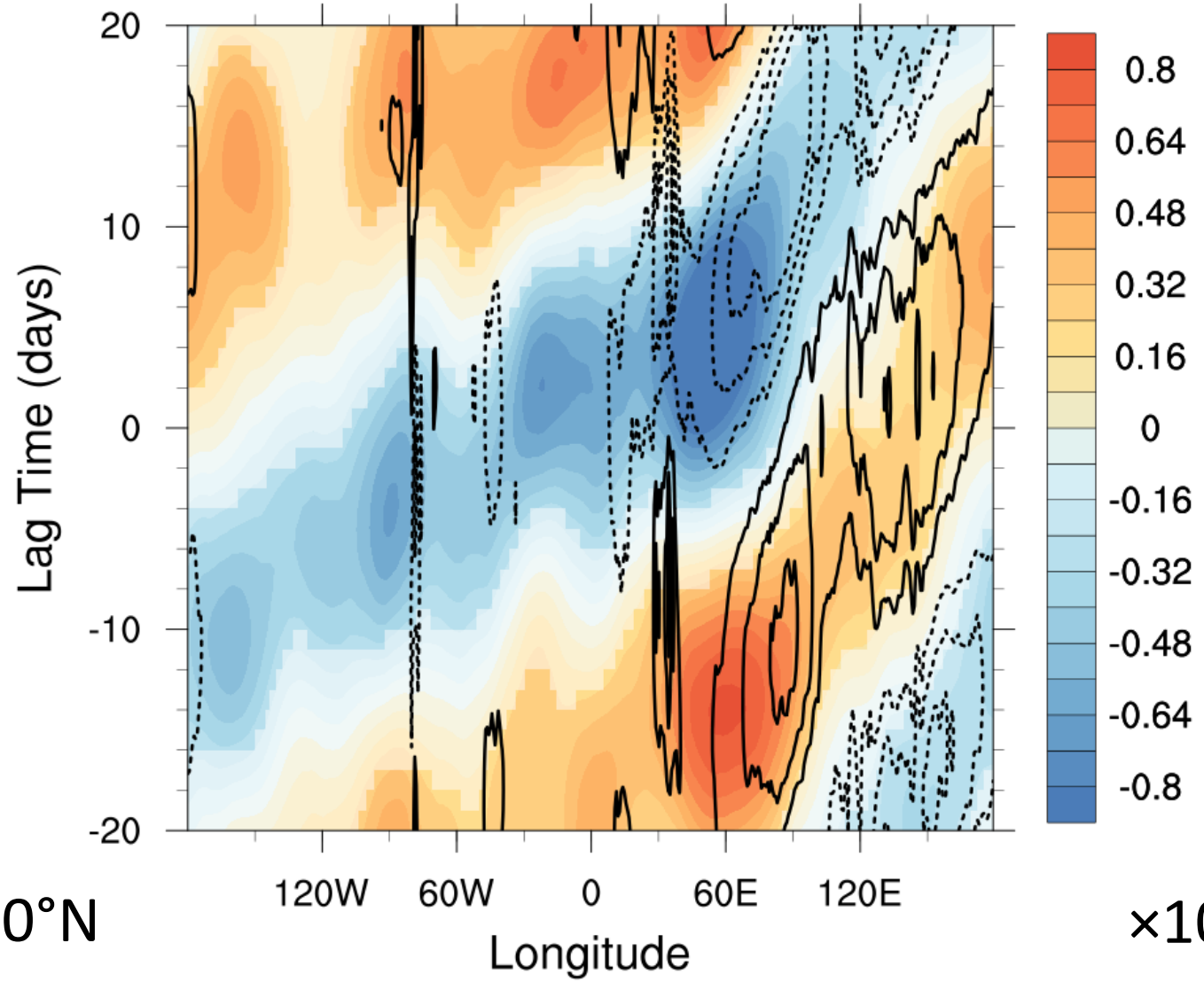

10°S-10°N

$\times 10^{-5}$ m s^{-2}

Upper tropospheric easterly acceleration on the west side of a region of westerlies leads to divergence which may help to provide large-scale upward motion

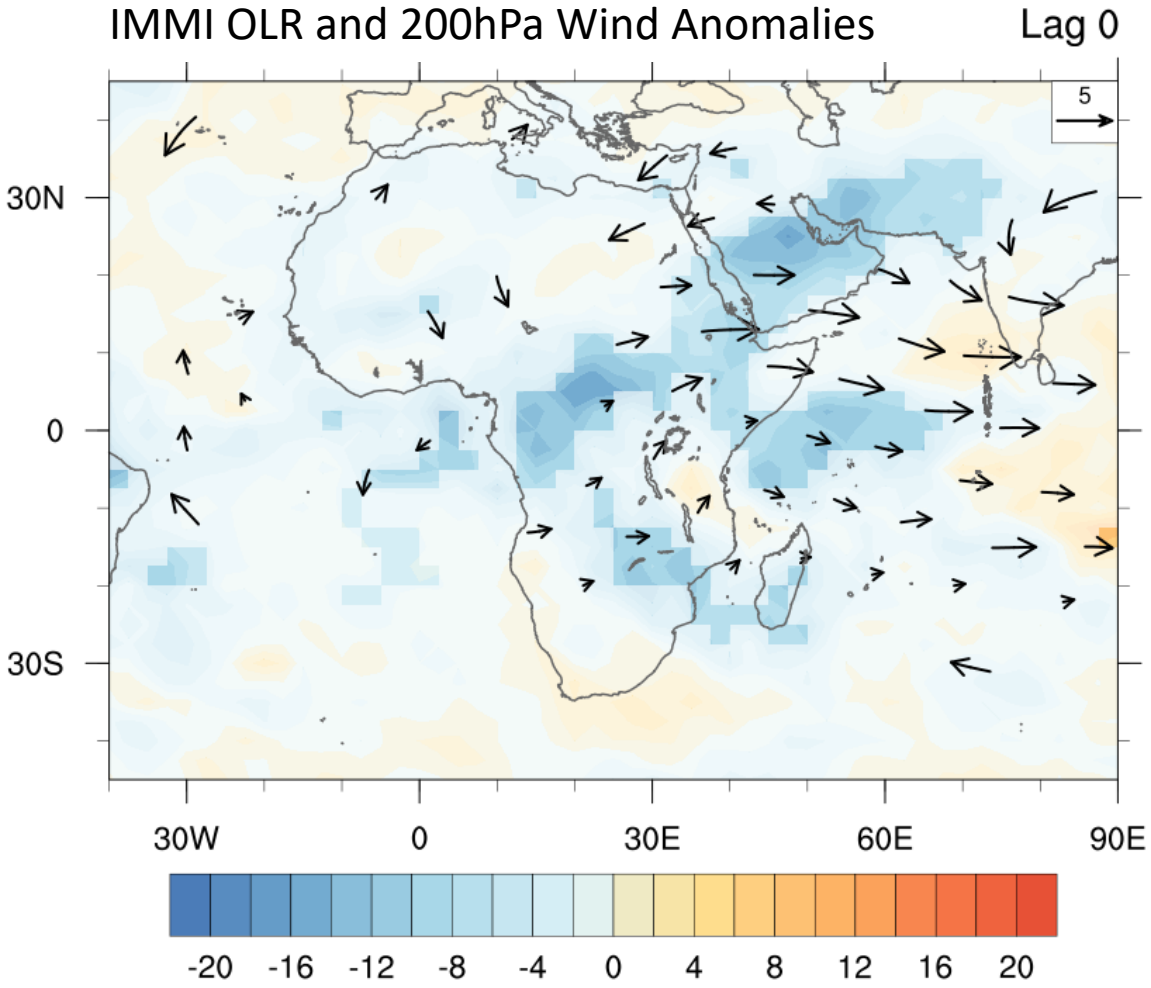

Easterly acceleration is maximized near 50-60°E and 10°S-10°N around the time of convective onset

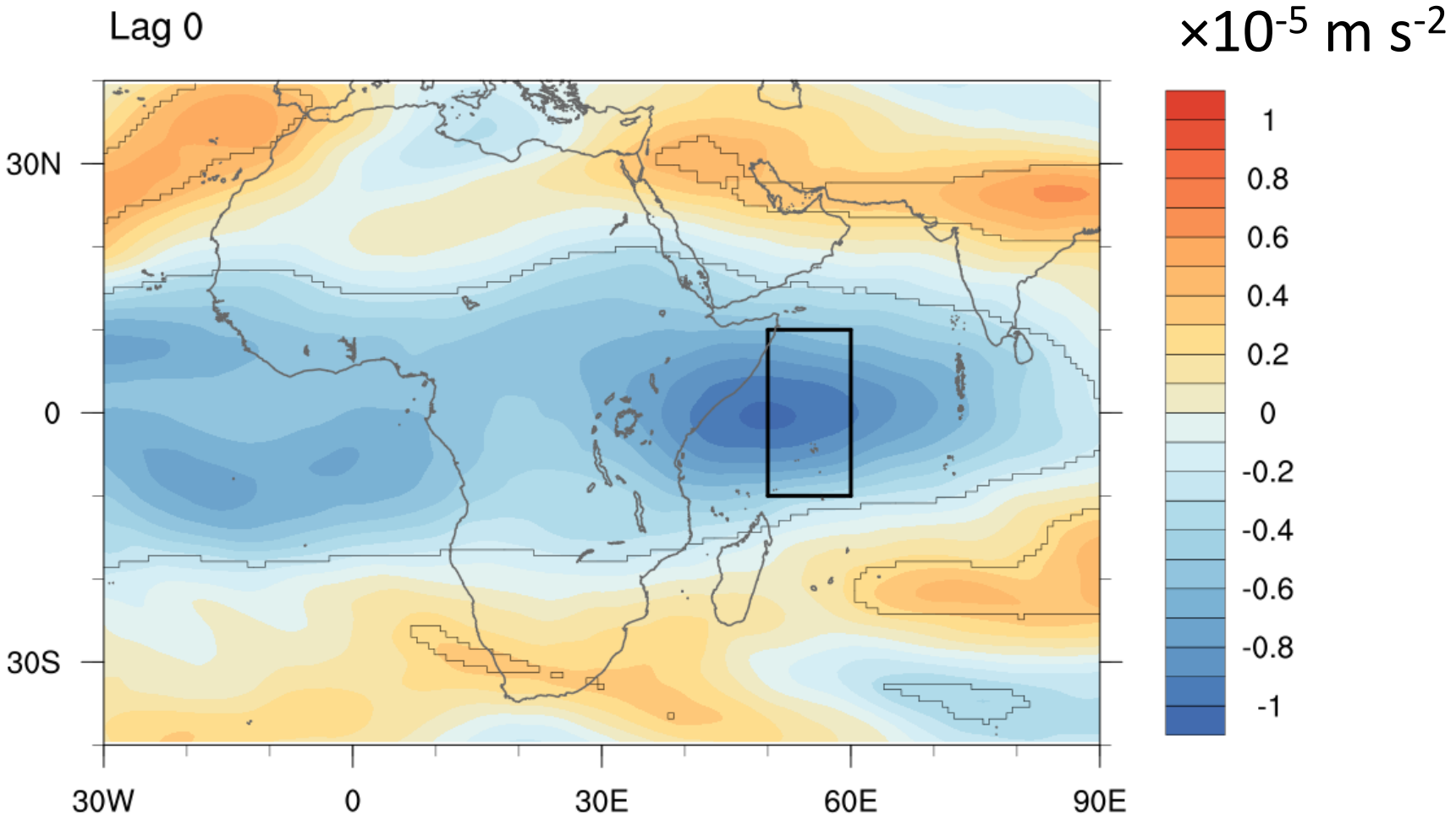

76/84
East

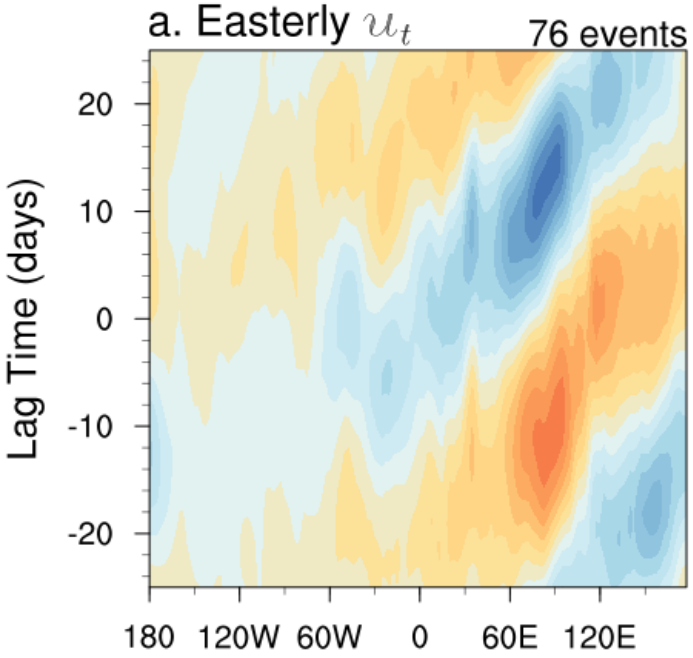

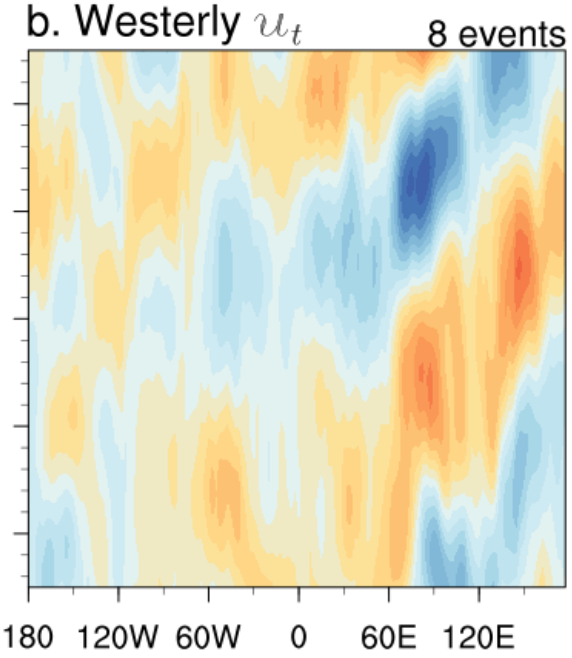

8/84
West

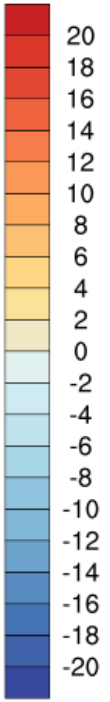

20-100d OLR
(shading)

East – West
Tendency
In box from
50-60°E and
10°S-10°N

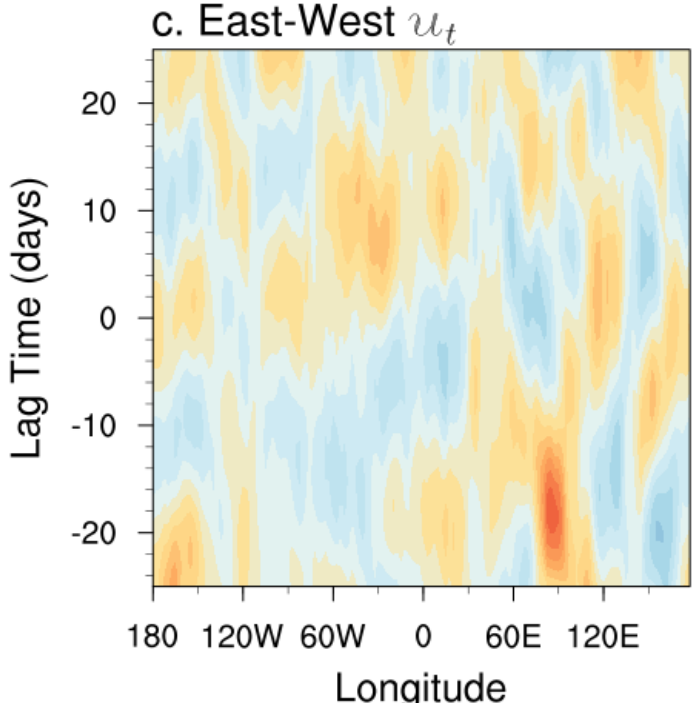

Negative OLR is
delayed for
westerly events

76/84
East

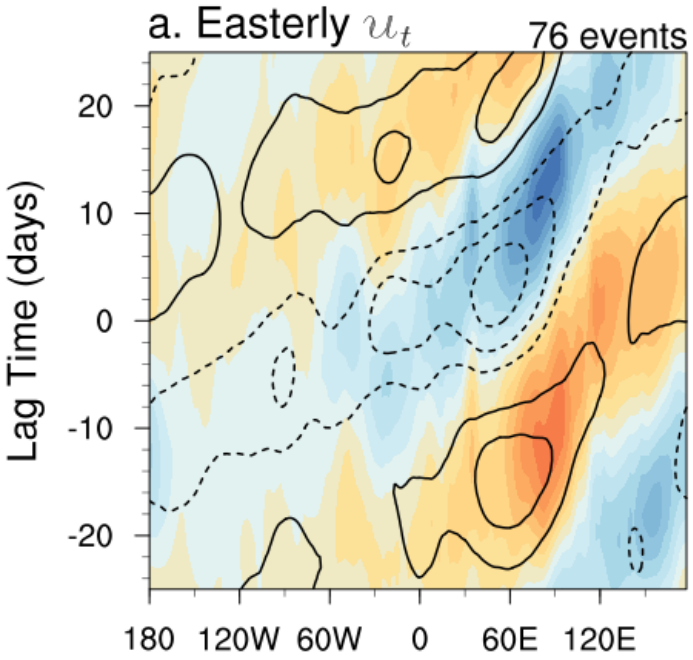

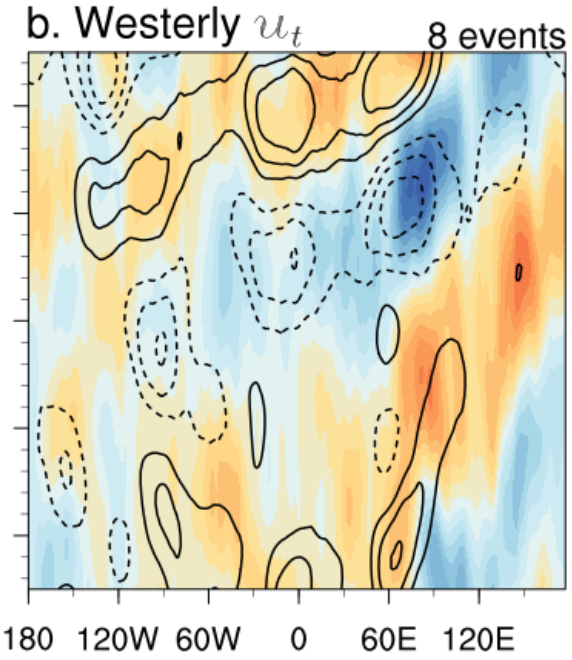

8/84
West

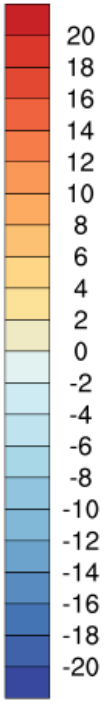

20-100d OLR (shading), Tendency (contours)

East – West

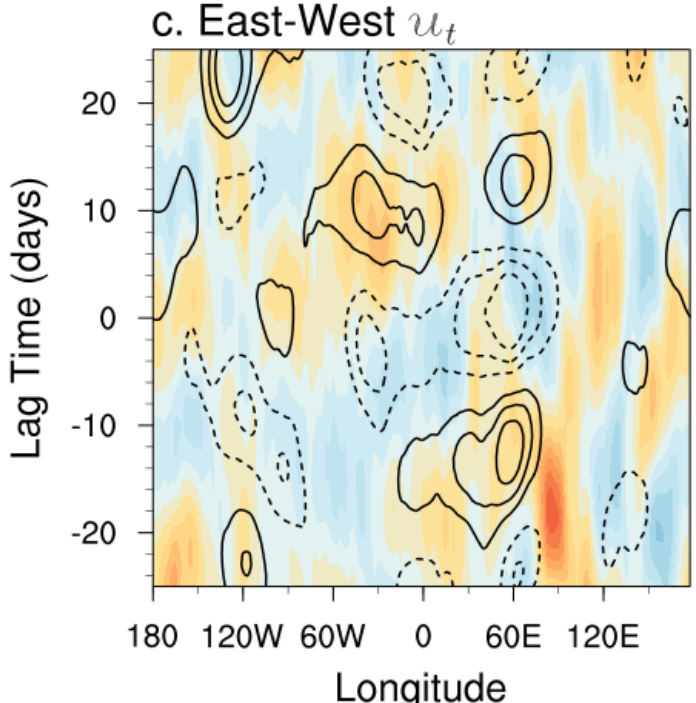

Negative OLR is in phase with zonal wind tendency

The time tendency is negative at lag zero (at its minimum a few days after lag 0)

Budget in box from 50-60°E and 10°S-10°N

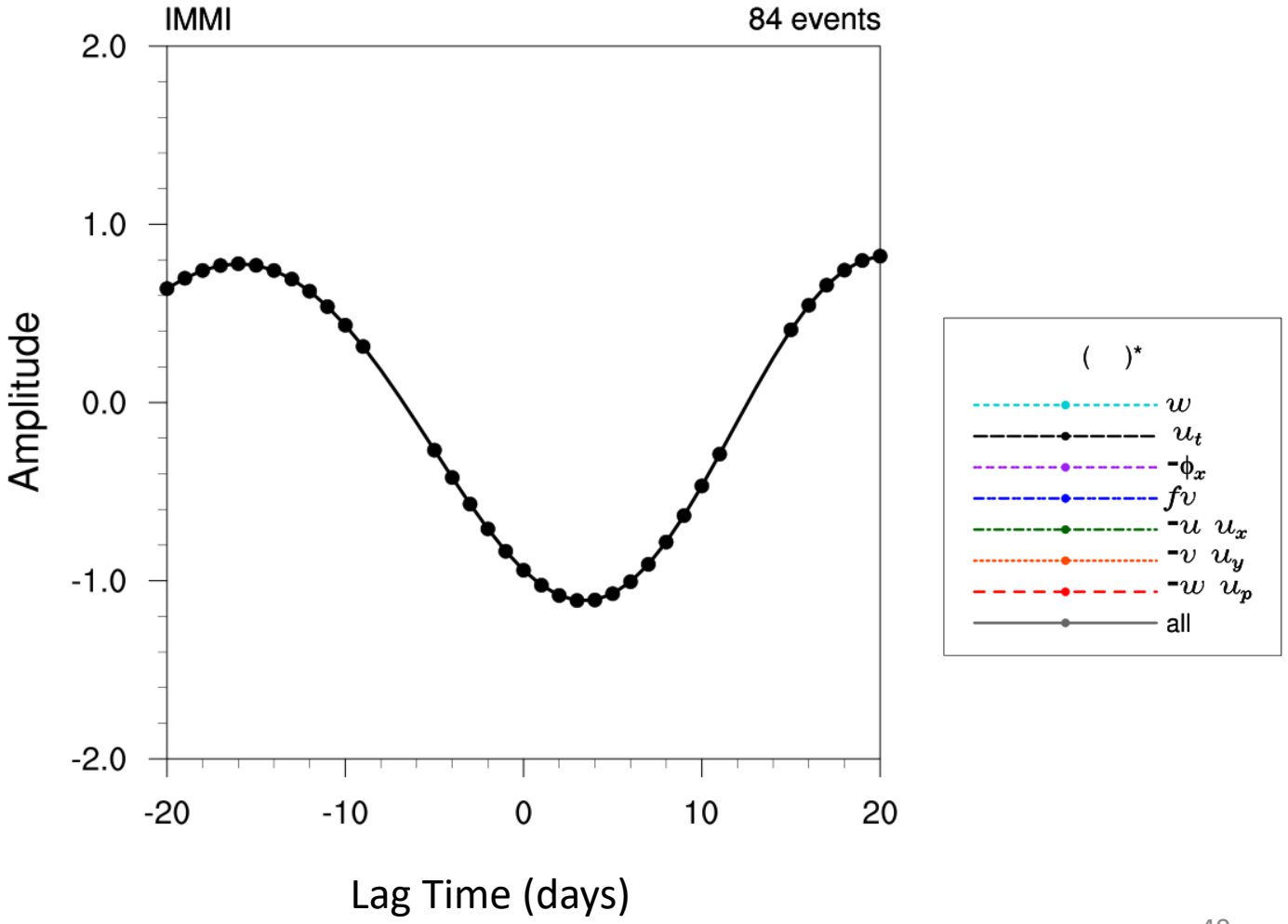

ω (cyan) is in phase with the time tendency

Budget in box from 50-60°E and 10°S-10°N

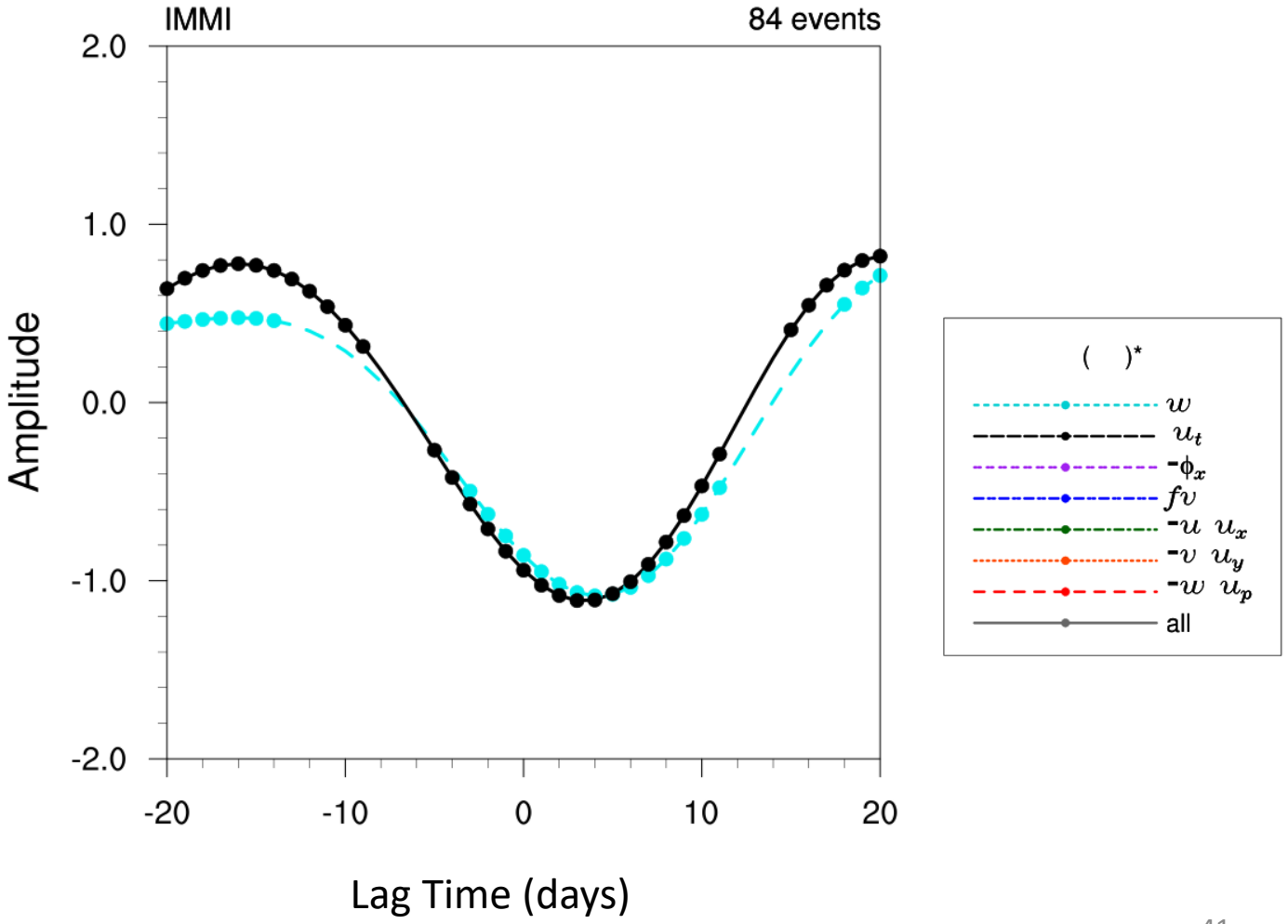

The zonal pressure gradient force is mainly in phase with the time tendency

Budget in box from 50-60°E and 10°S-10°N

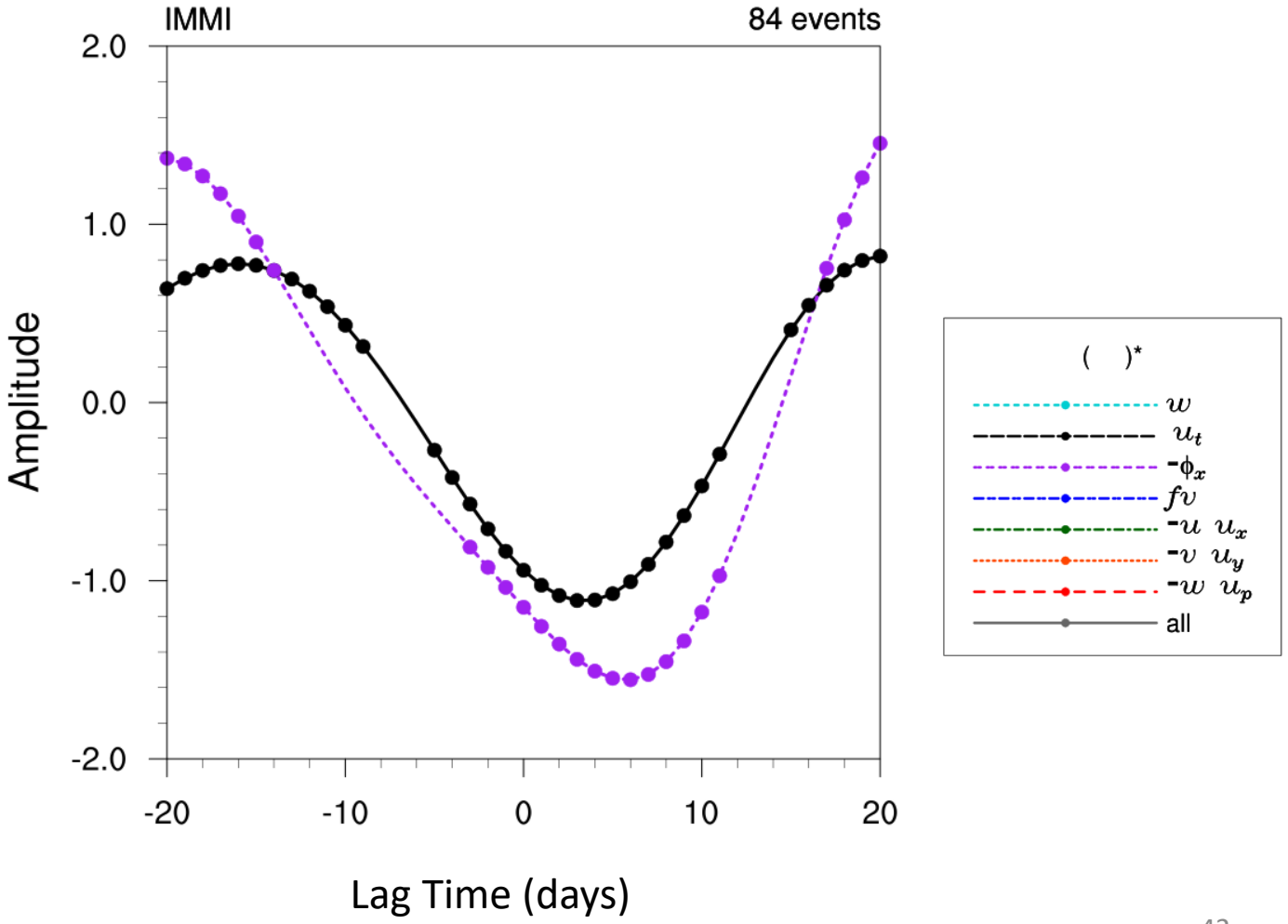

The Coriolis is not statistically significant for the average of all events

Budget in box from 50-60°E and 10°S-10°N

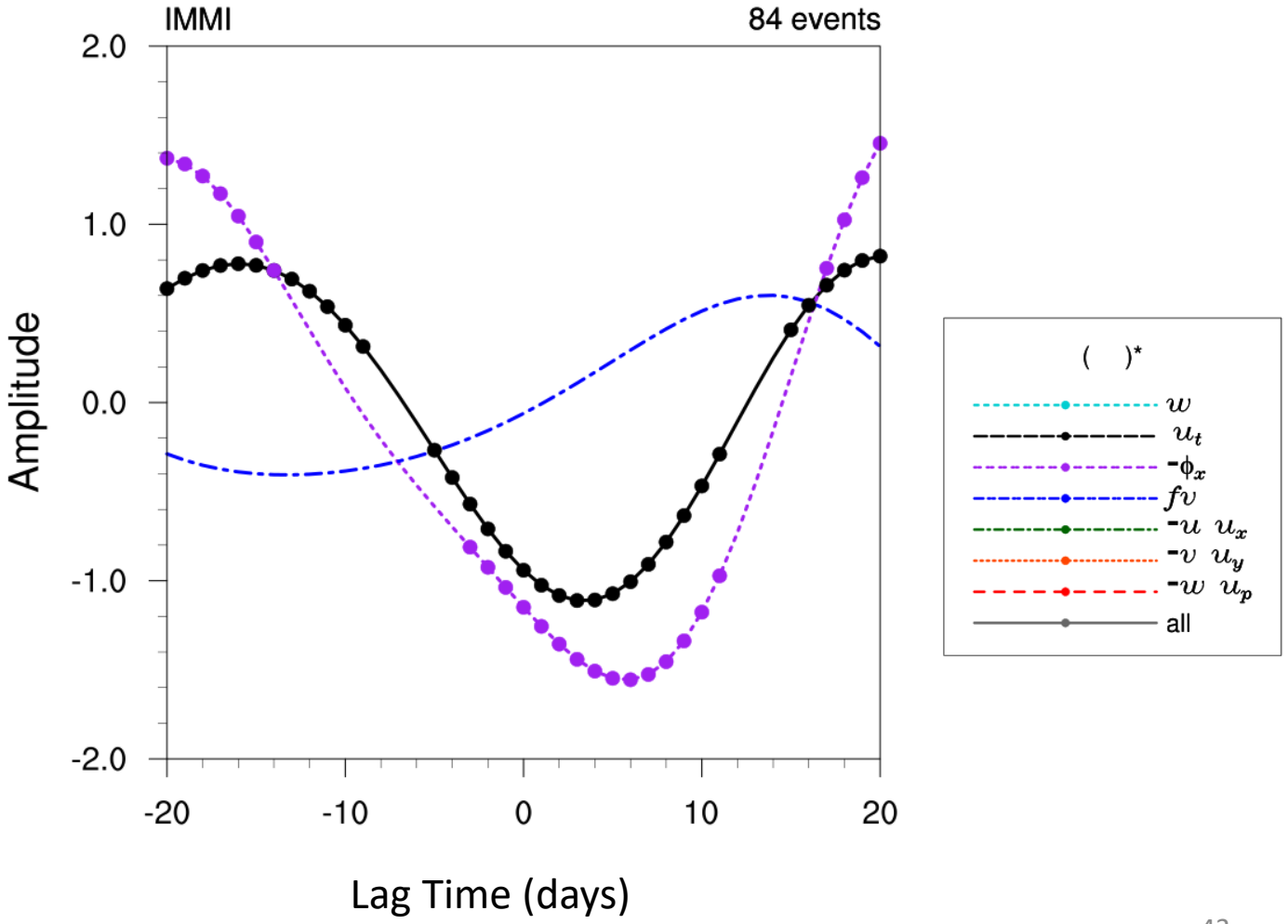

The zonal advection is westerly

Budget
in box from
50-60°E and
10°S-10°N

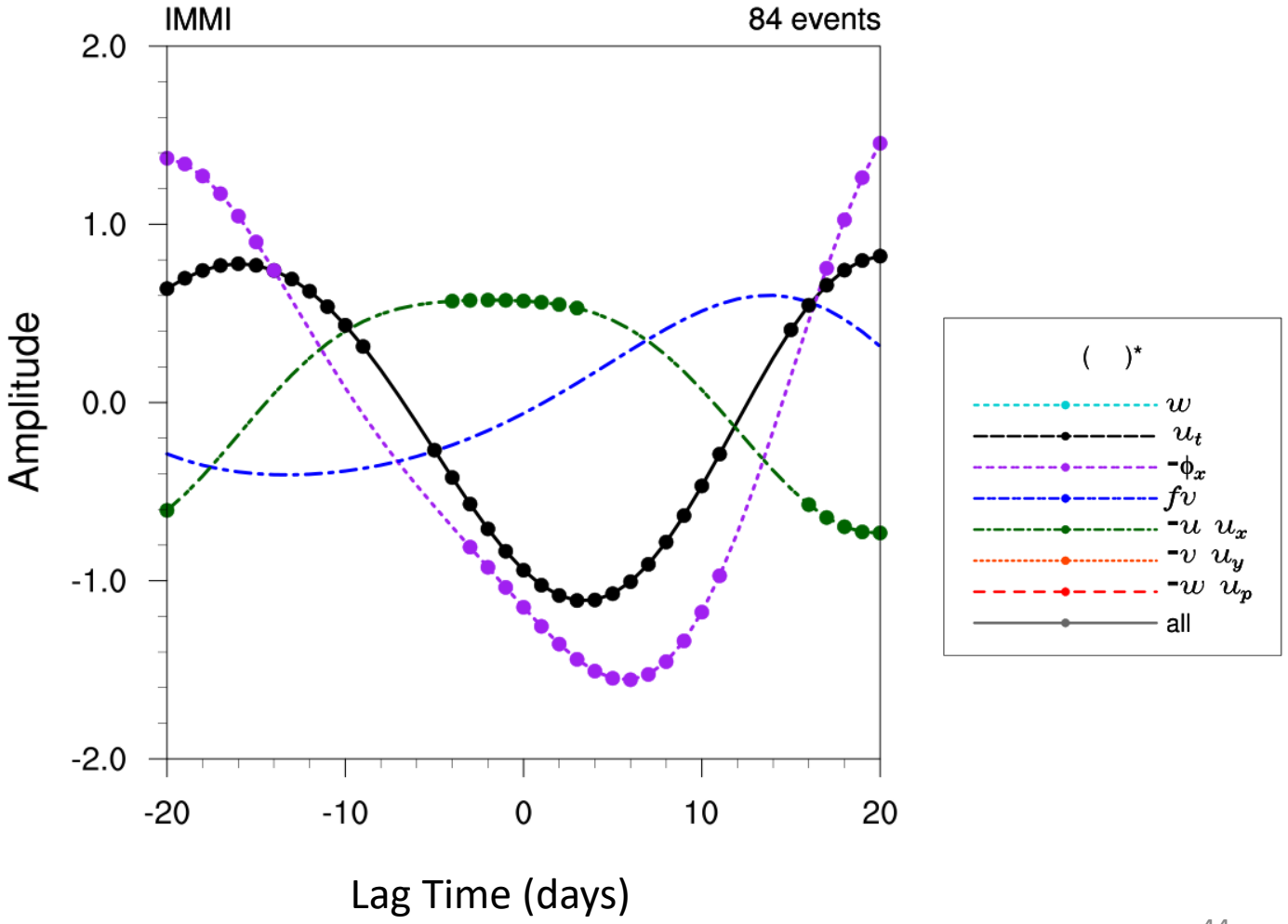

The meridional advection is not statistically significant for the average of all events

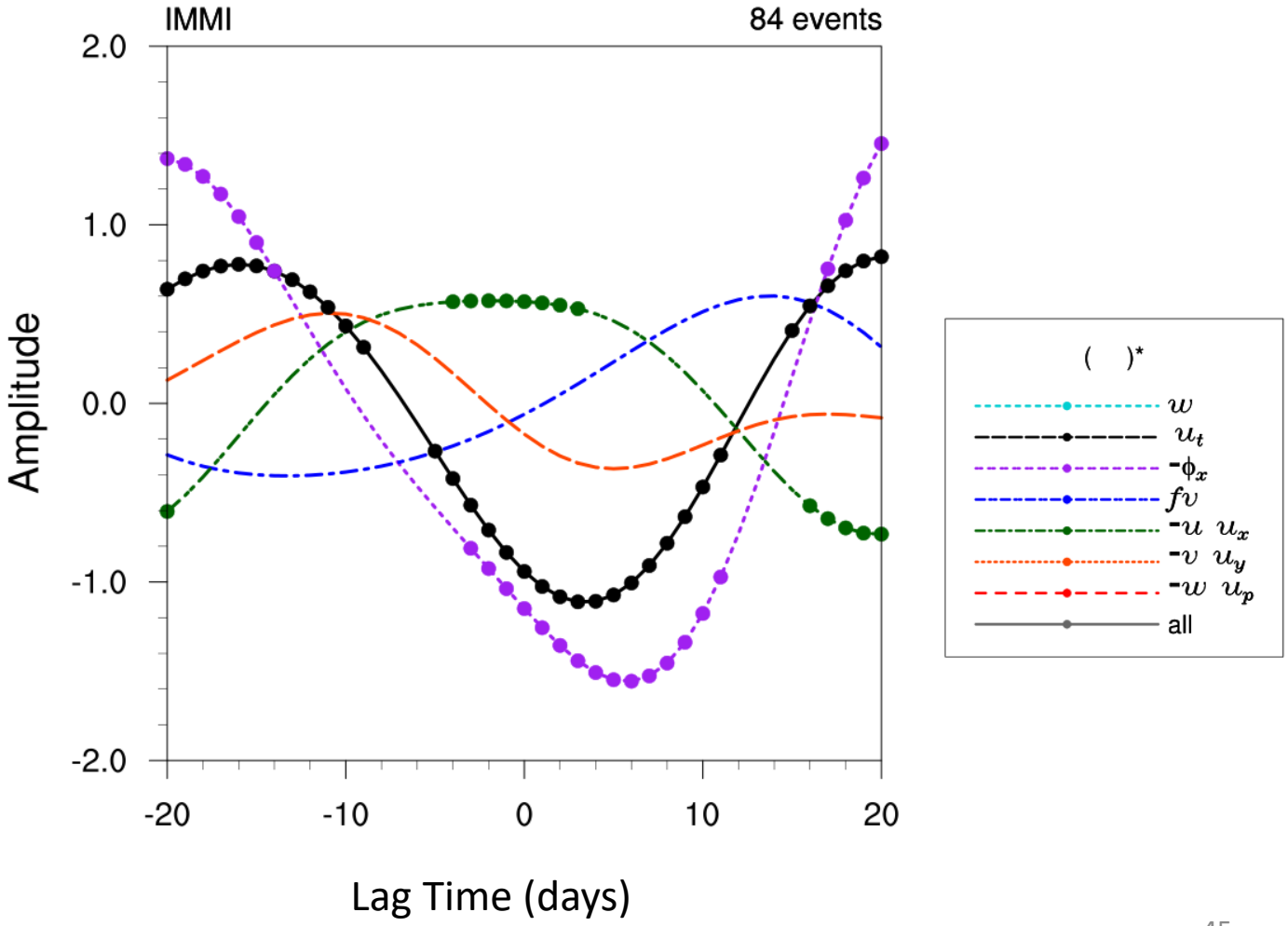

Budget in box from 50-60°E and 10°S-10°N

The vertical advection is not statistically significant for the average of all events

Budget in box from 50-60°E and 10°S-10°N

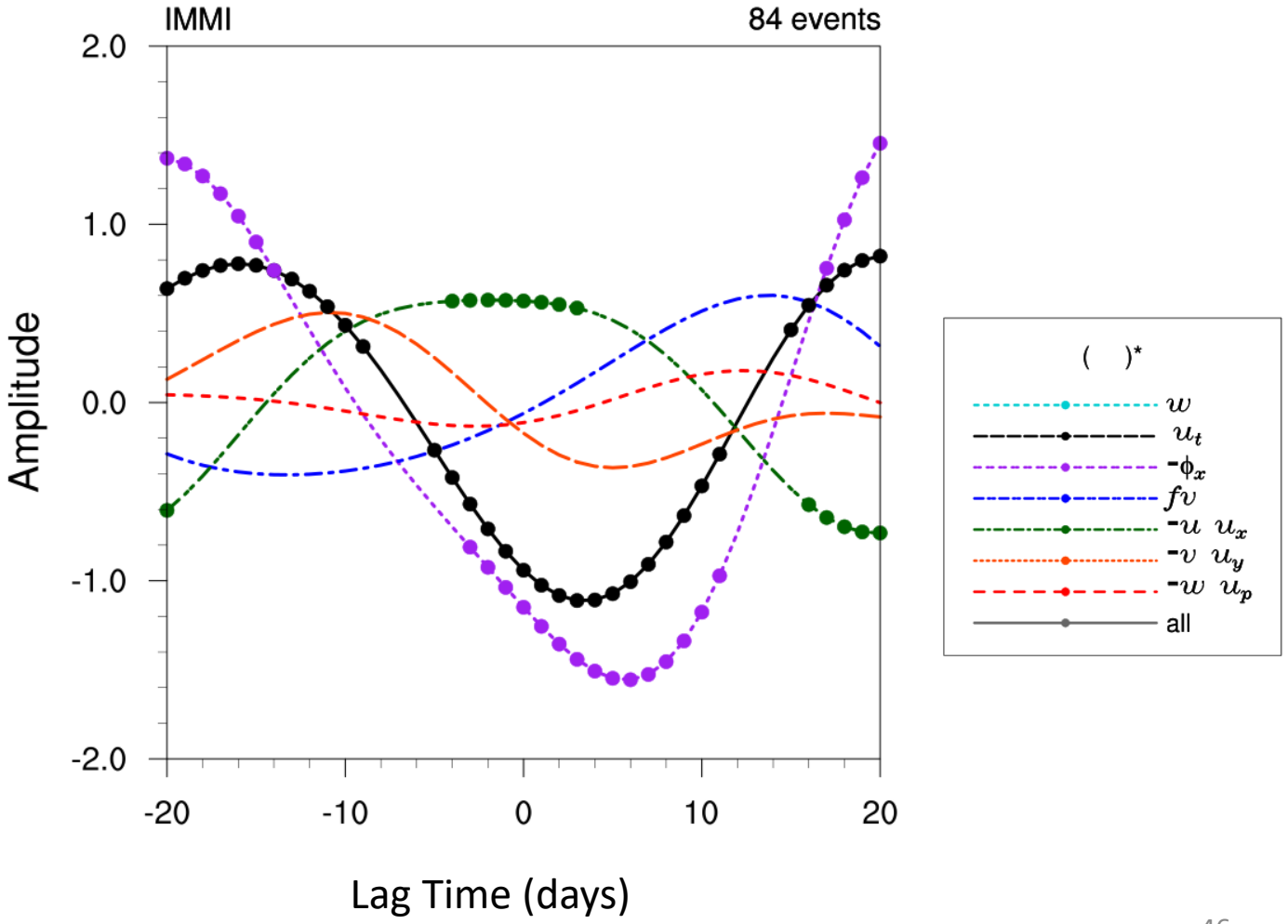

The sum of all terms is close to the value of the tendency -> residual is small

Budget
in box from
50-60°E and
10°S-10°N

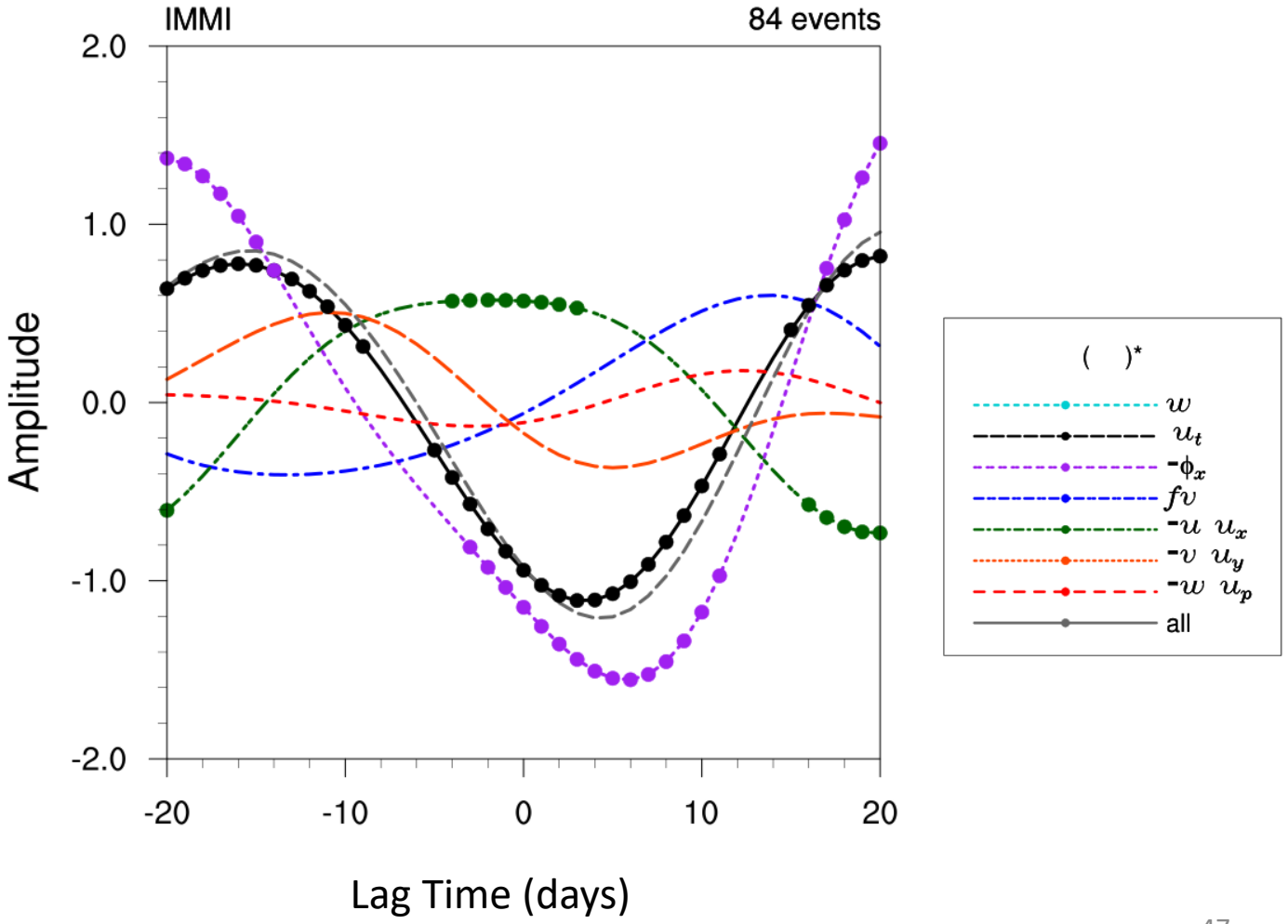

The zonal pressure gradient force term contributes most of the easterly acceleration at lag zero

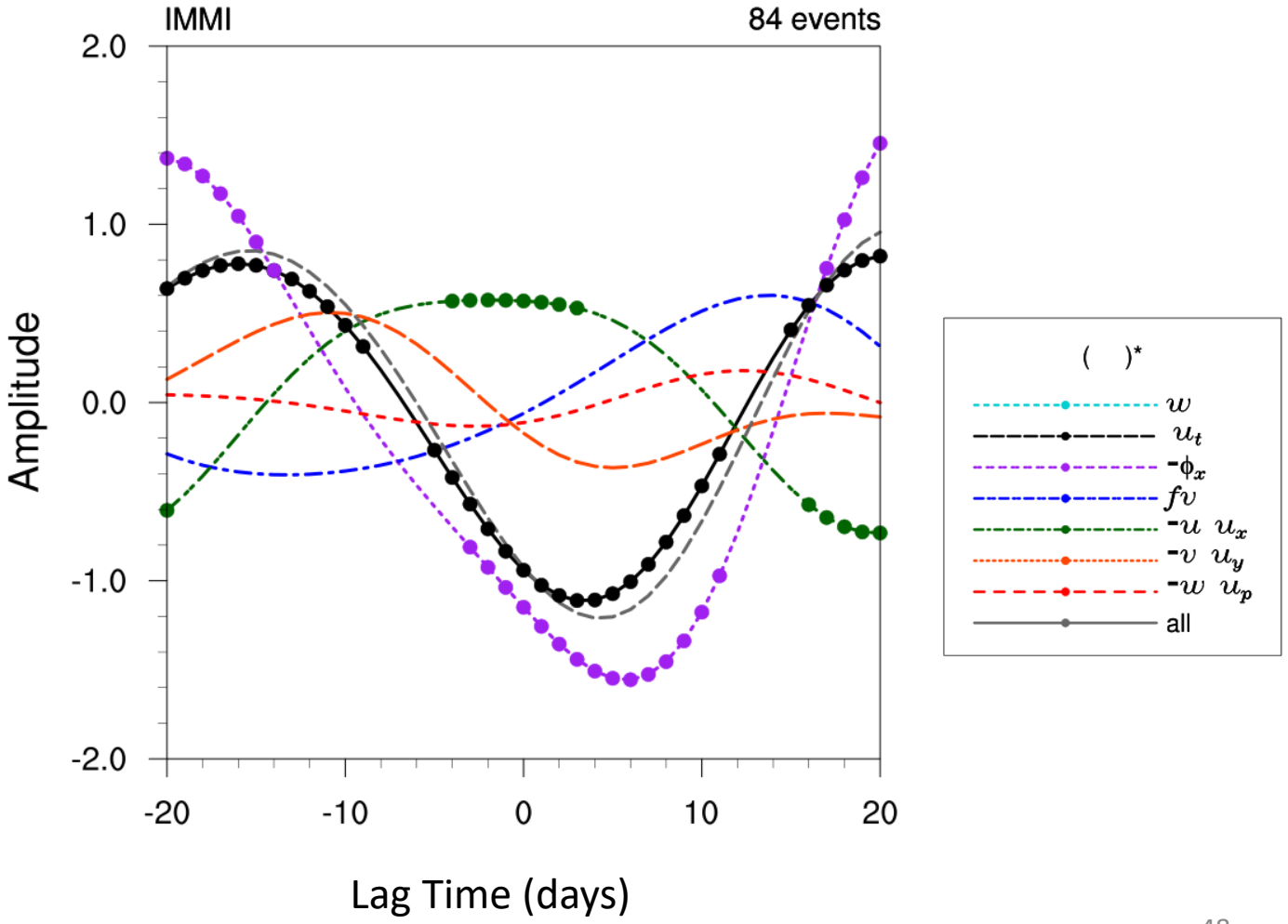

Budget in box from 50-60°E and 10°S-10°N

61/84
East

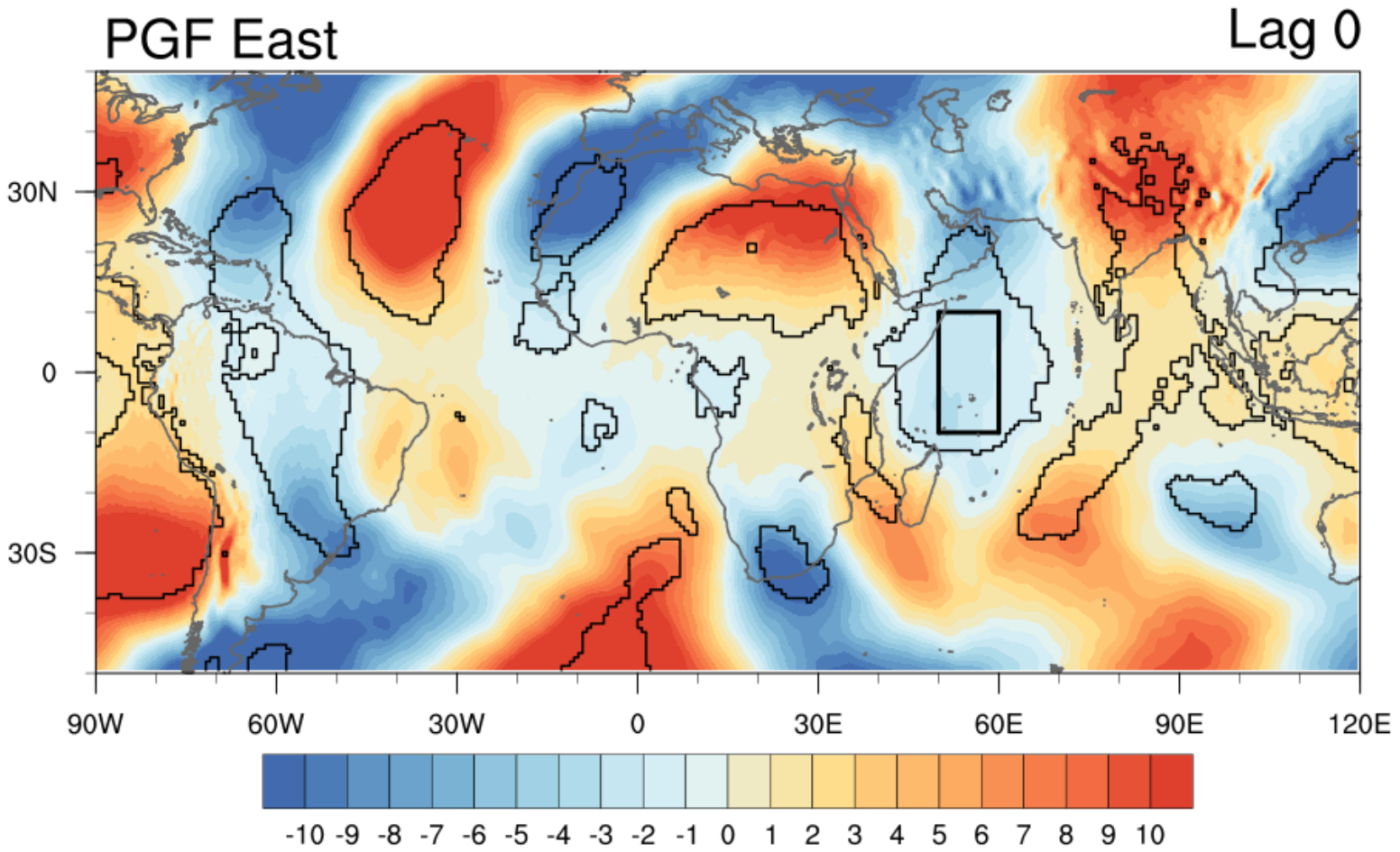

Focus only on events with PGF Easterly in the box

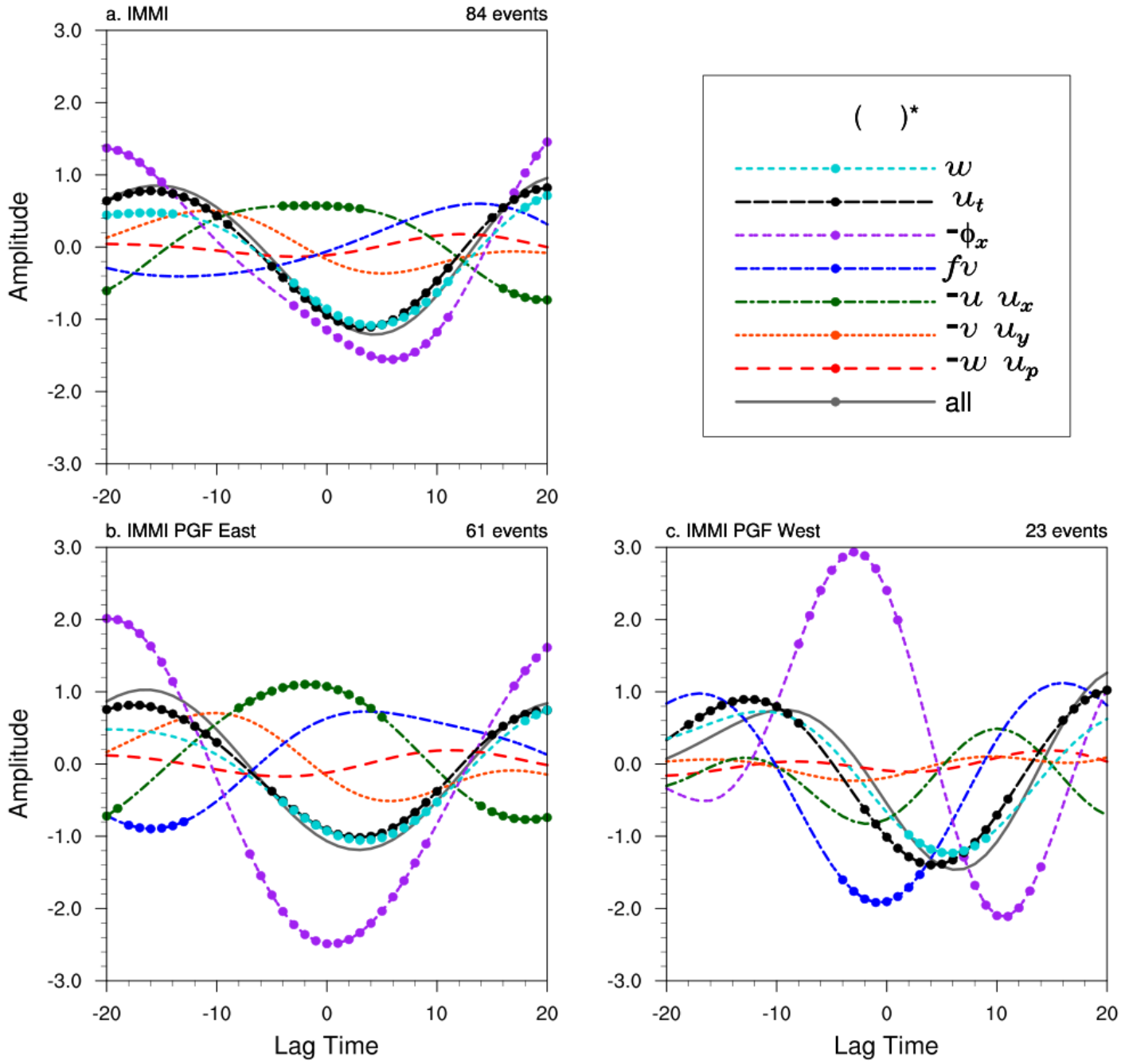
a. IMMI
84 events
b. IMMI PGF East
61 events
c. IMMI PGF West
23 events
Amplitude
Lag Time
( )*
w
u_t
$-\phi_x$
fv
$-u\ u_x$
$-v\ u_y$
$-w\ u_p$
all

The zonal pressure gradient force leads time tendency for PGF easterly cases

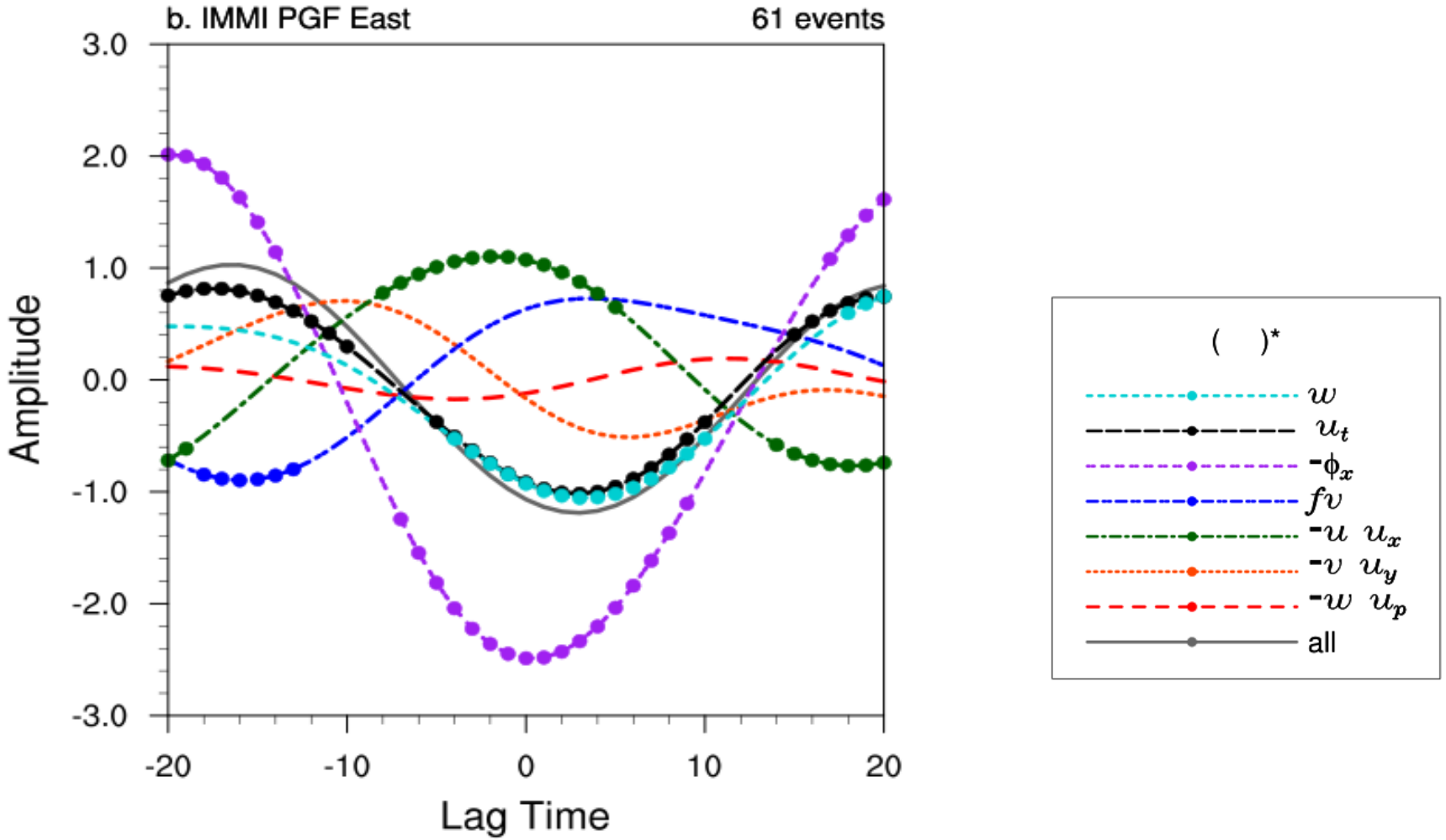

Dominance of PGF term could indicate Kelvin wave type dynamics, however…

PGF term does not circumnavigate equatorially

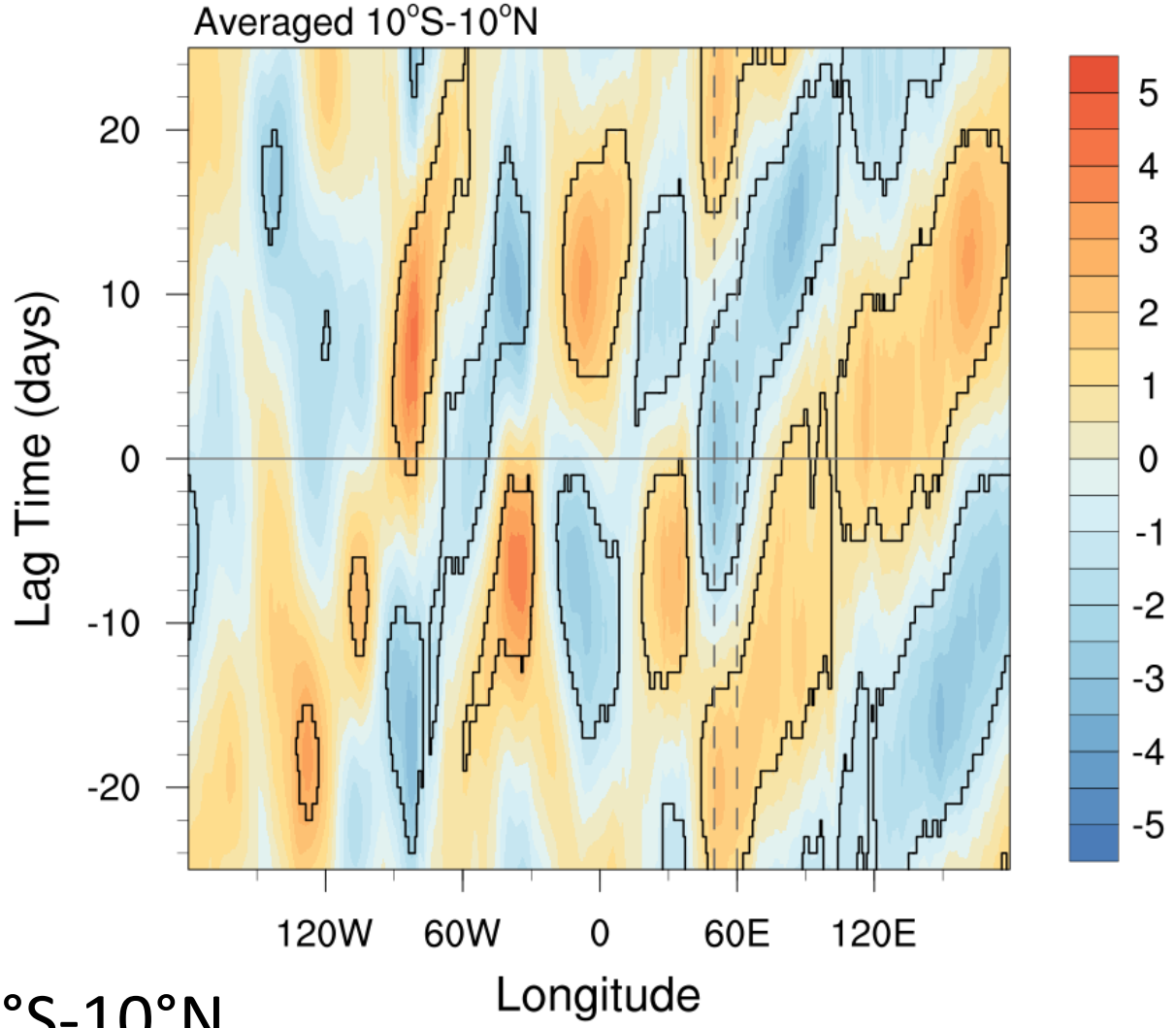

PGF: shading,

10°S-10°N

$\times 10^{-5}$ m s^{-2}

Easterly PGF moves equatorward from the extratropics between 50-60°E

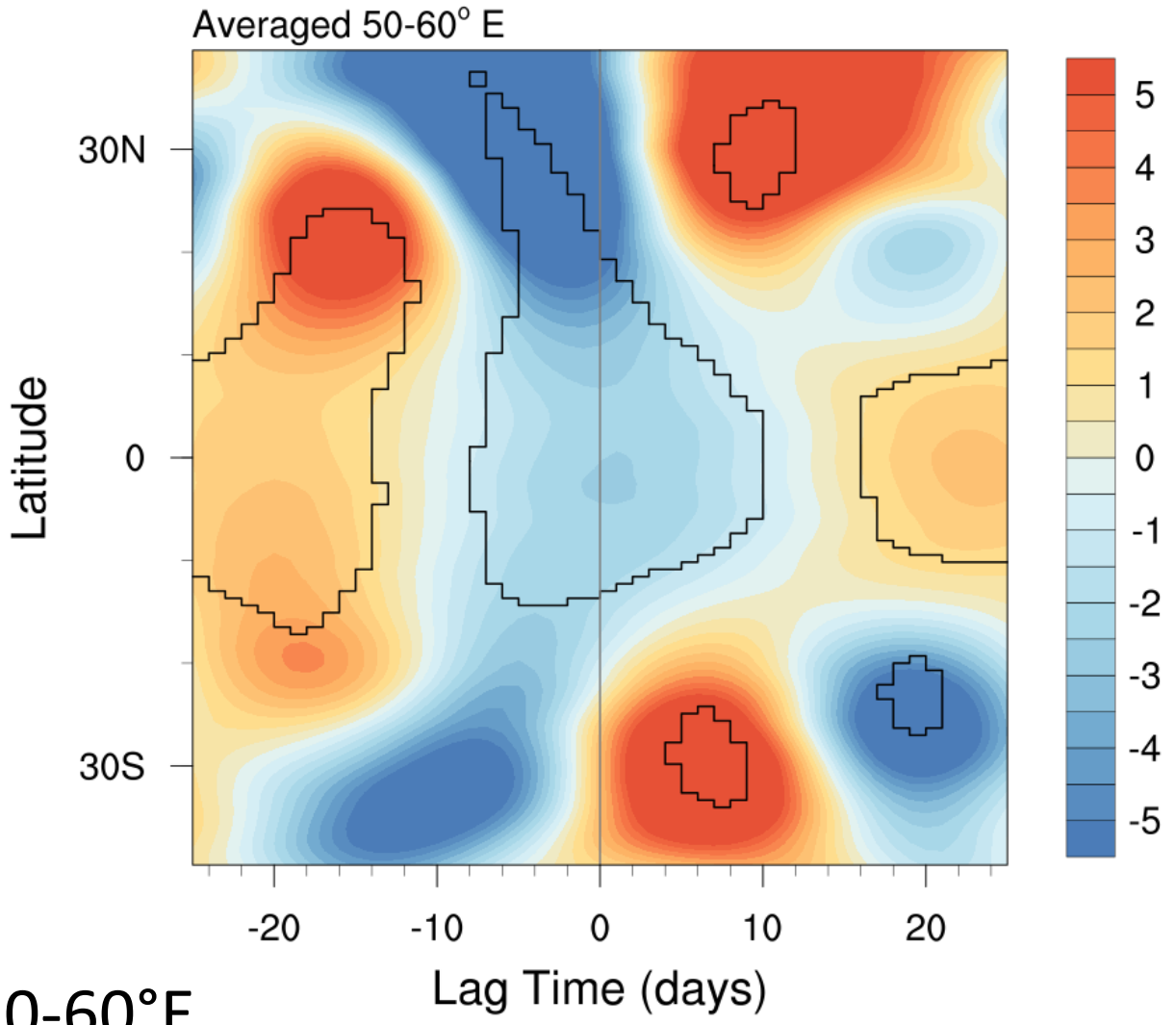

PGF: shading,

50-60°E

$\times 10^{-5}$ m s^{-2}

Easterly PGF moves equatorward from the extratropics between 50-60°E

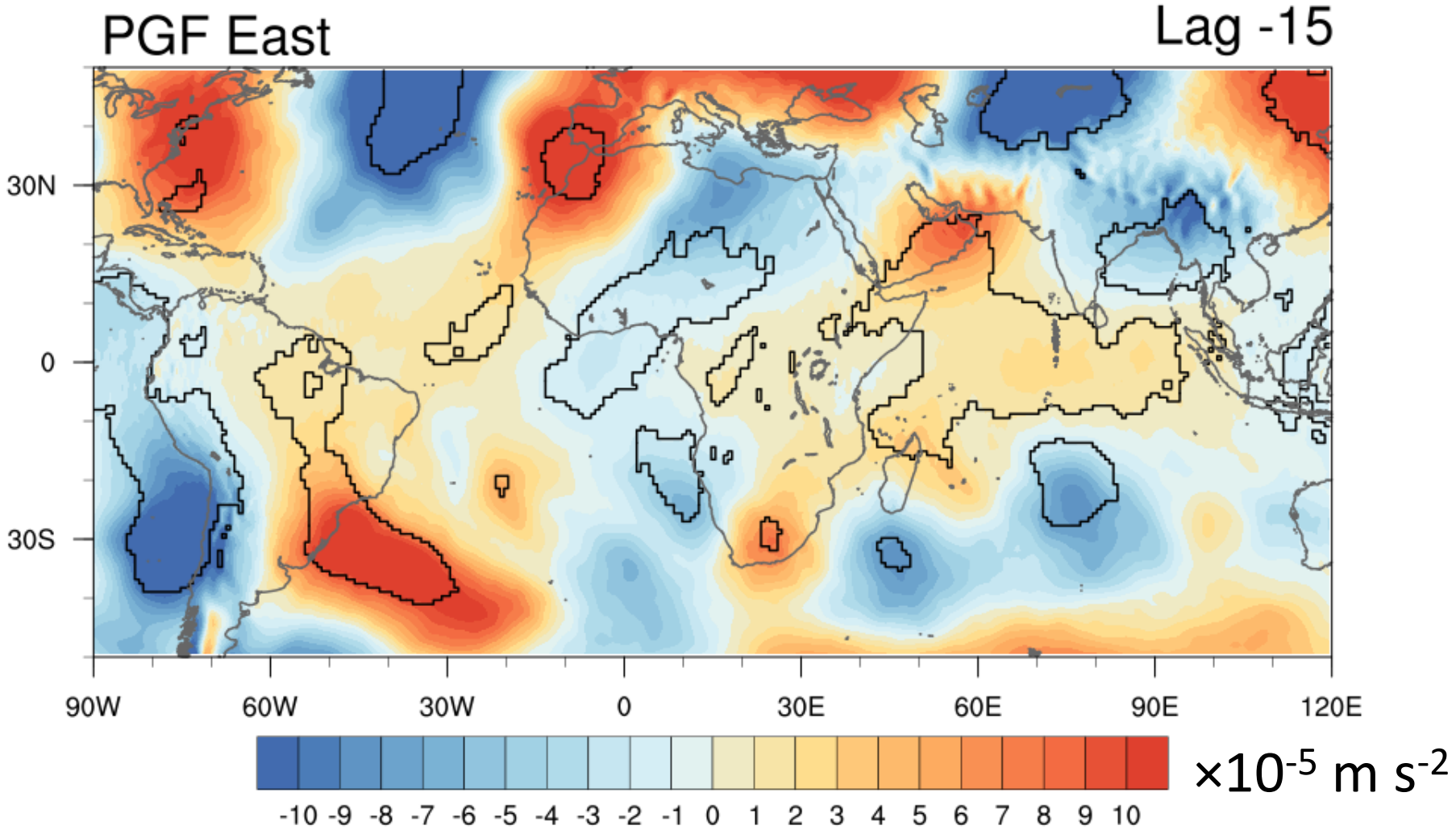

Easterly PGF moves equatorward from the extratropics between 50-60°E

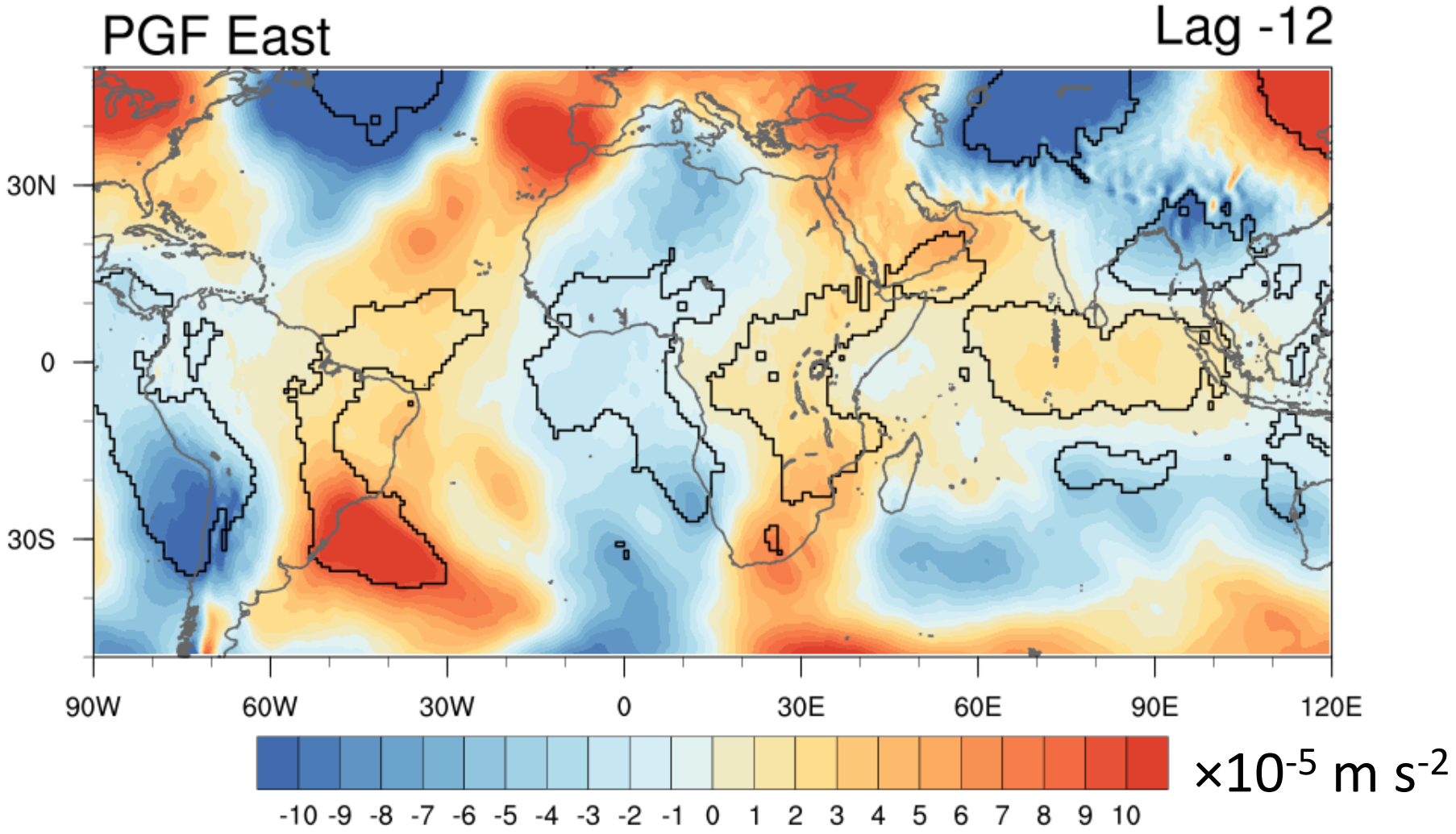

Easterly PGF moves equatorward from the extratropics between 50-60°E

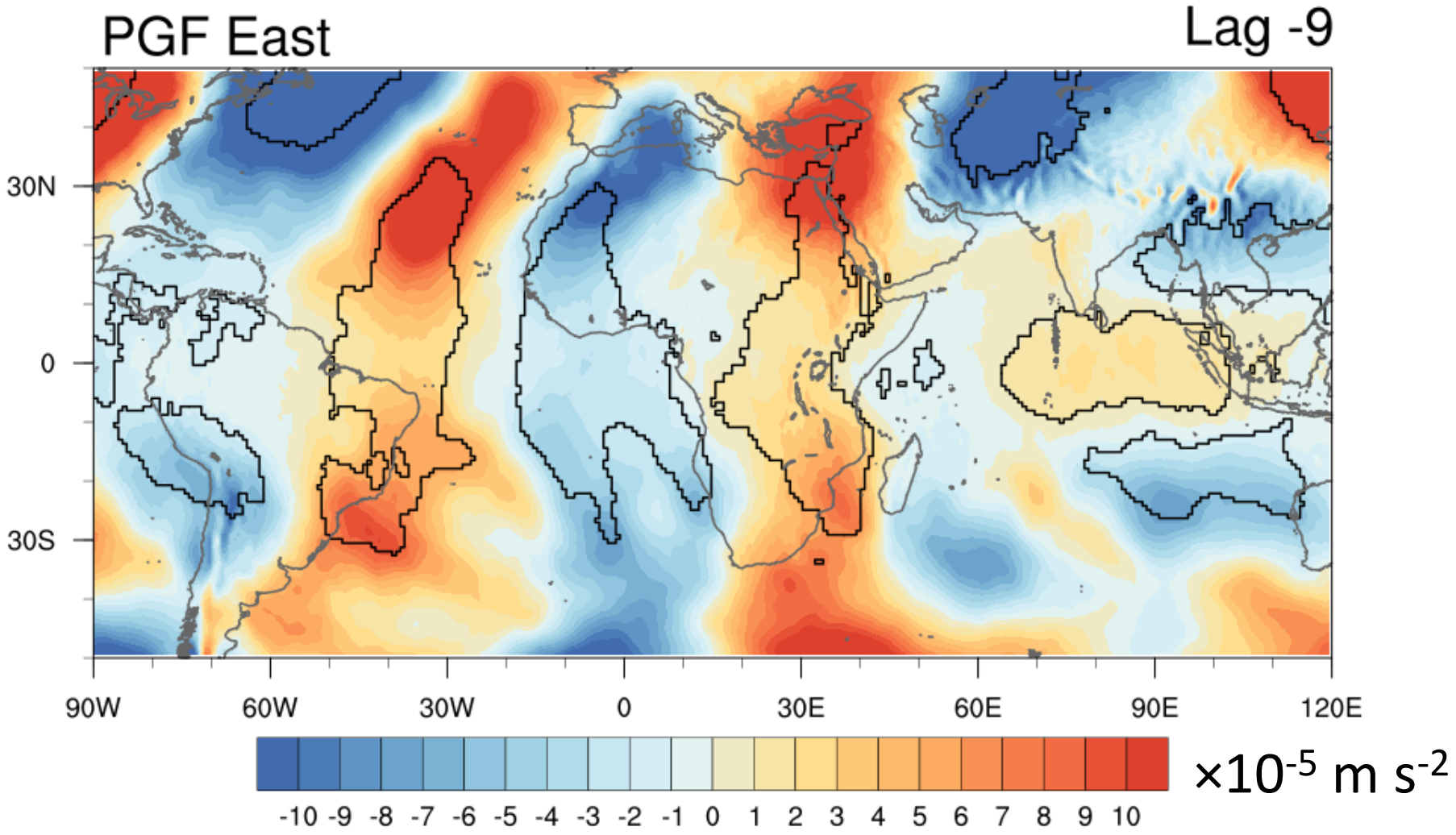

Easterly PGF moves equatorward from the extratropics between 50-60°E

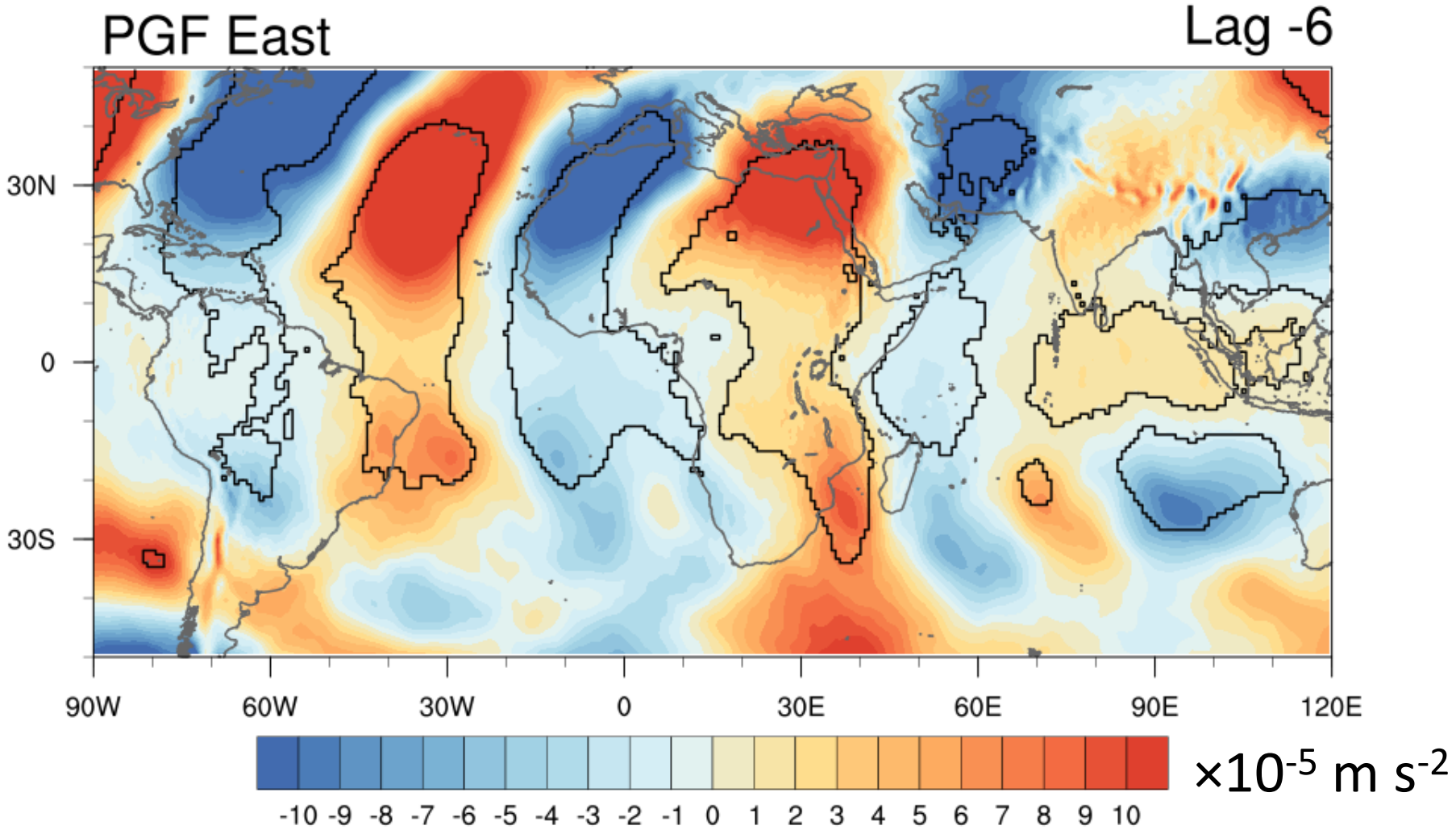

Easterly PGF moves equatorward from the extratropics between 50-60°E

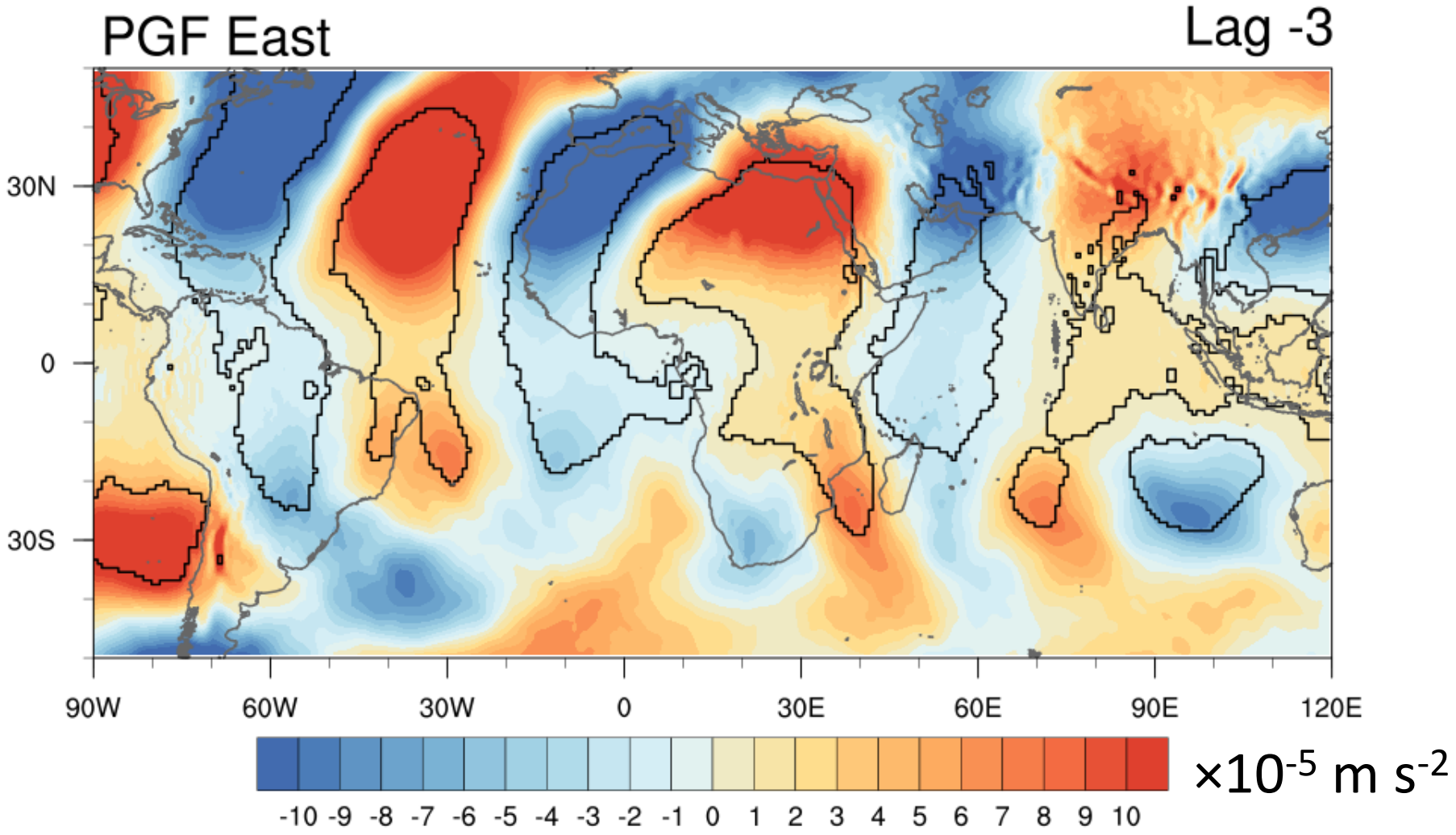

Easterly PGF moves equatorward from the extratropics between 50-60°E

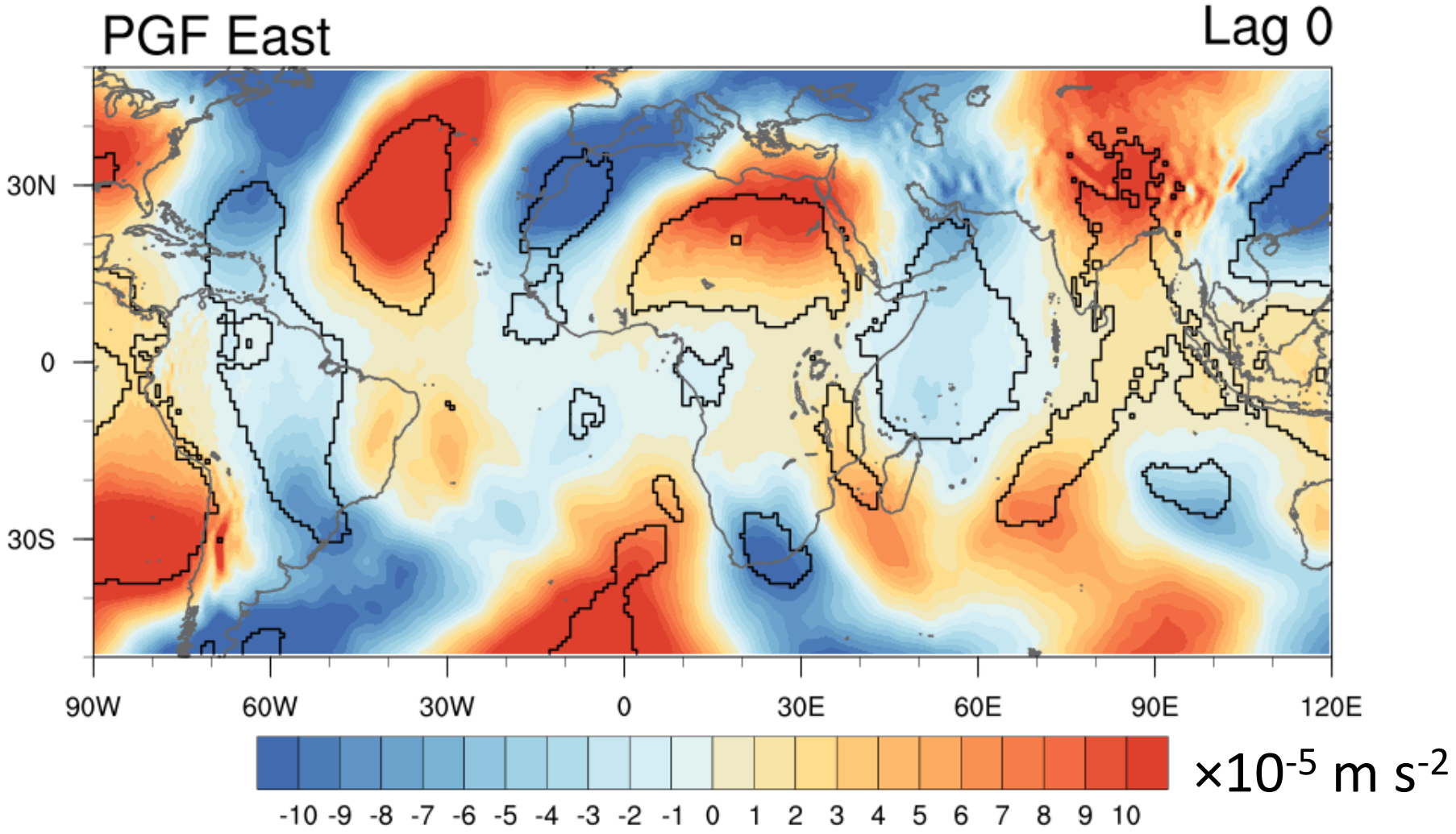

Easterly PGF moves equatorward from the extratropics between 50-60°E

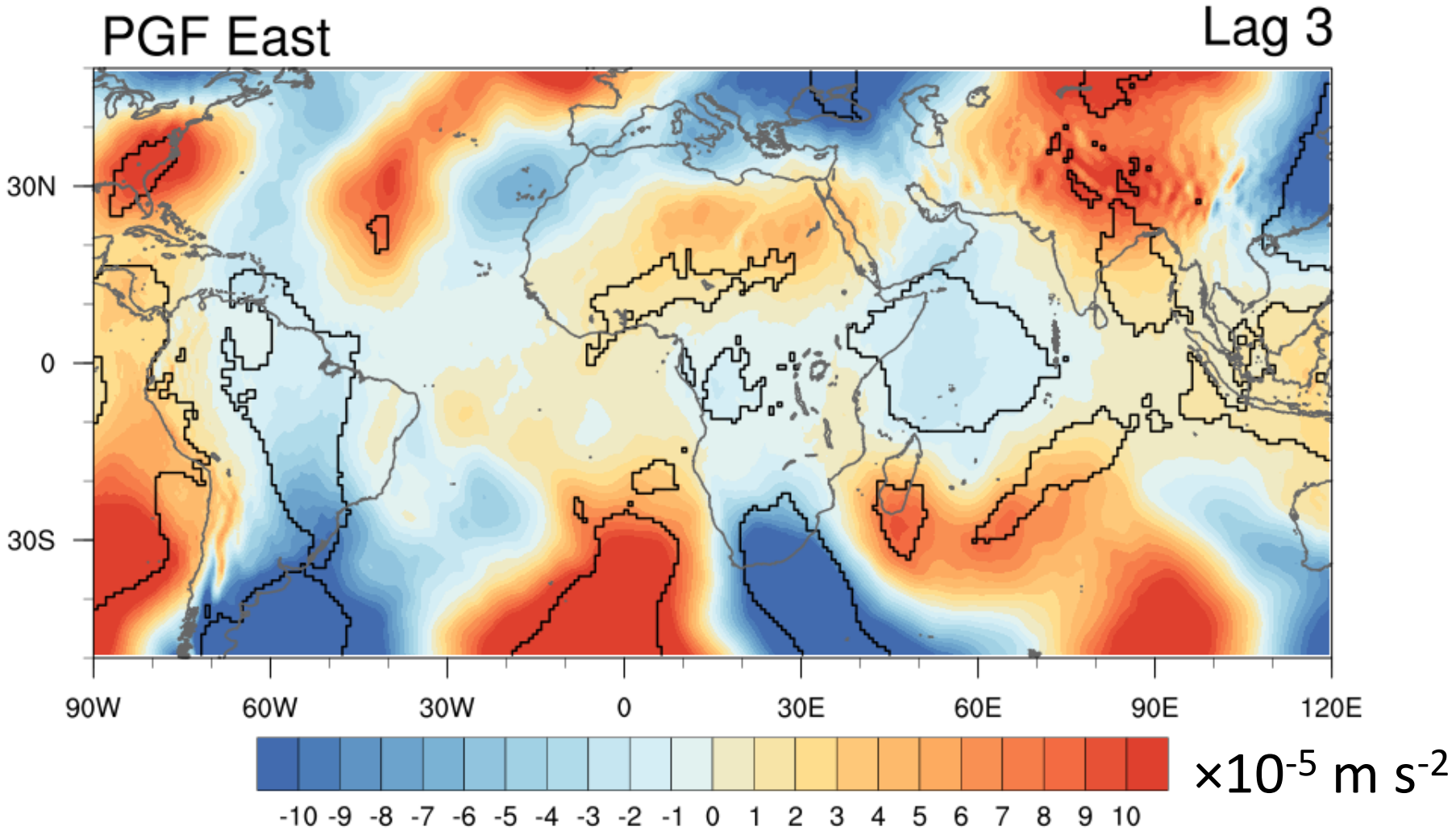

Easterly PGF moves equatorward from the extratropics between 50-60°E

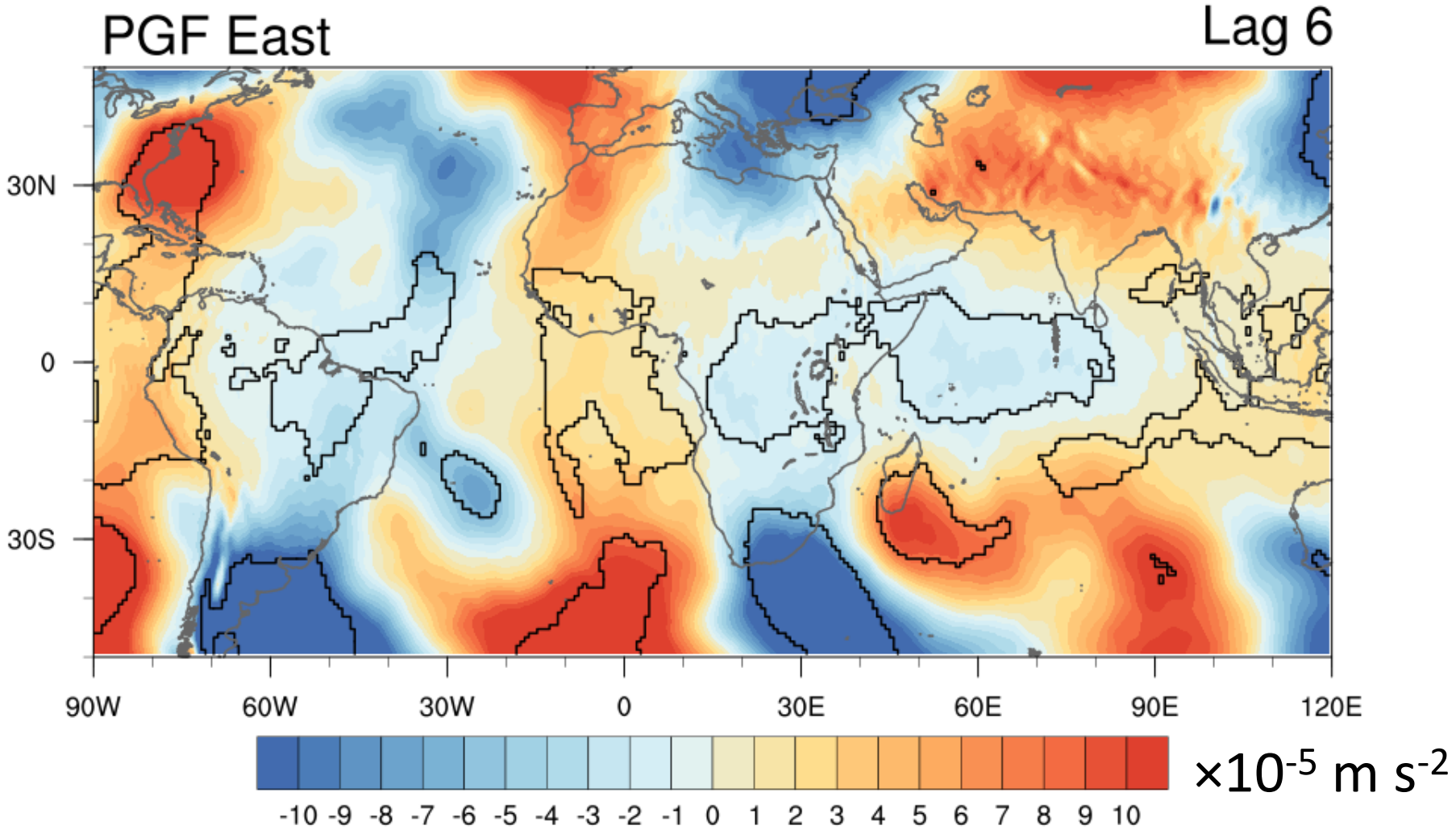

Easterly PGF moves equatorward from the extratropics between 50-60°E

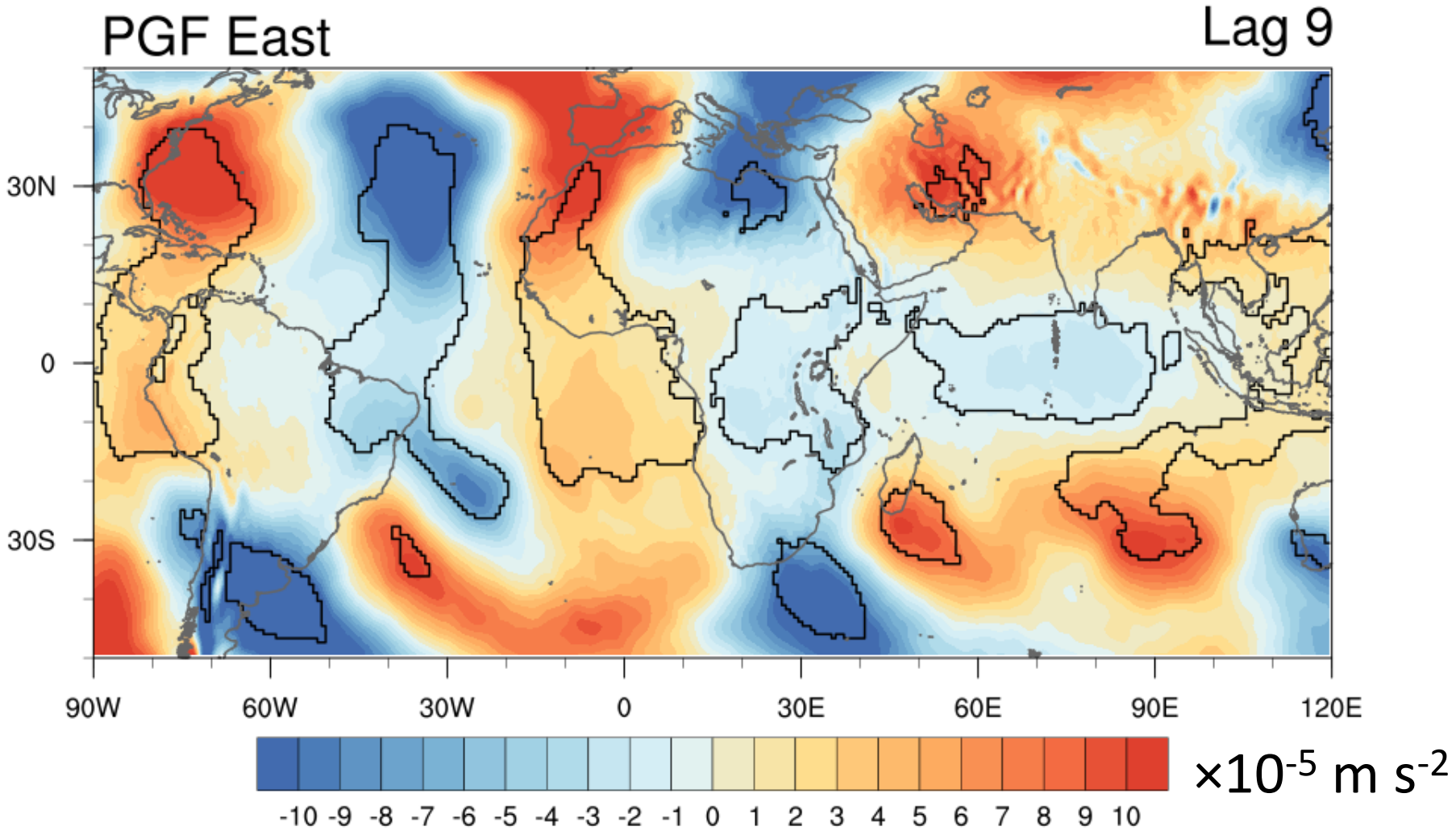

Negative GH anomalies move equatorward 35-45° E

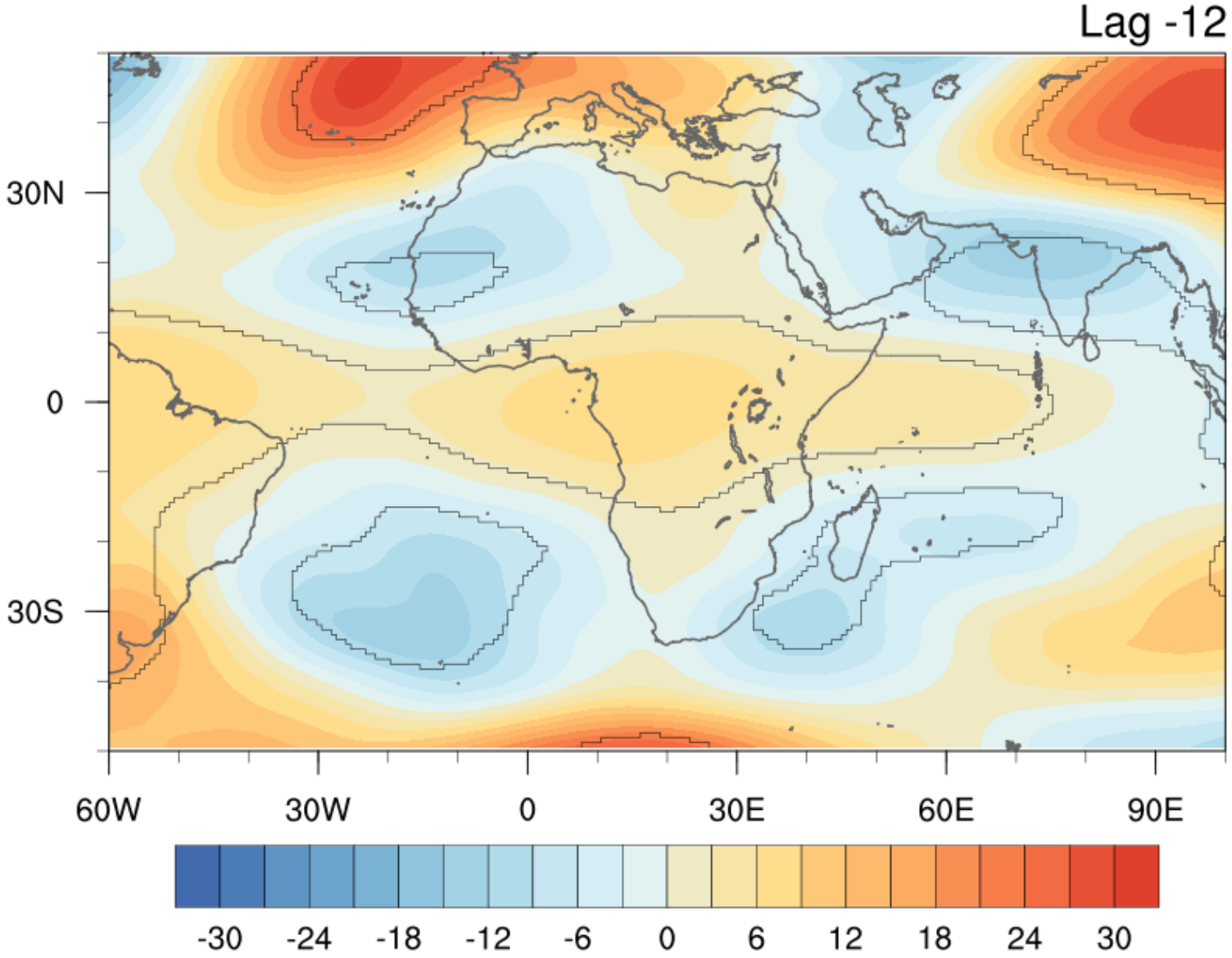

Negative GH anomalies move equatorward 35-45° E

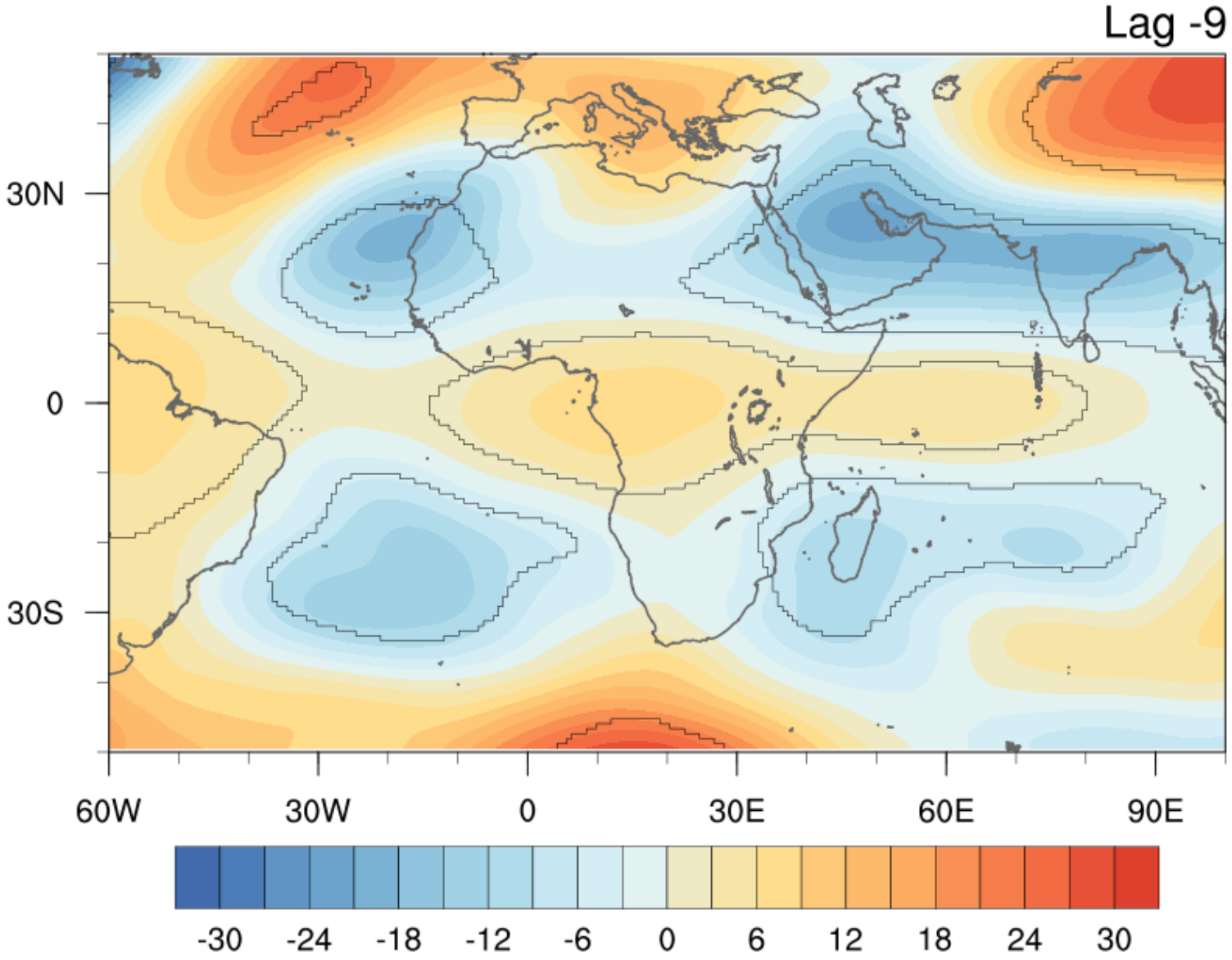

Negative GH anomalies move equatorward 35-45° E

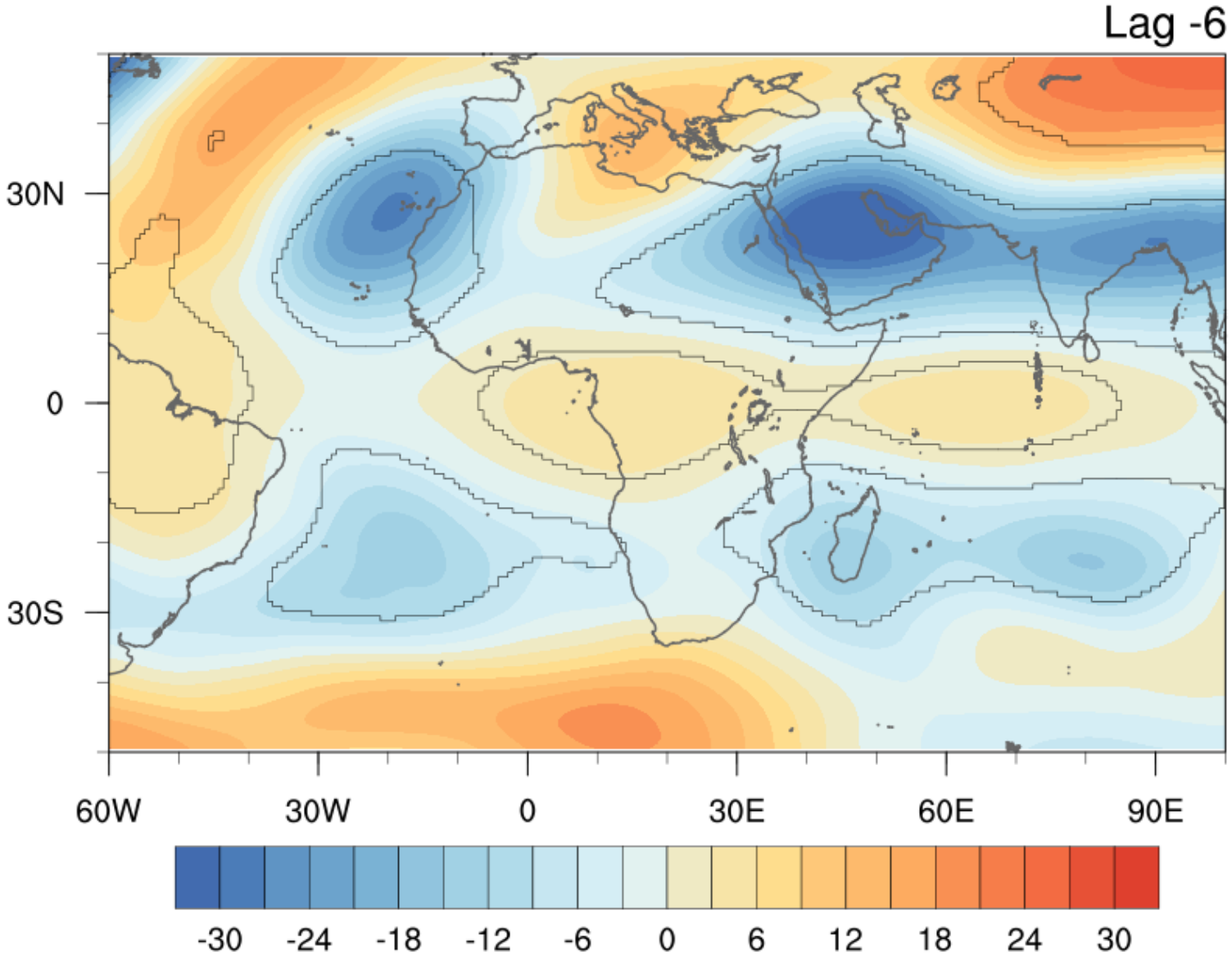

Negative GH anomalies move equatorward 35-45° E

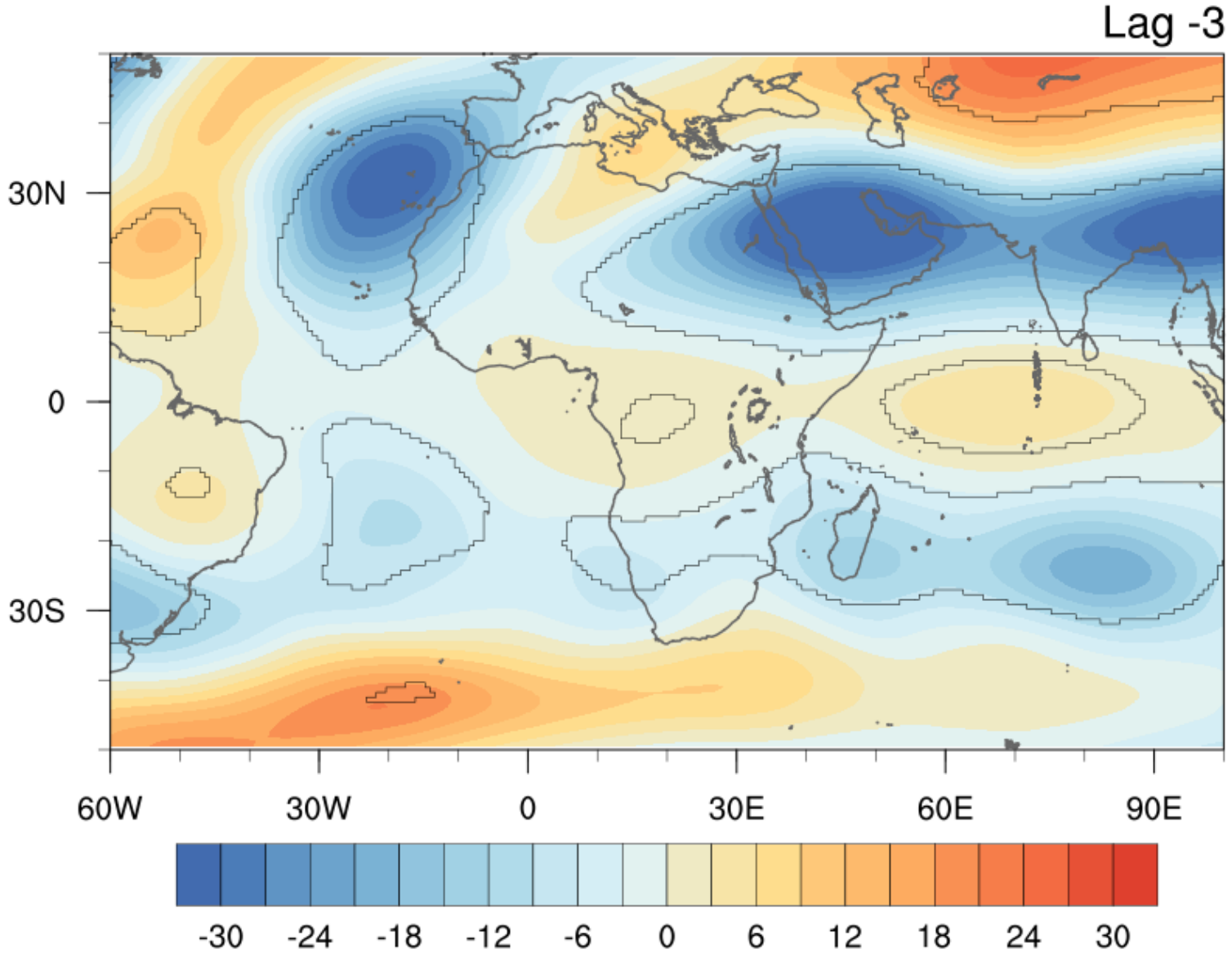

Negative GH anomalies move equatorward 35-45° E

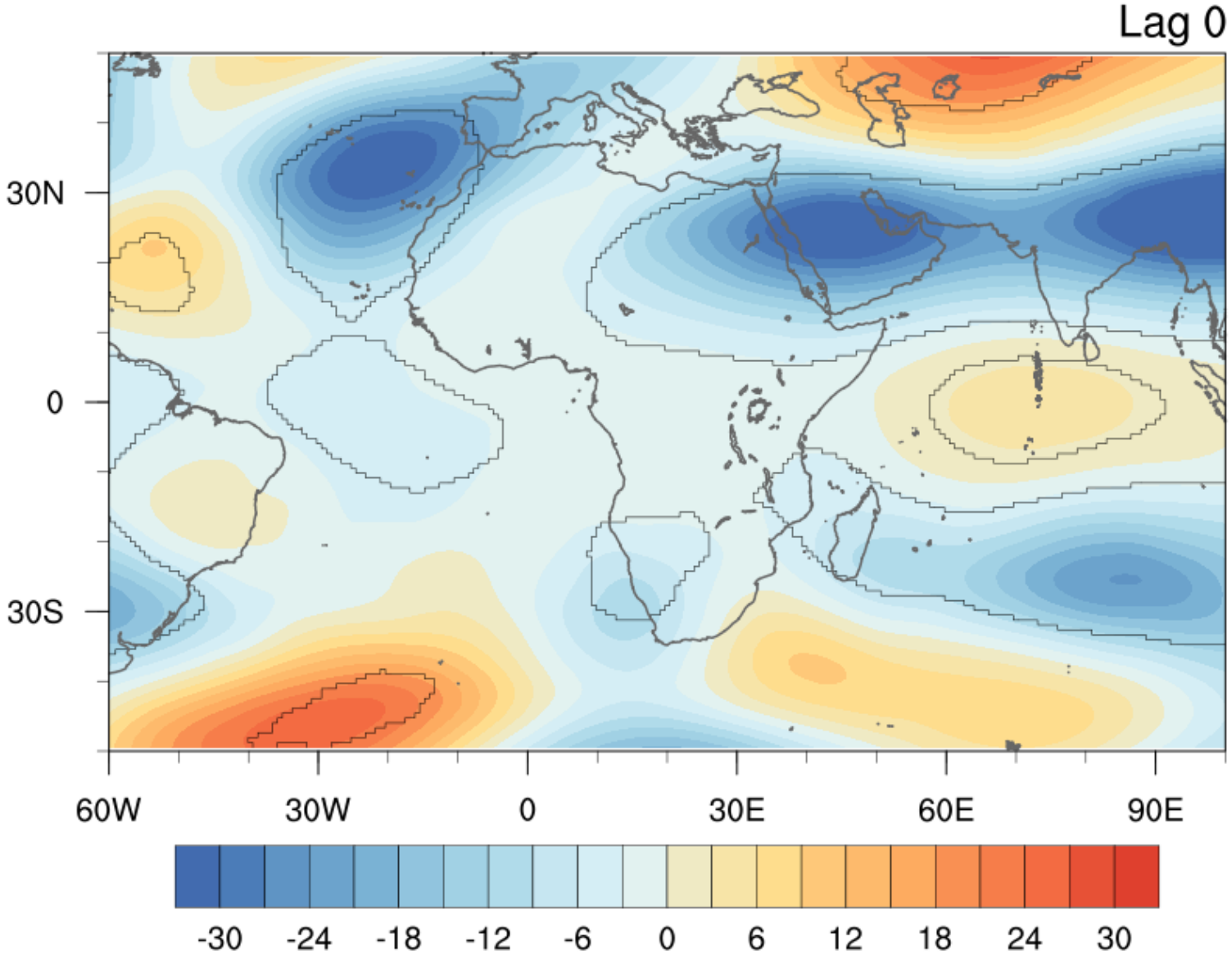

Negative GH anomalies move equatorward 35-45° E

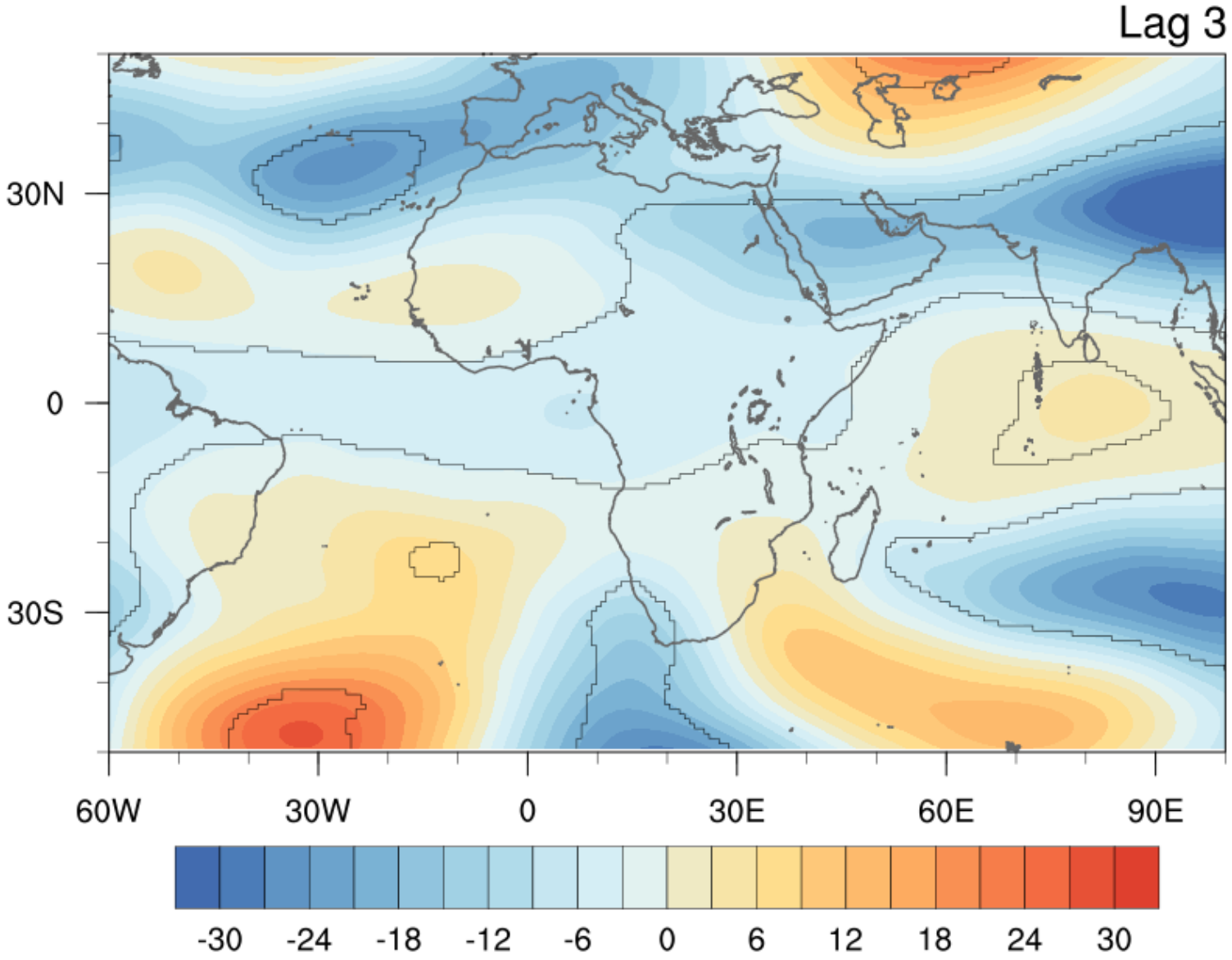

Negative GH anomalies move equatorward 35-45° E

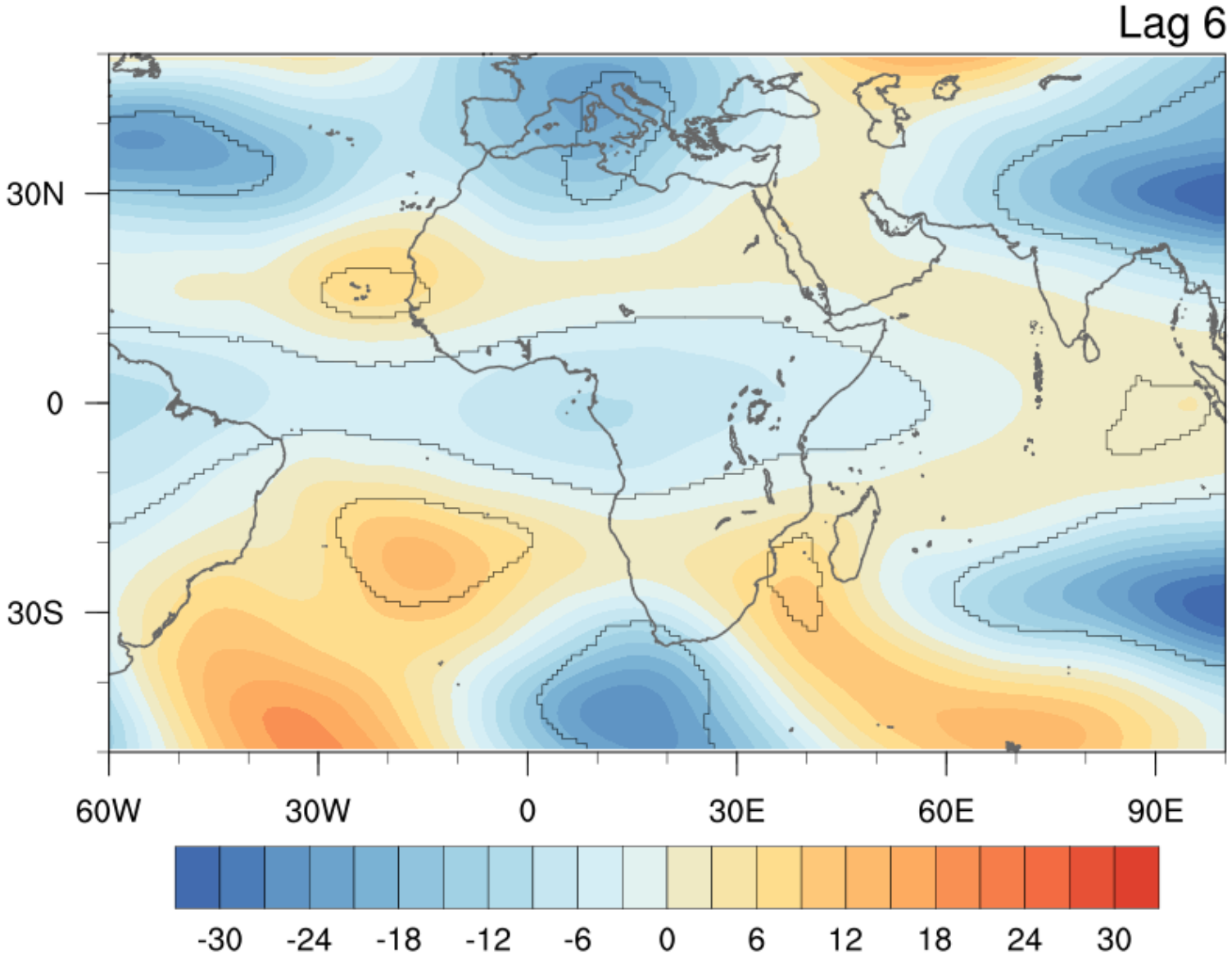

GH does not circumnavigate equatorially

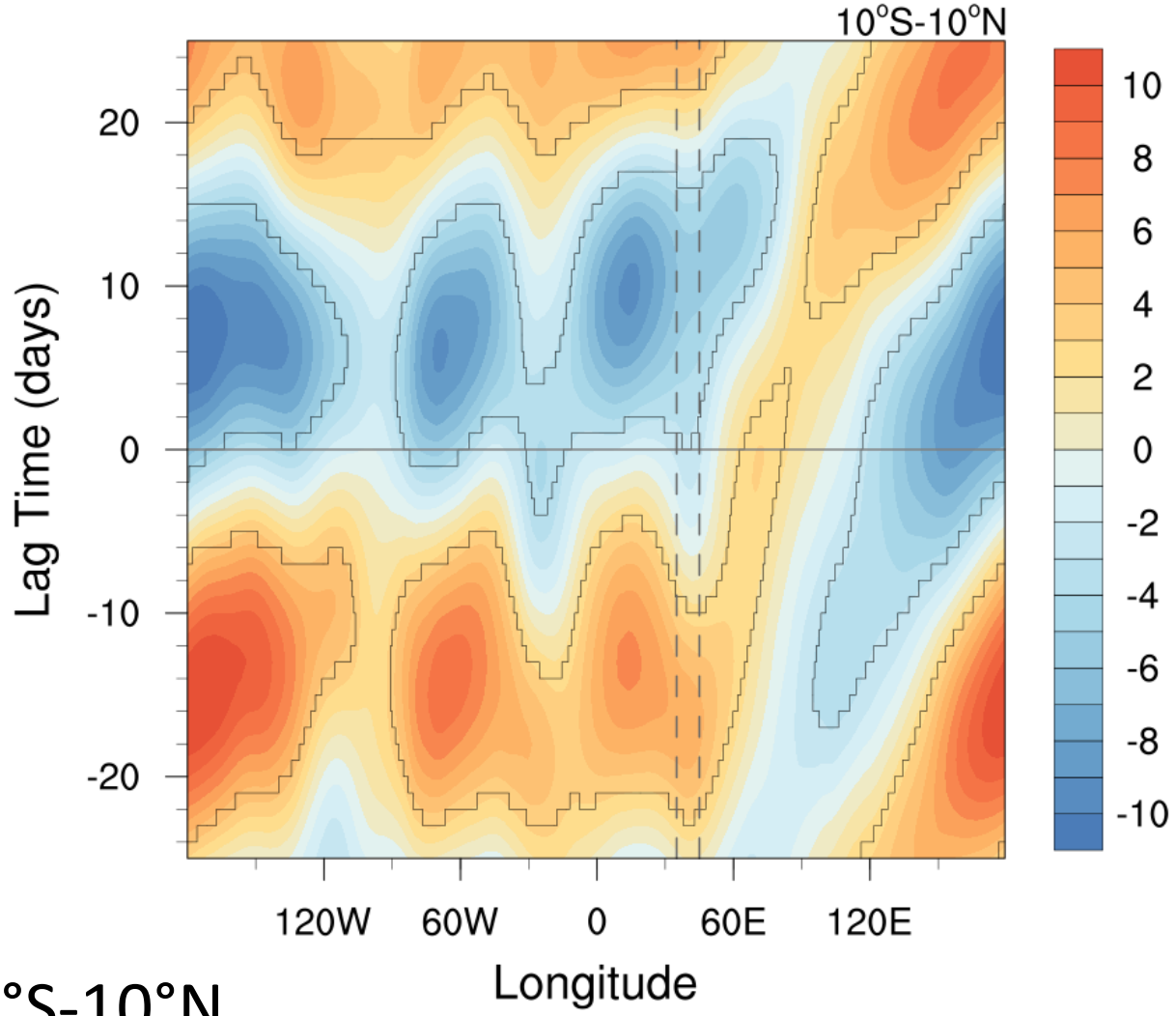

GH: shading

10°S-10°N

Negative GH anom moves equatorward from the extratropics between 35-45°E

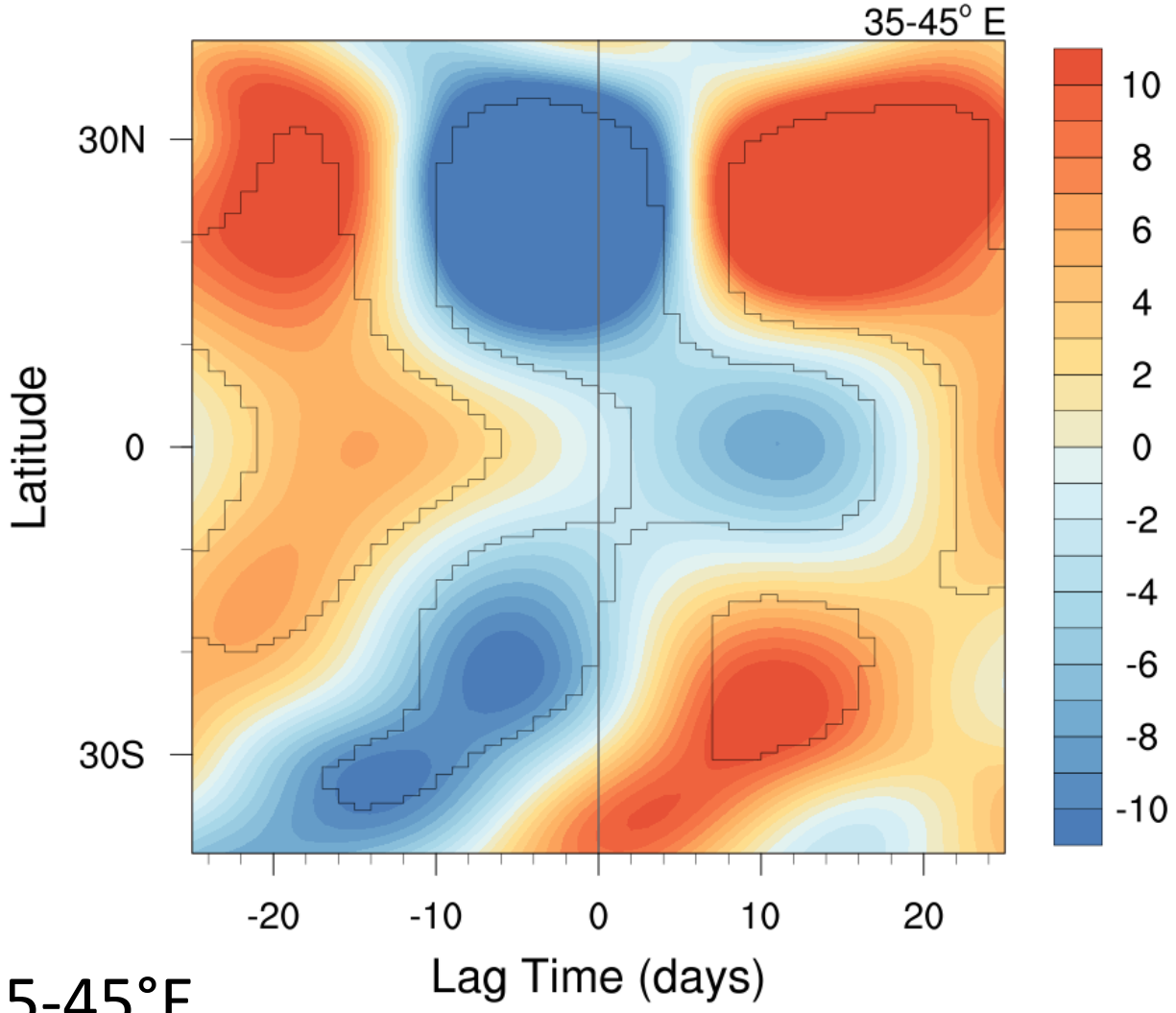

GH: shading

35-45°E

Gahtan, J. and P. Roundy, 2019: Extratropical Influence on 200-hPa Easterly Acceleration over the Western Indian Ocean Preceding Madden–Julian Oscillation Convective Onset. *J. Atmos. Sci.*, **76**, 265–284, https://doi.org/10.1175/JAS-D-18-0069.1

Next step is to identify meridionally moving features separately from the MJO

To identify meridionally propagating features separately from the MJO we use meridional-temporal wavelets

- Real portion of the Morlet wavelet (Roundy 2018)
- Wavelets initially centered in the subtropics at 20°N or 20°S

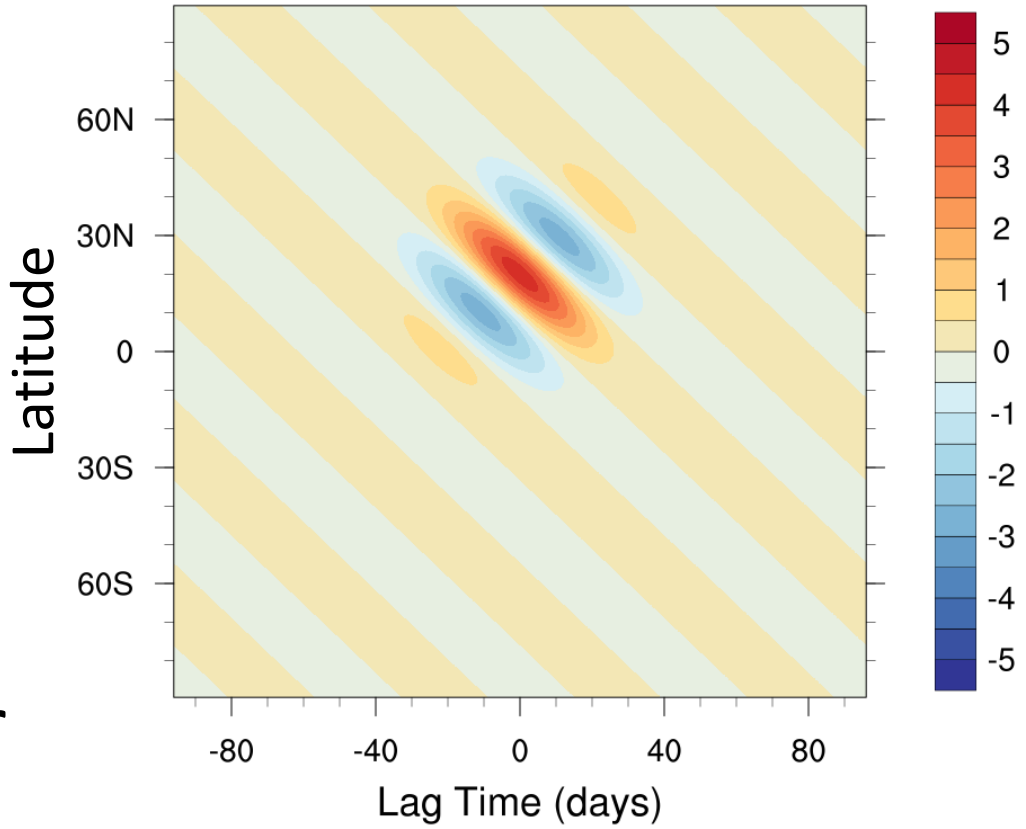

wavelet structure at 20° N for equatorward scale of 30° latitude and period of 48 days

To identify meridionally propagating features separately from the MJO we use meridional-temporal wavelets

- Find transform by multiplying with 200hPa normalized geopotential height anomalies from 35-45°E
- Power is given by the wavelet transform squared

More overall power is equatorward than poleward in this region, yet this power is centered at shorter periods

20° N

20° S

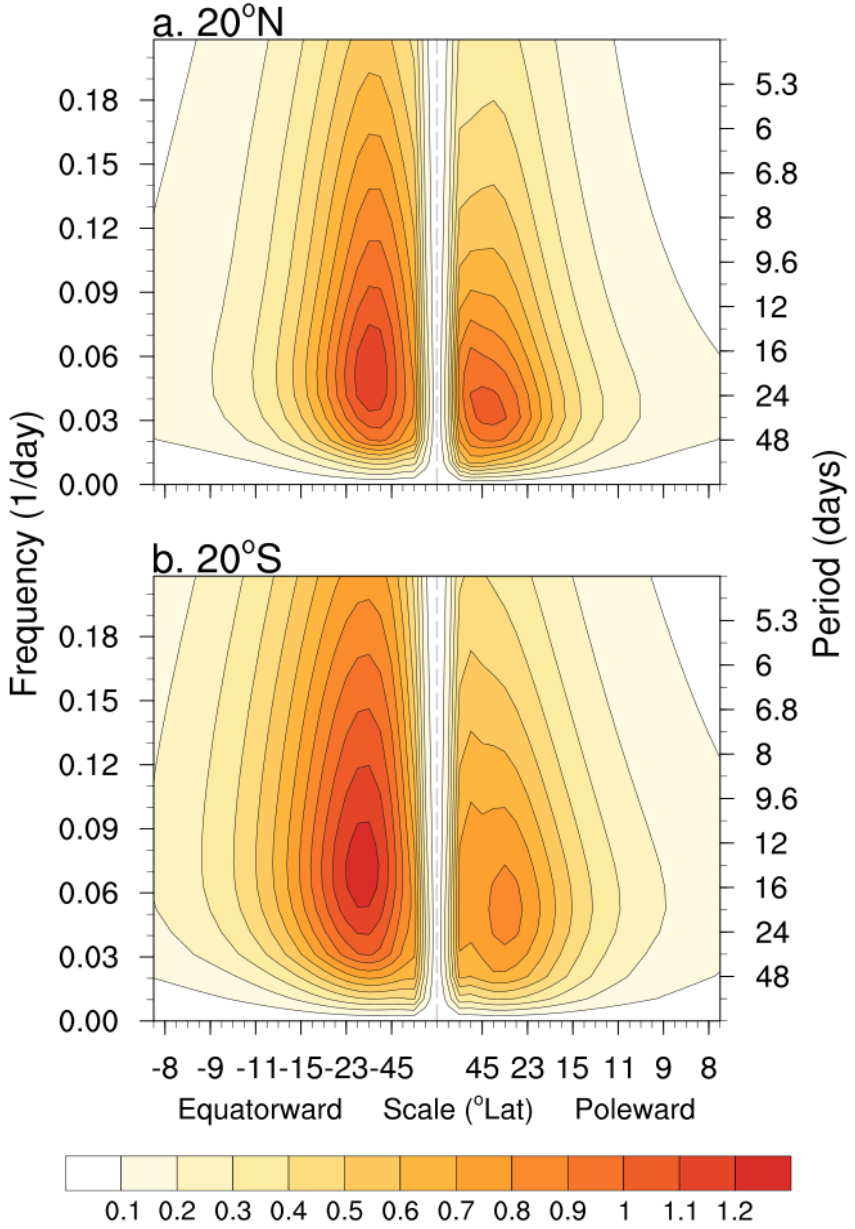

November-April
35-45°E

Power is increased for equatorward intraseasonal waves when amplitudes of MJO indices are greater than 1

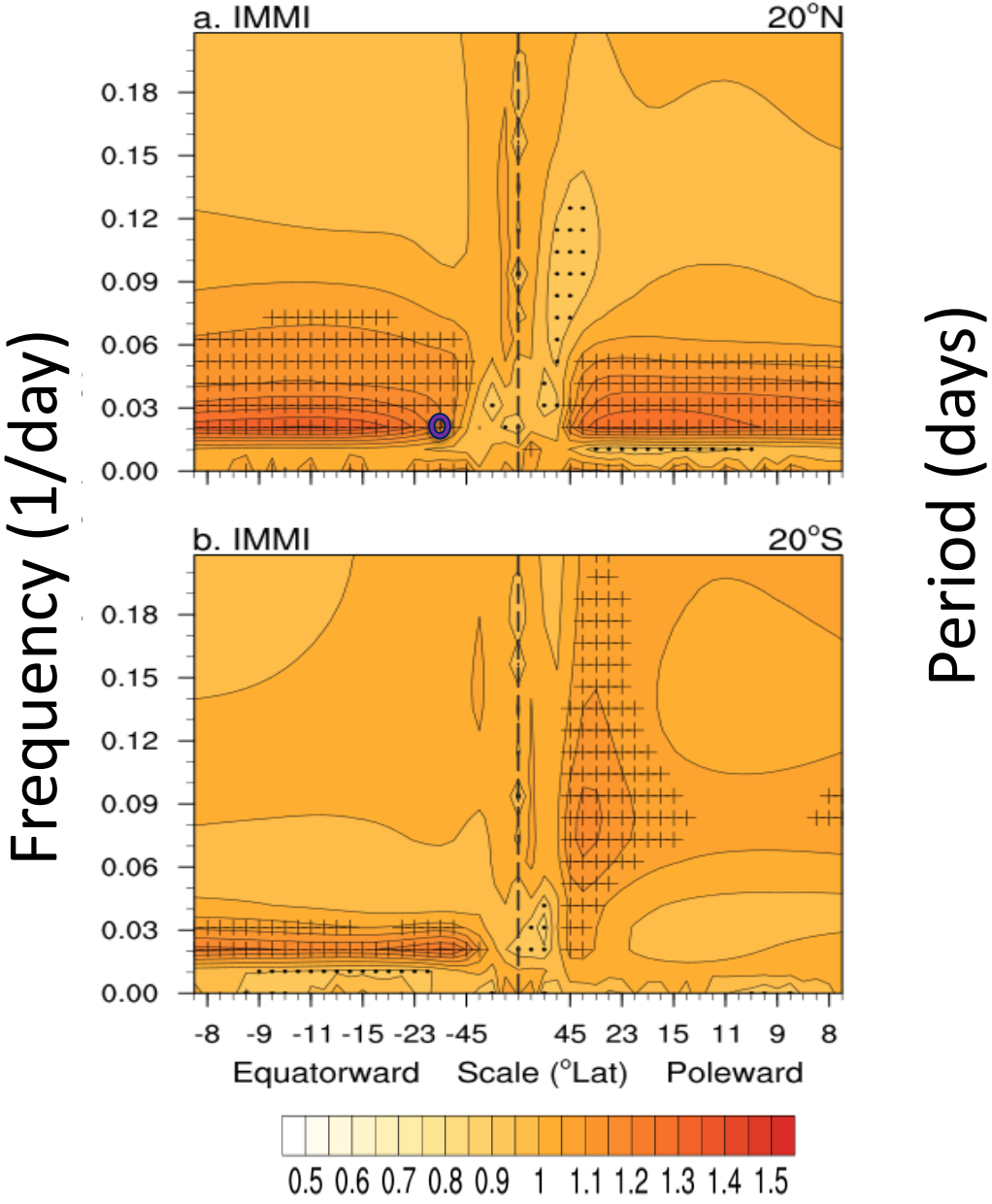

- NH equatorward scale of 30° latitude and period of 48 days

Regressions show equatorward moving negative GH anomalies from 35-45°E with easterly acceleration from the zonal PGF between 50-60°E

GH

PGF

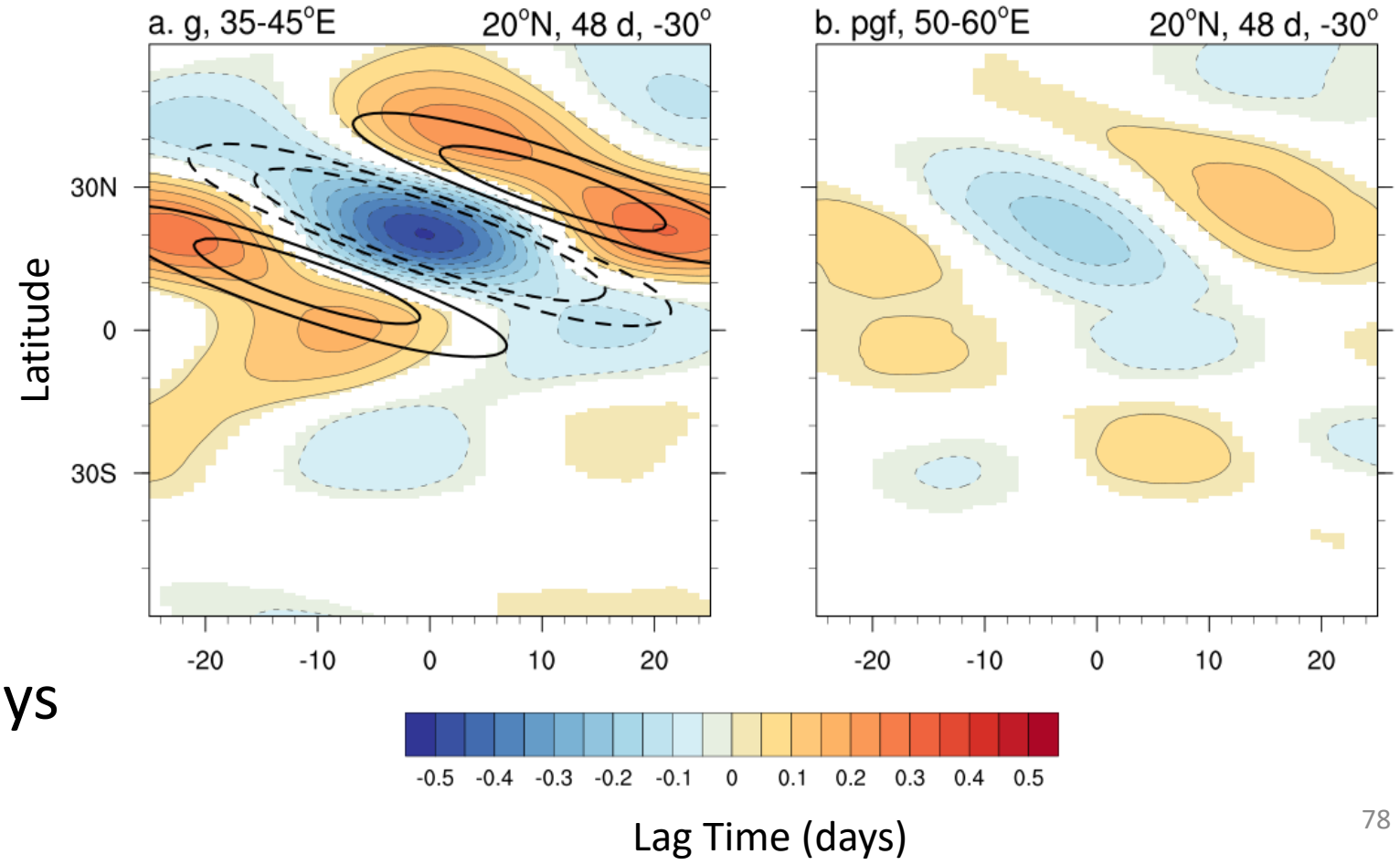

20° N
48 days
-30°

Regressions of equatorial OLR against the wavelet transforms are similar to RMM1, but with less amplitude

RMM1

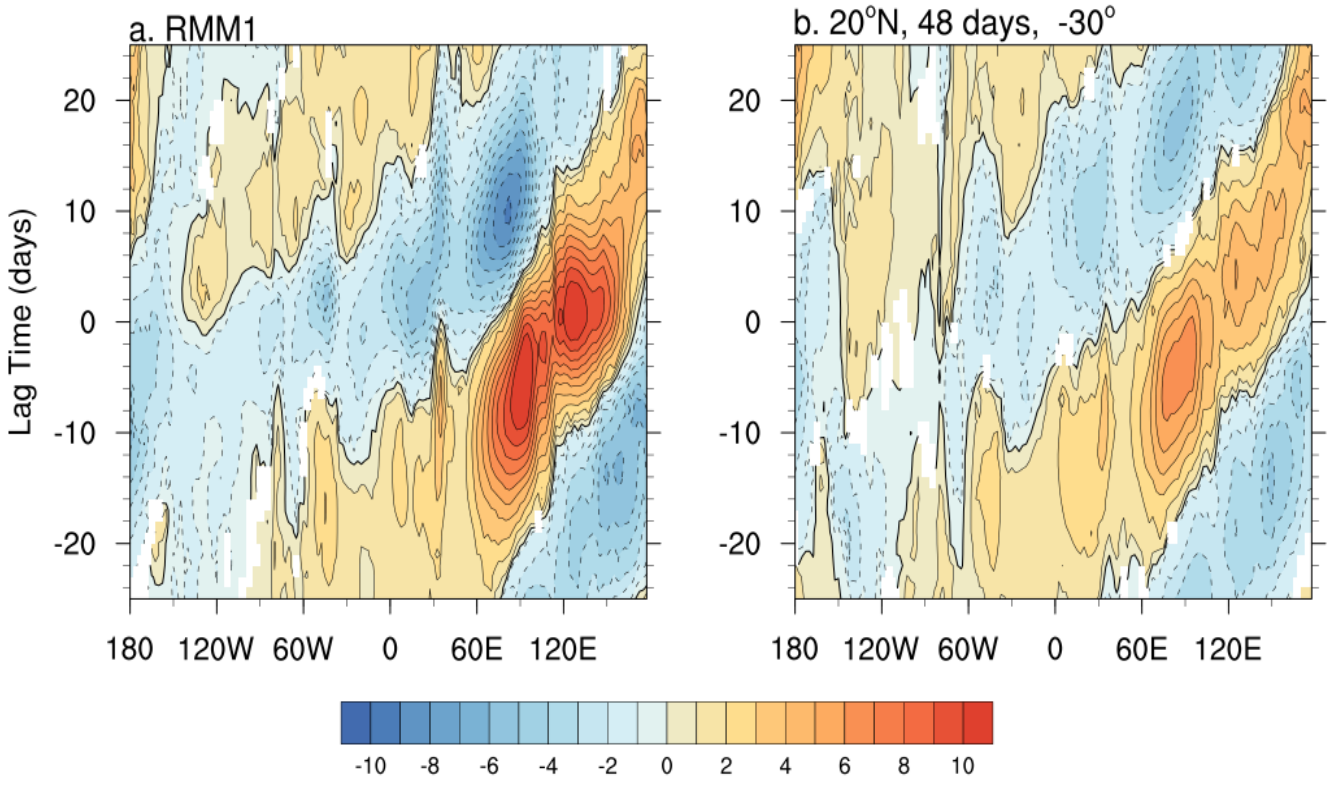

20° N
48 days
-30°

Averaged 10°S -10°N

Regression against wavelet transforms for 20° N with periods of 48 days and meridional scales of 30° latitude

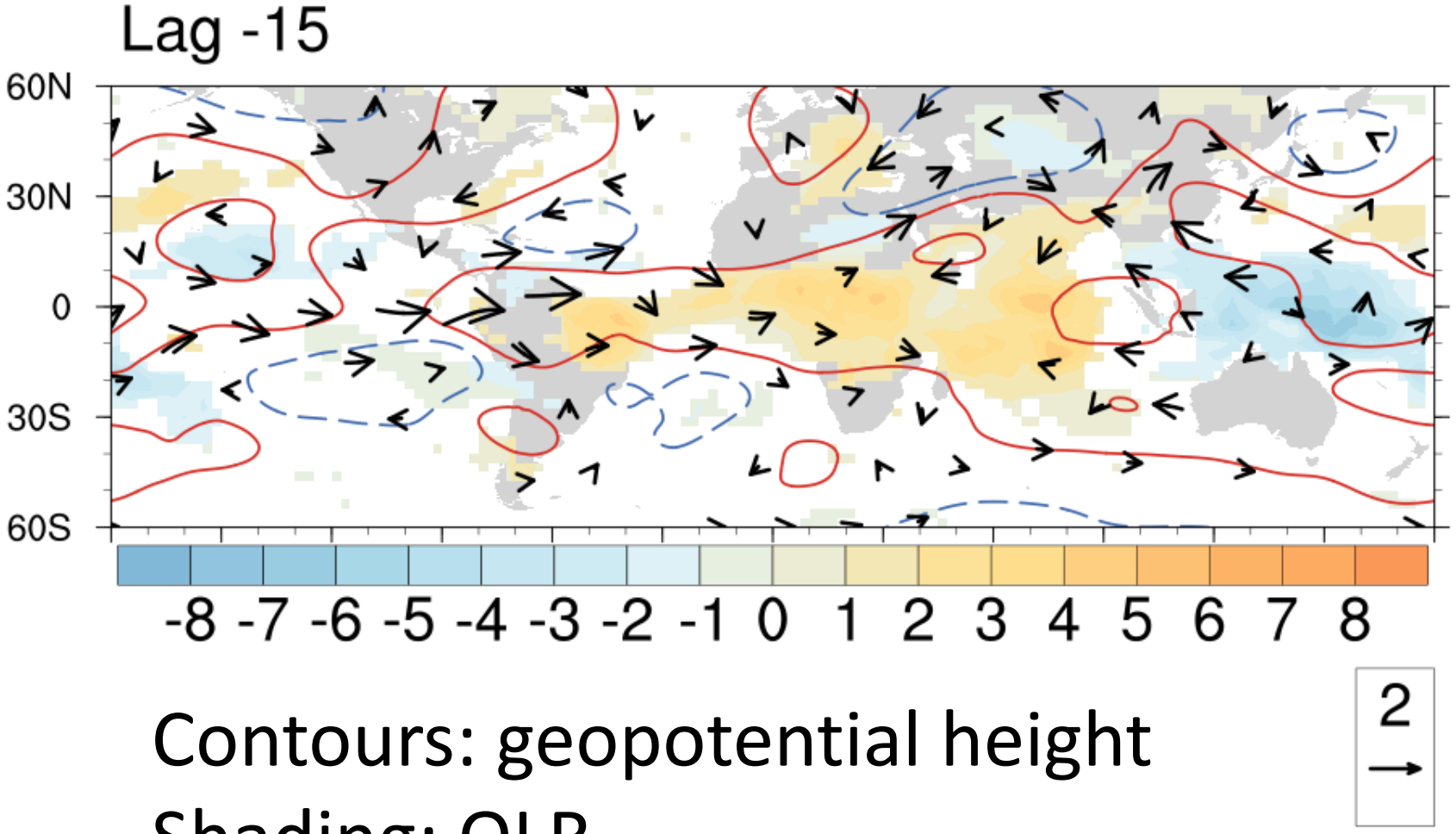

Contours: geopotential height

Shading: OLR

Regression against wavelet transforms for 20° N with periods of 48 days and meridional scales of 30° latitude

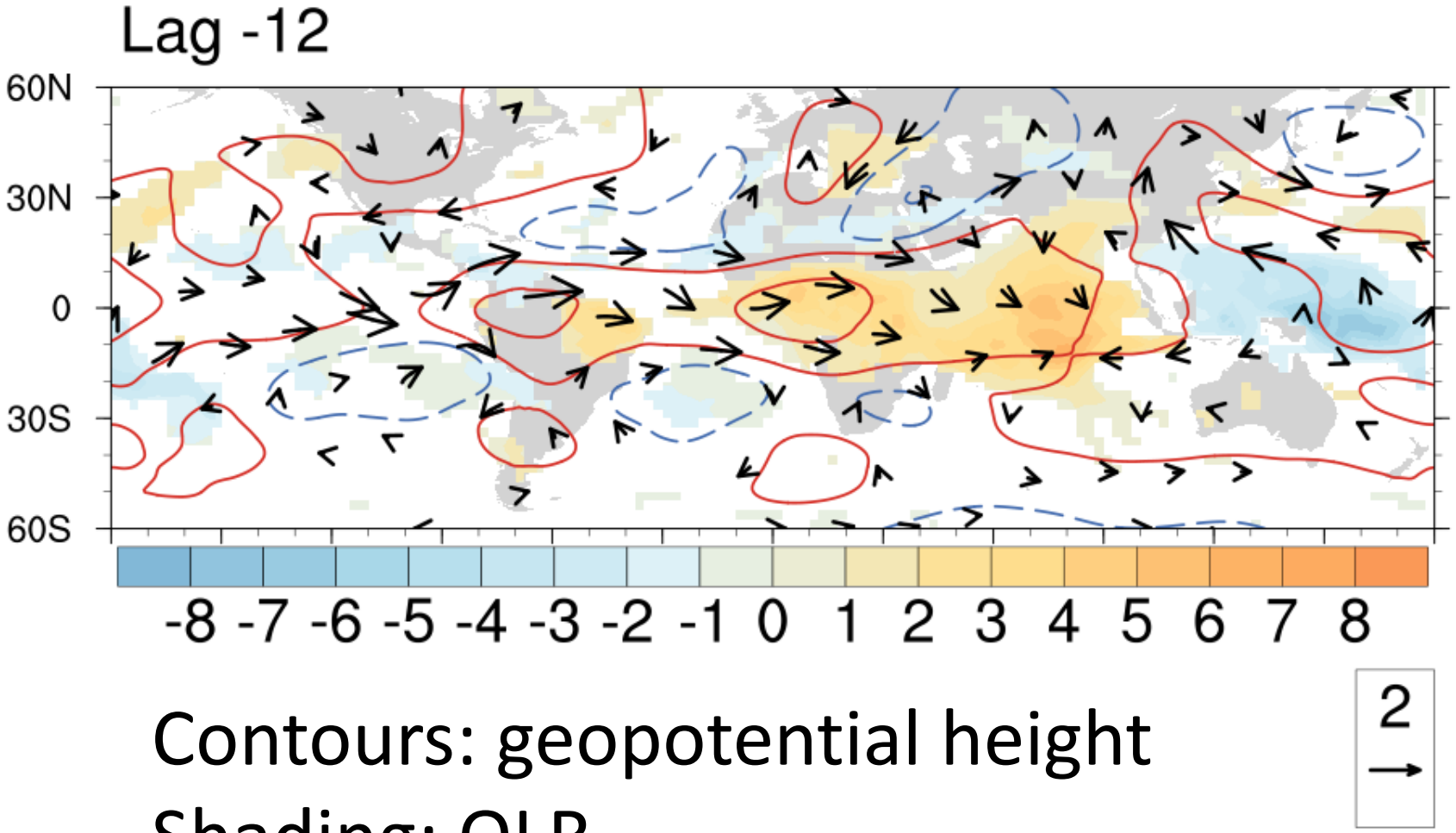

Contours: geopotential height

Shading: OLR

Regression against wavelet transforms for 20° N with periods of 48 days and meridional scales of 30° latitude

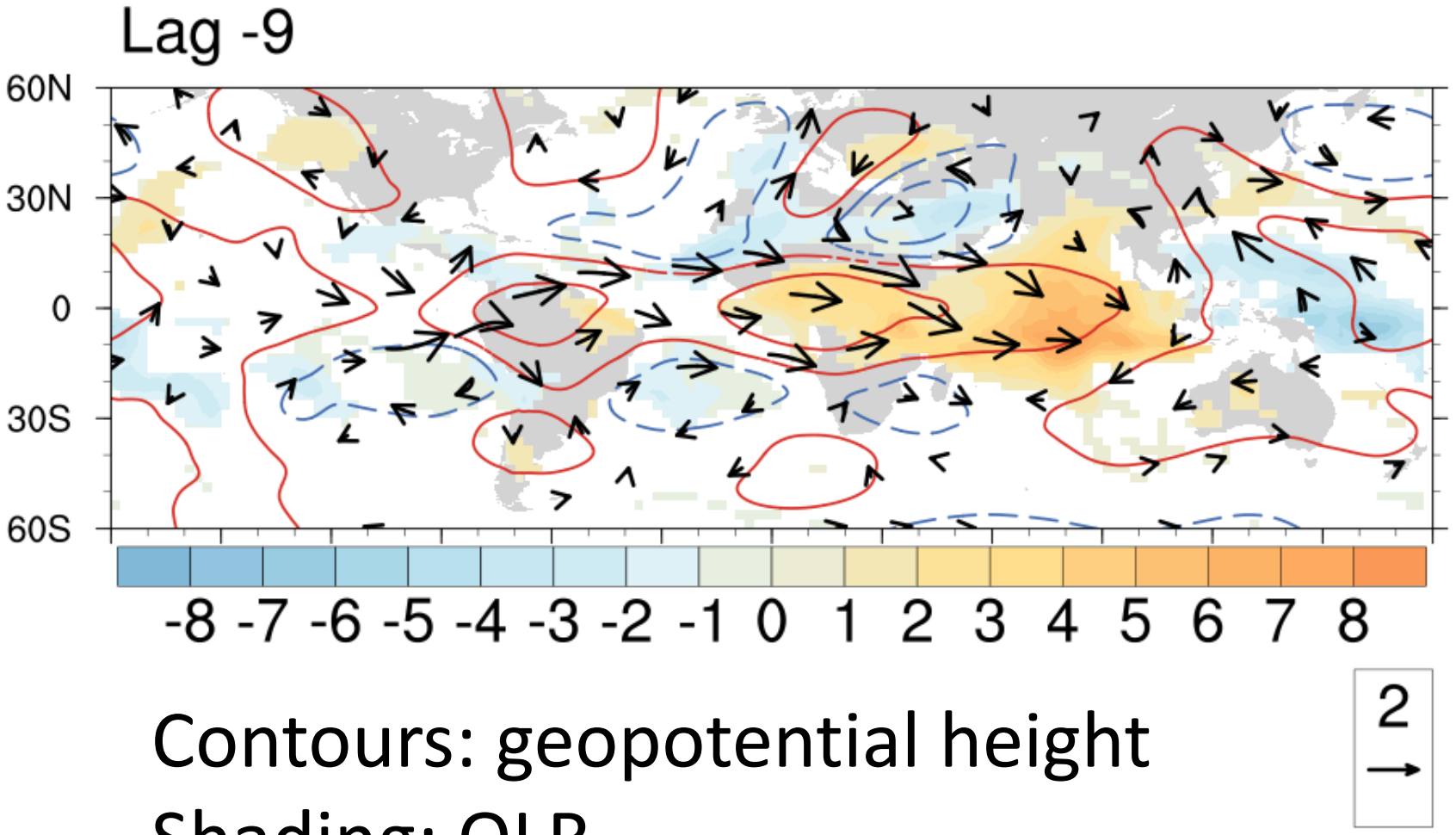

Contours: geopotential height

Shading: OLR

Regression against wavelet transforms for 20° N with periods of 48 days and meridional scales of 30° latitude

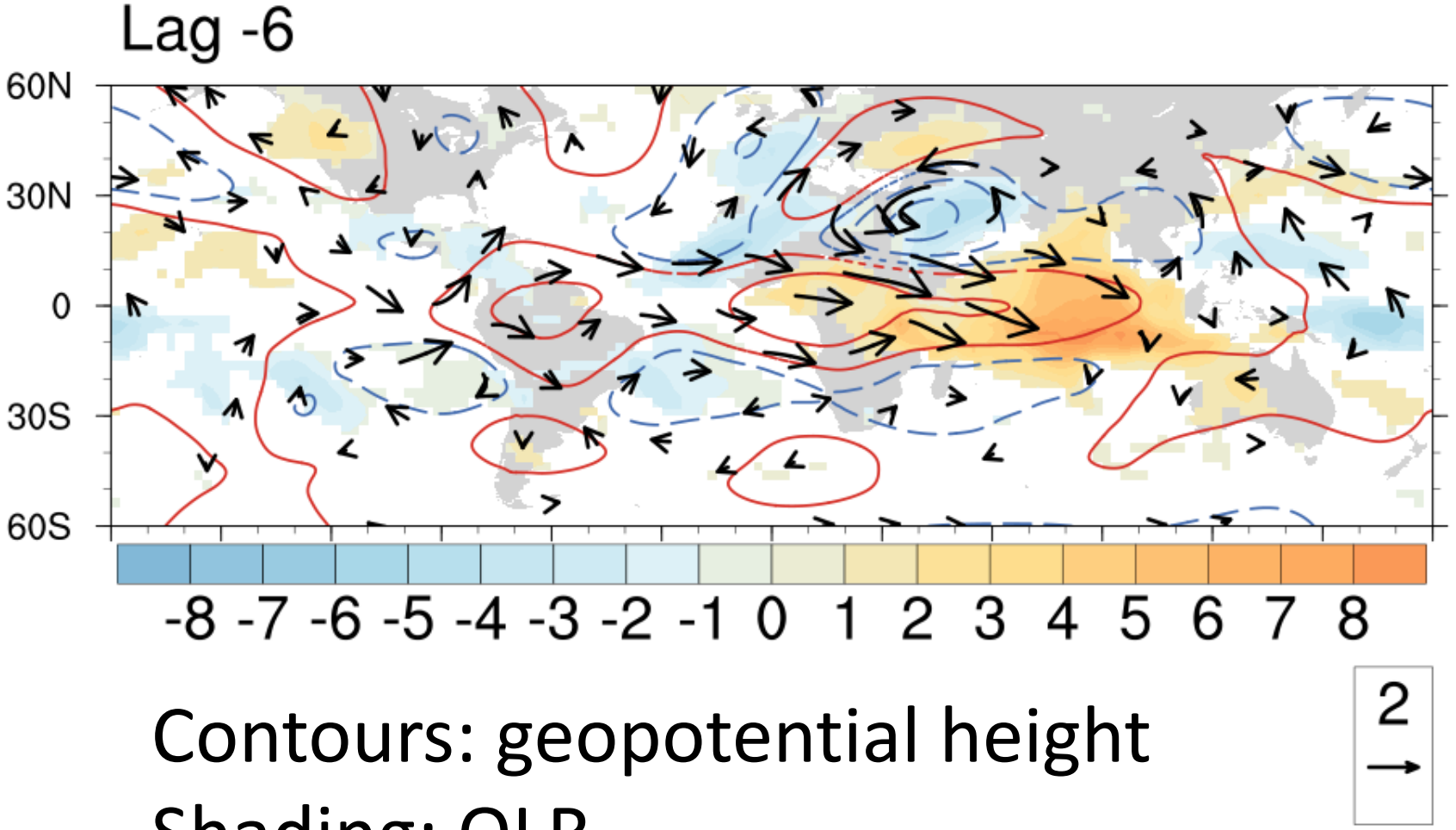

Contours: geopotential height

Shading: OLR

Regression against wavelet transforms for 20° N with periods of 48 days and meridional scales of 30° latitude

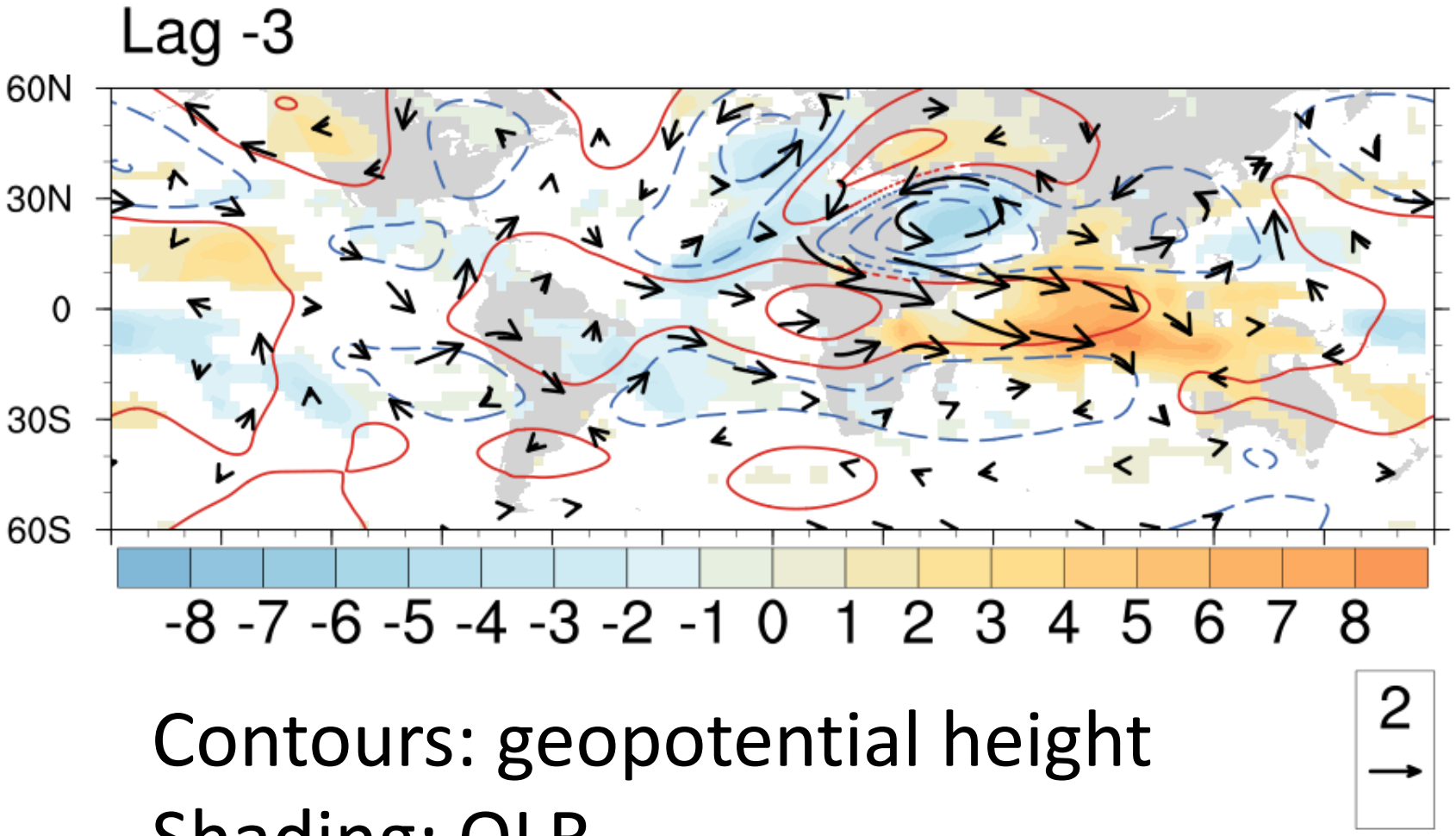

Contours: geopotential height

Shading: OLR

Regression against wavelet transforms for 20° N with periods of 48 days and meridional scales of 30° latitude

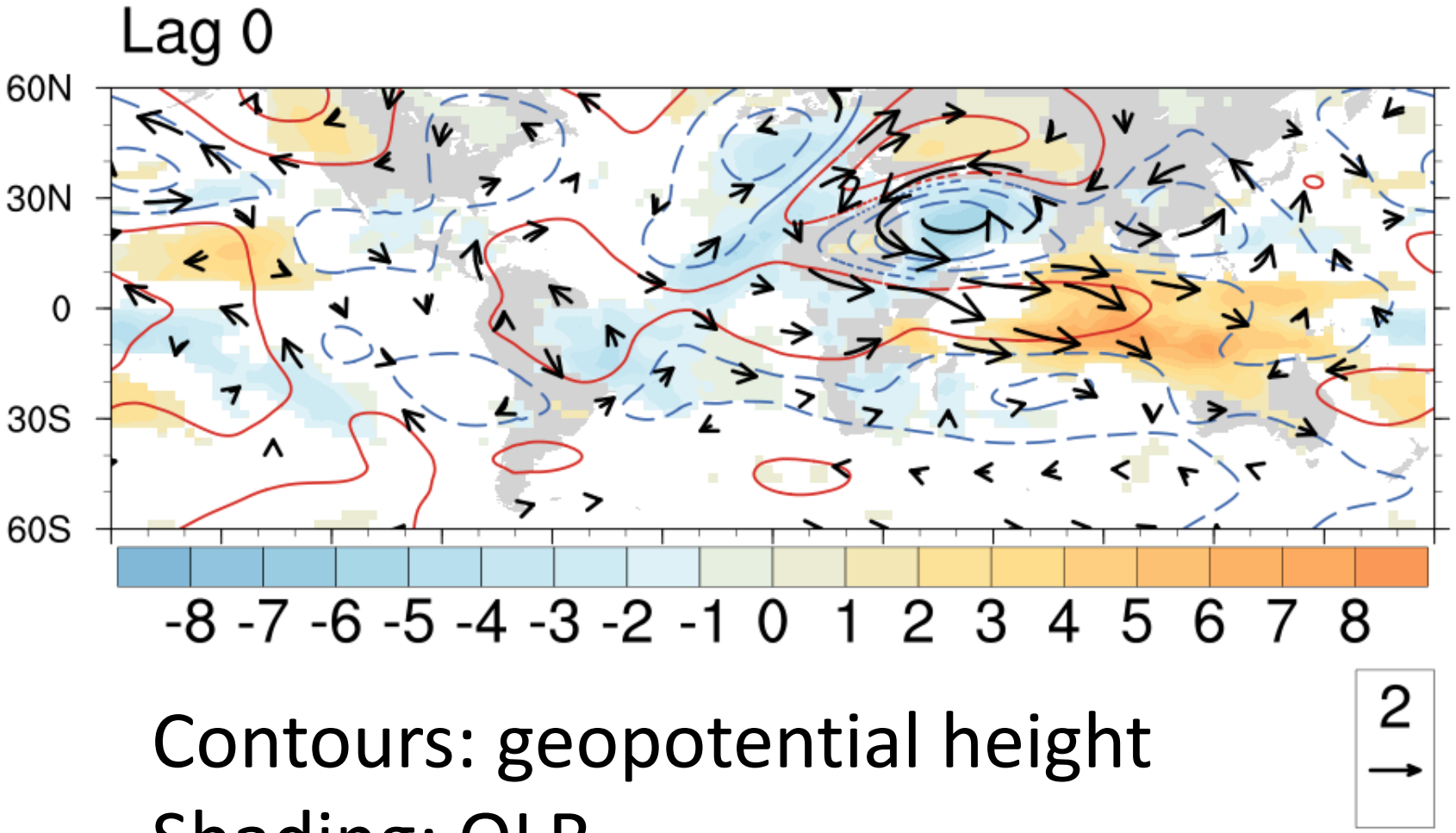

Contours: geopotential height

Shading: OLR

Regression against wavelet transforms for 20° N with periods of 48 days and meridional scales of 30° latitude

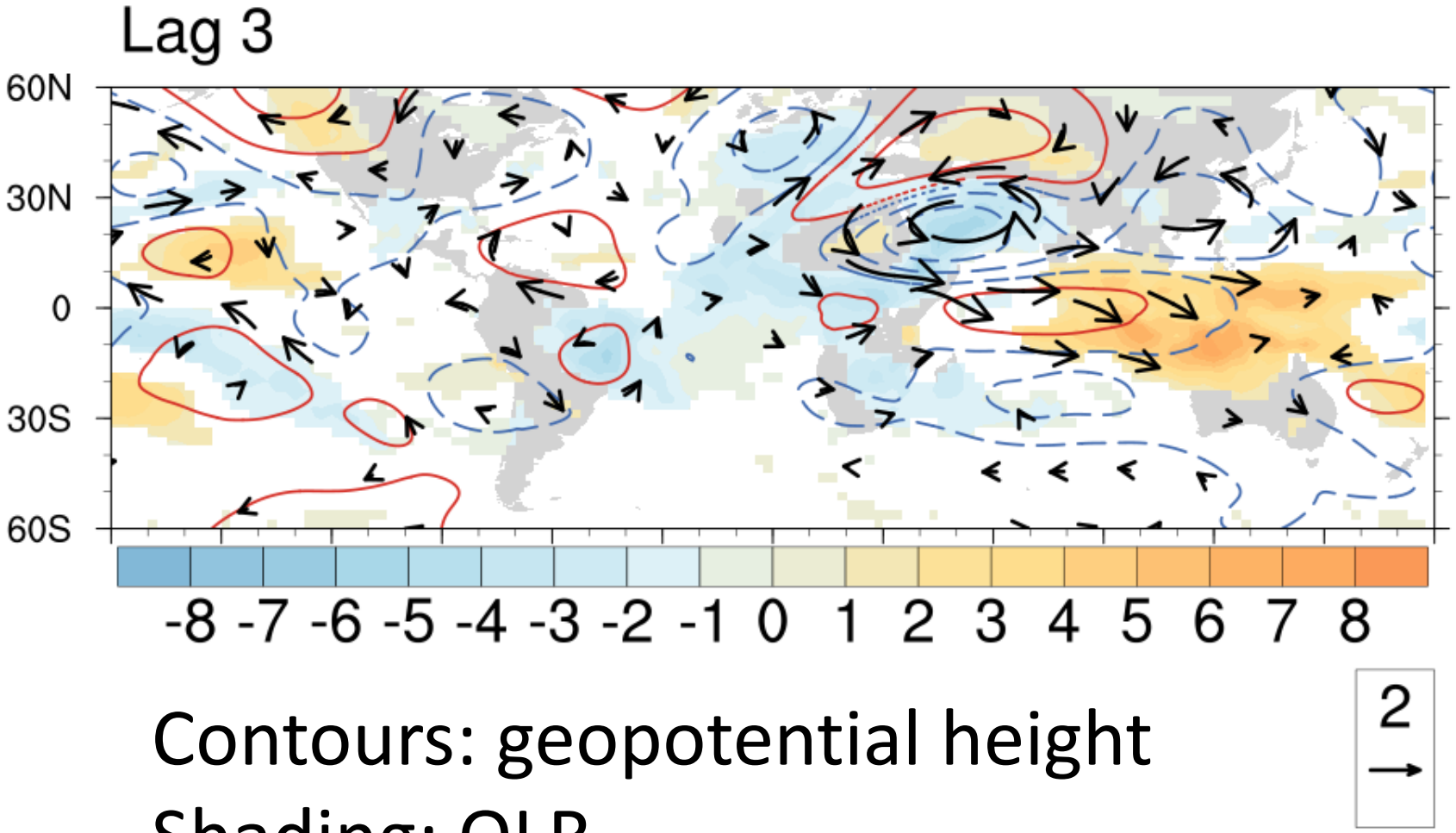

Contours: geopotential height

Shading: OLR

Regression against wavelet transforms for 20° N with periods of 48 days and meridional scales of 30° latitude

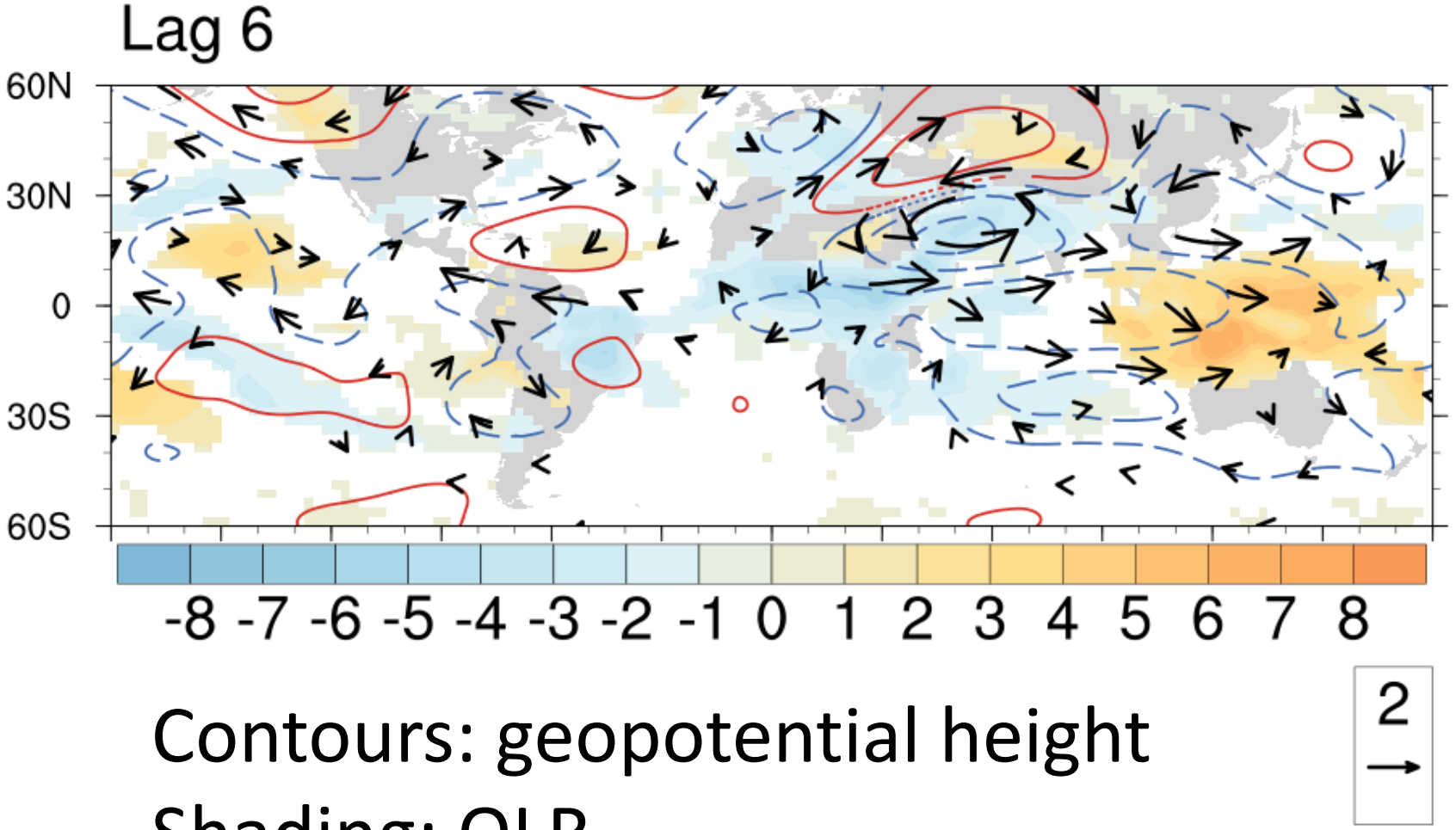

Contours: geopotential height

Shading: OLR

Regression against wavelet transforms for 20° N with periods of 48 days and meridional scales of 30° latitude

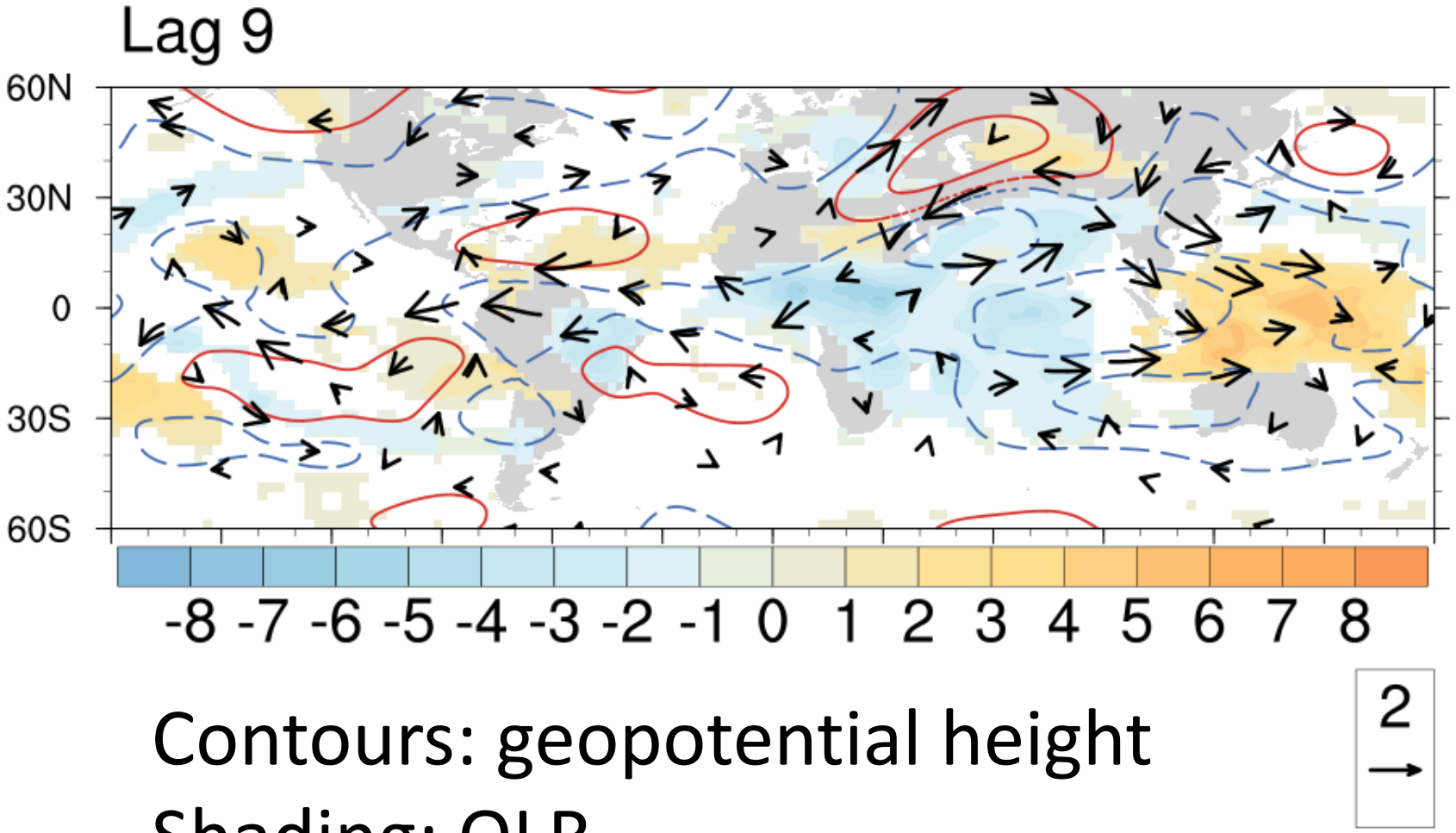

Contours: geopotential height

Shading: OLR

Regression against wavelet transforms for 20° N with periods of 48 days and meridional scales of 30° latitude

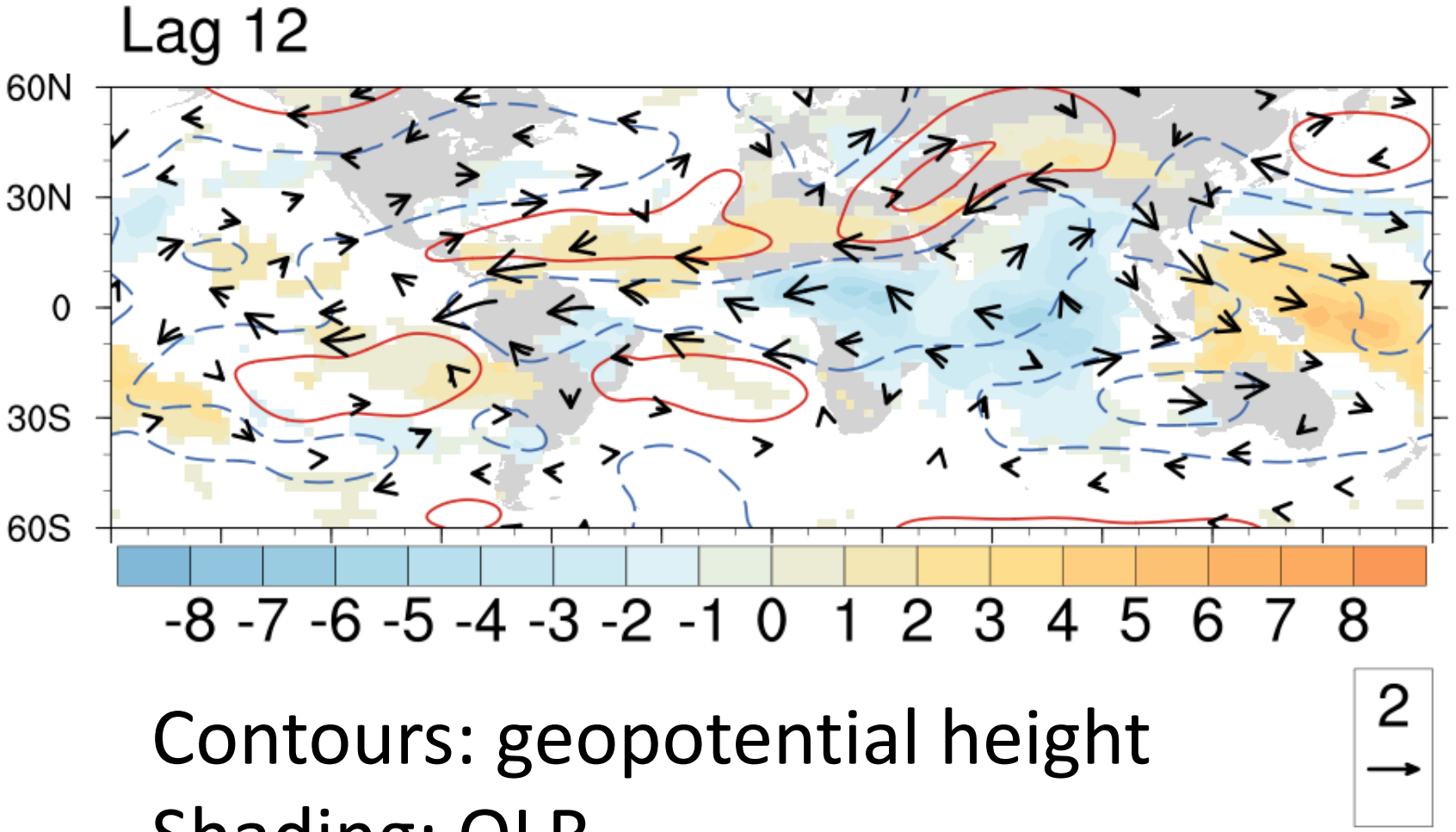

Contours: geopotential height

Shading: OLR

Regression against wavelet transforms for 20° N with periods of 48 days and meridional scales of 30° latitude

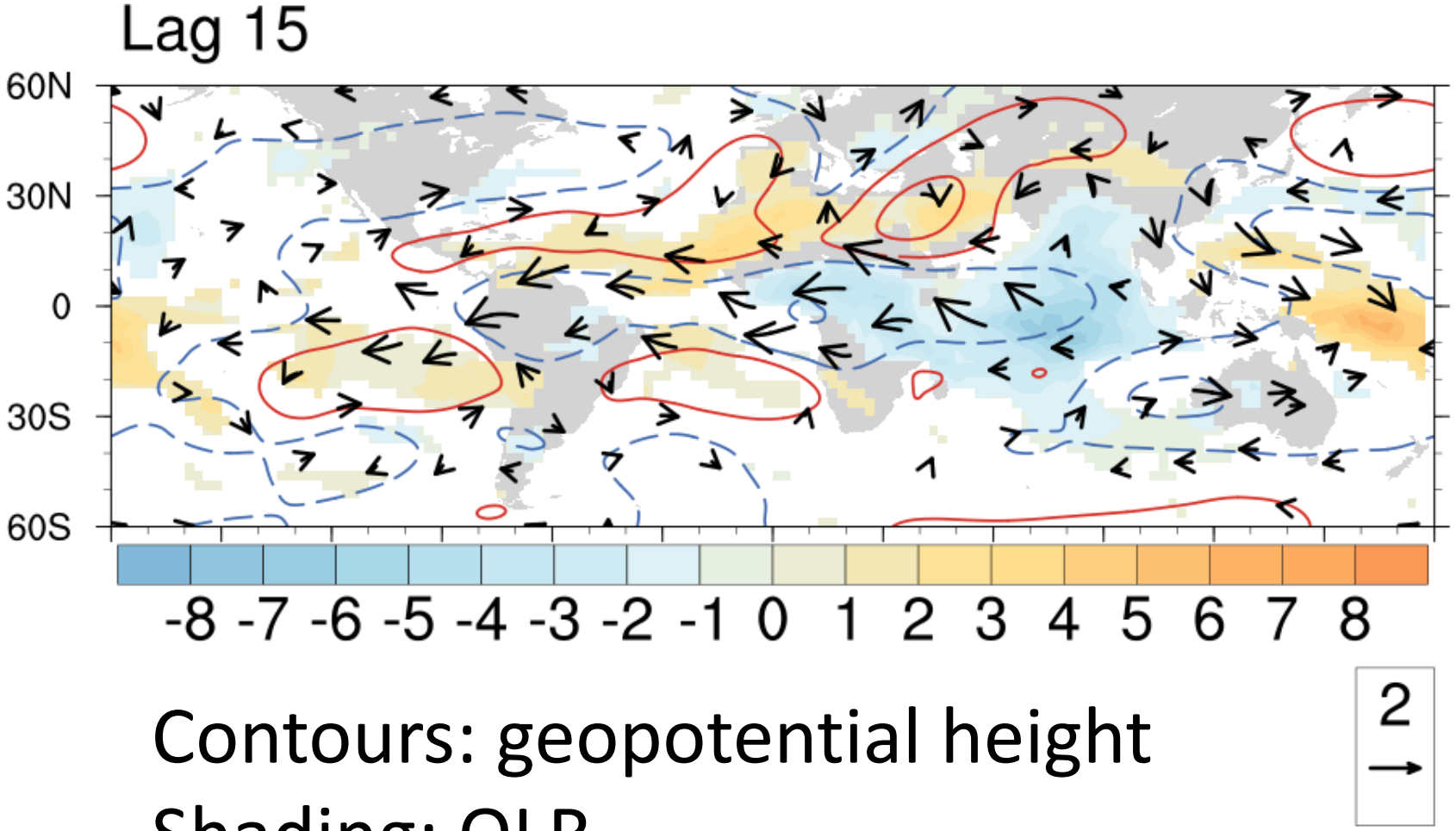

Contours: geopotential height

Shading: OLR

Local power spectra (35-45°E) divided by global power spectra show increased equatorward power on intraseasonal timescales

- equatorward scale of 30° latitude and period of 48 days

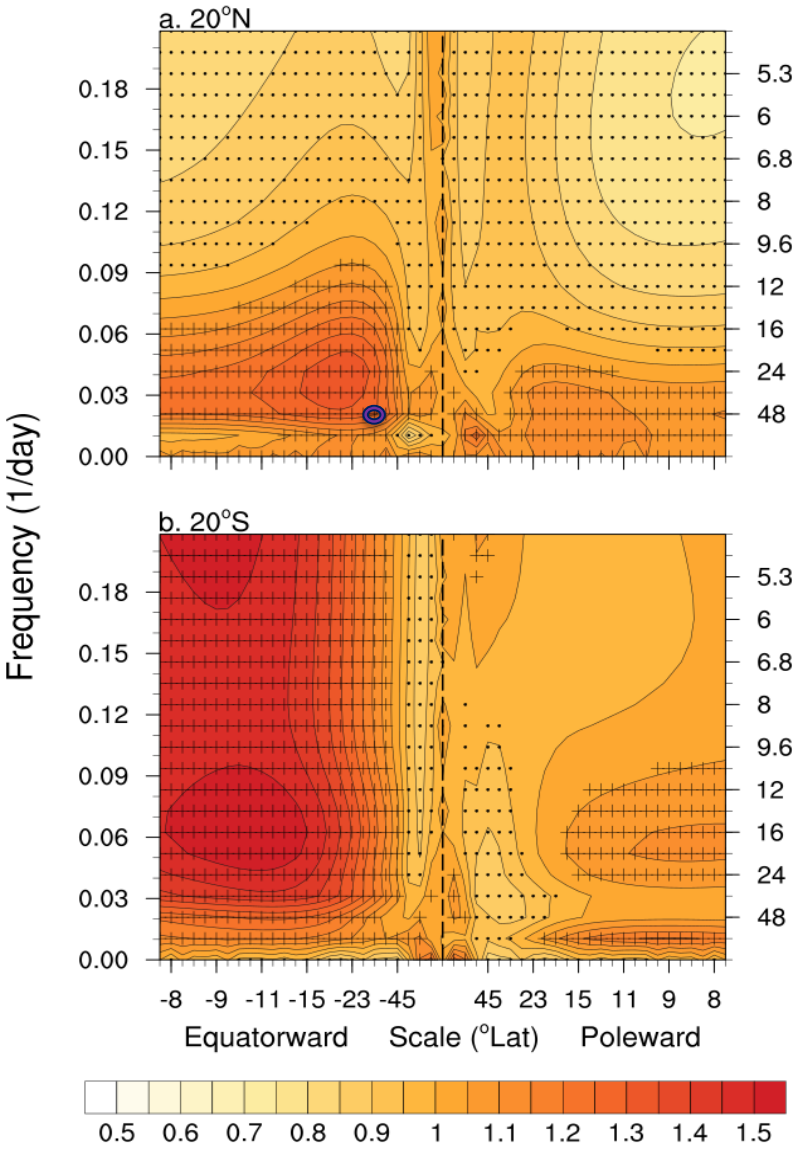

20° N

20° S

Gahtan, J and Roundy PE. Wavelet isolation of meridionally moving geopotential height perturbations near the subtropics of eastern Africa and their relationship with the Madden–Julian Oscillation. Q J R Meteorol Soc. 2019. https://doi.org/10.1002/qj.3681

Next: A global understanding of these subtropical signals

Equatorward propagation at 20°N on intraseasonal timescales is maximized over Eastern Africa and the Indian Ocean

20° N

20° S

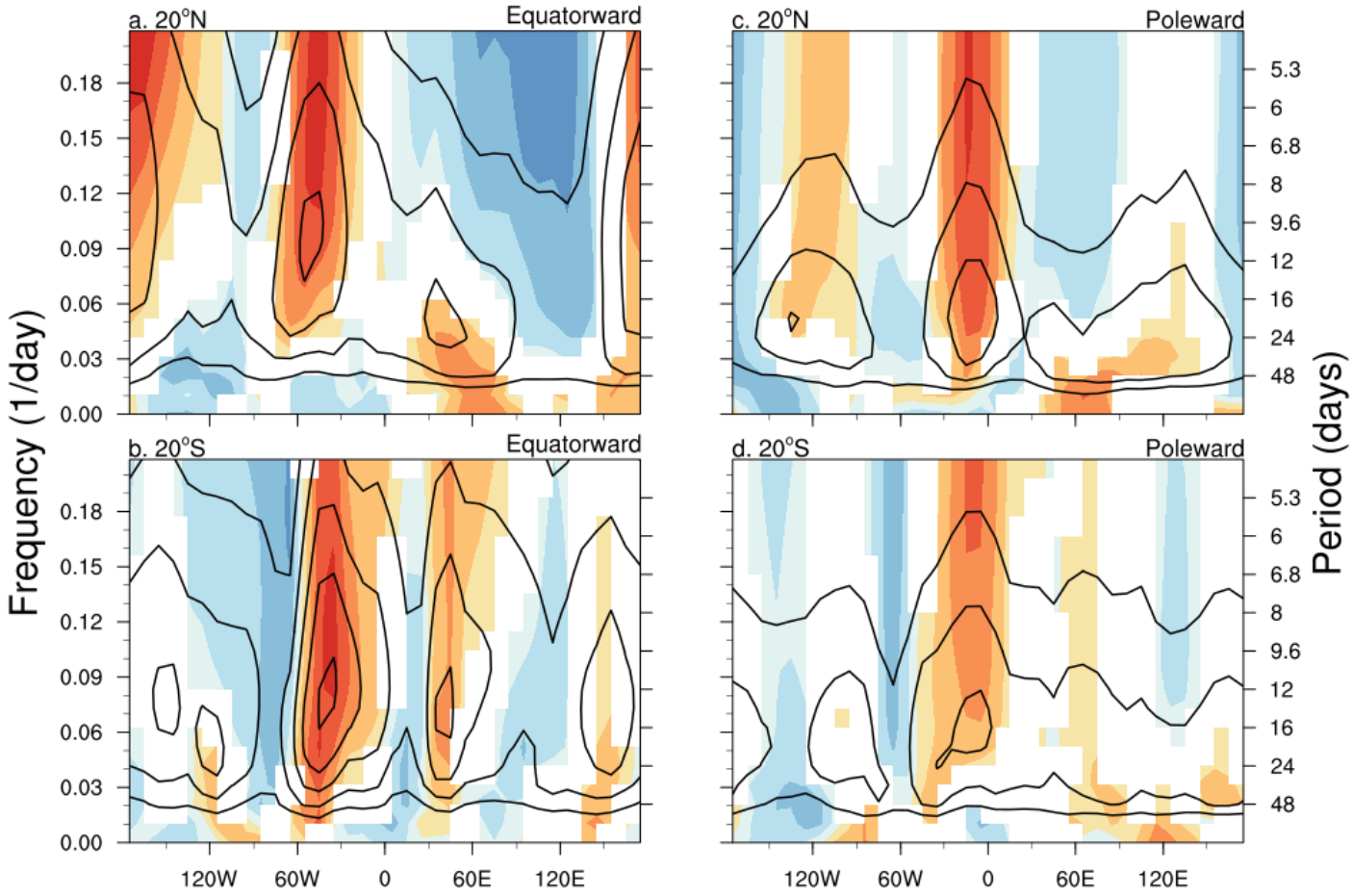

Avg. for all equatorward meridional scales

Avg. for all poleward meridional scales

Longitude

Longitudes of increased power on synoptic timescales tend to be near tropical westerlies or minima in easterlies

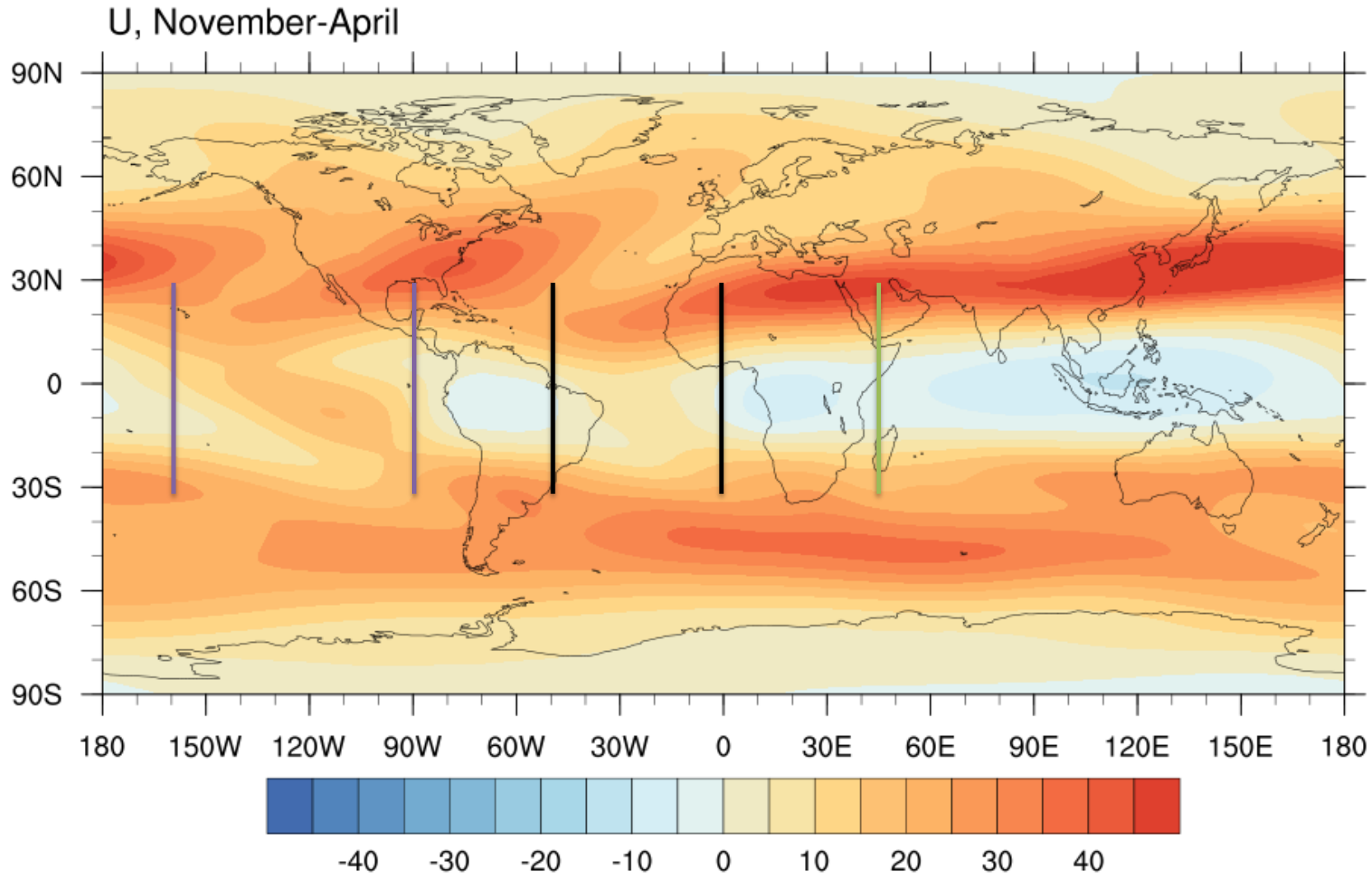

Longitudes of increased power on synoptic timescales tend to be near tropical westerlies or minima in easterlies

20° N

20° S

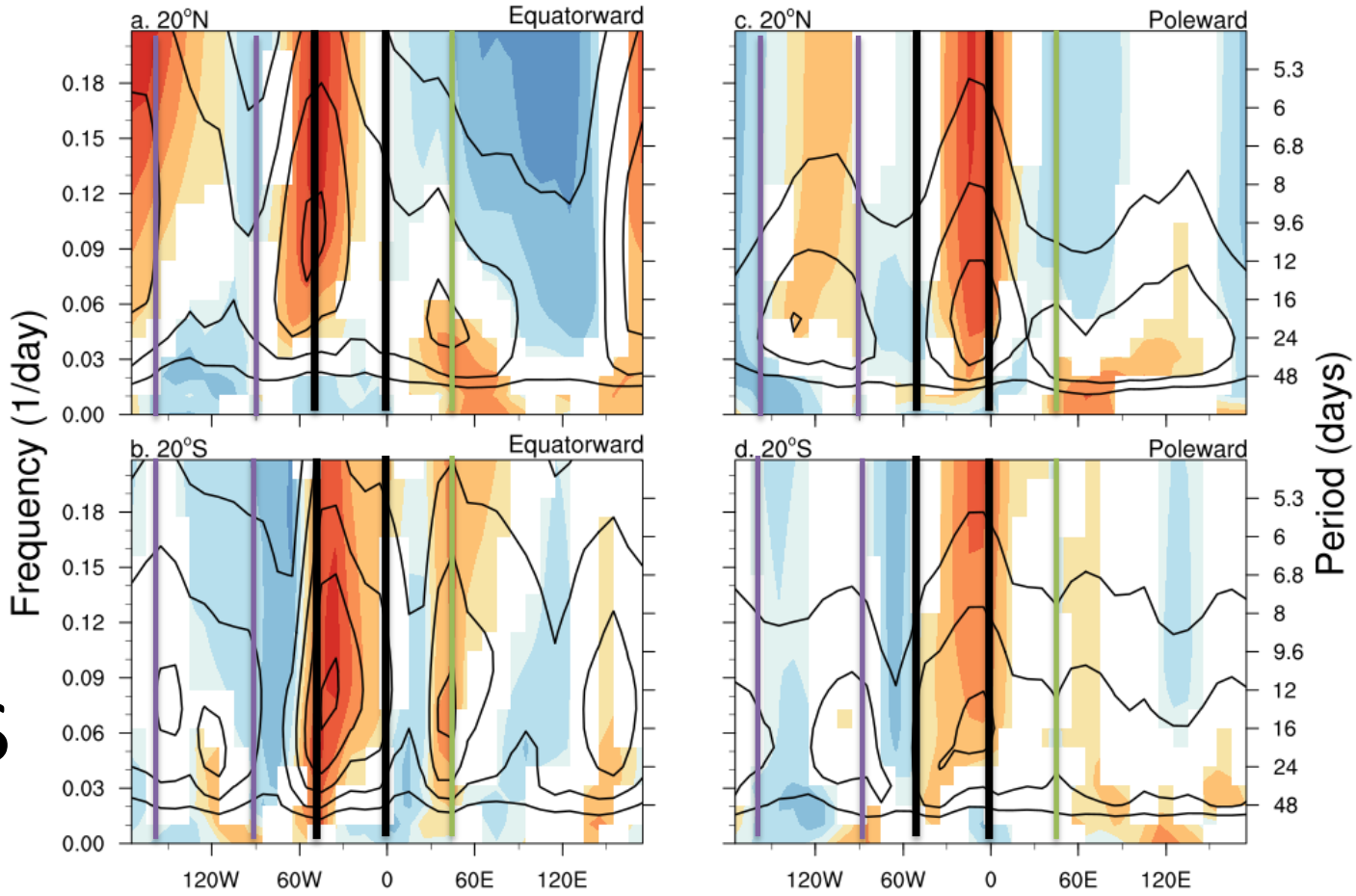

Avg. for all southward meridional scales

Avg. for all northward meridional scales

Longitude

Longitudes of increased equatorward power tend to be near subtropical jet exit regions

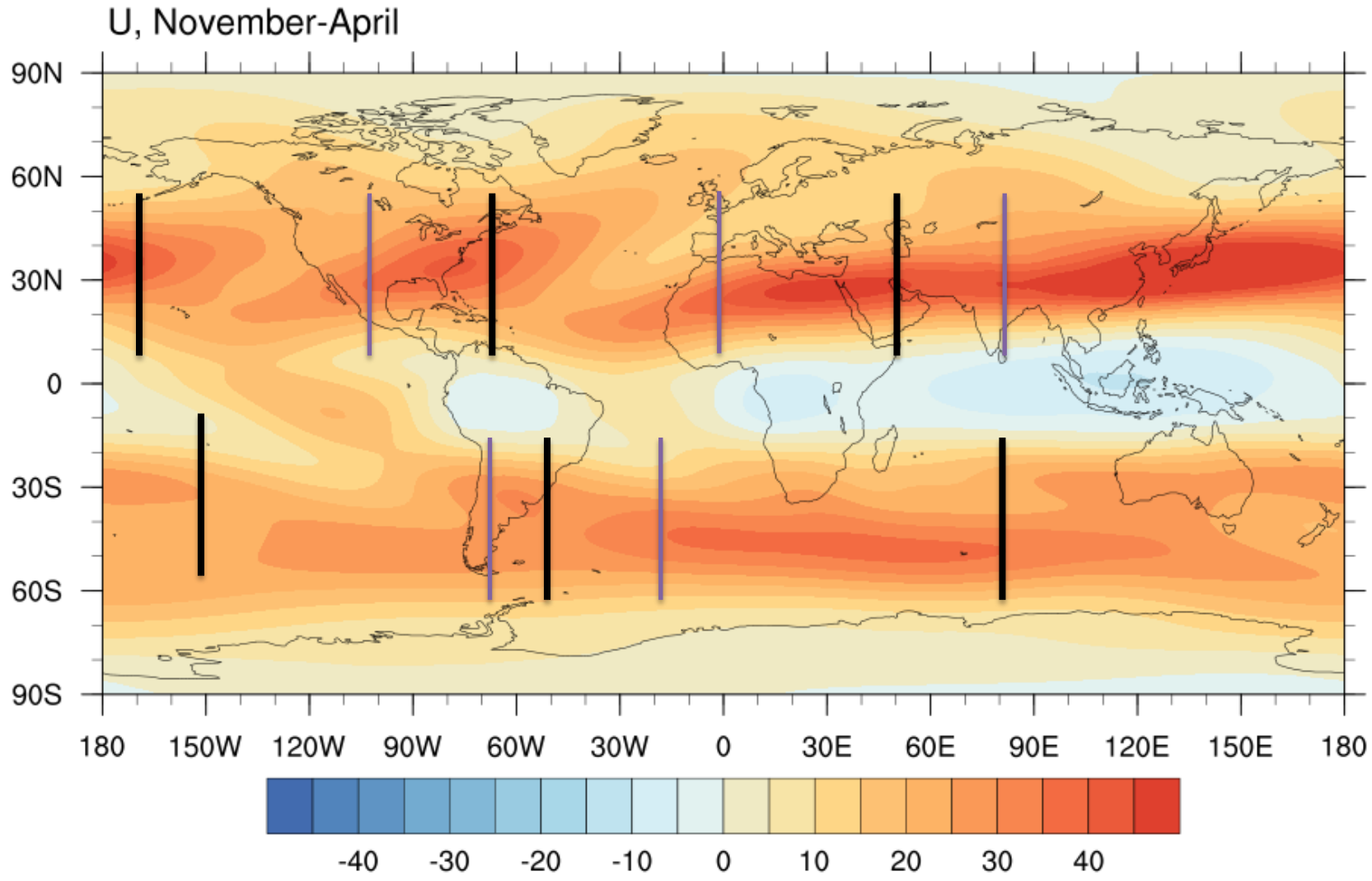

Longitudes of increased equatorward power tend to be near subtropical jet exit regions (black lines)

20° N

20° S

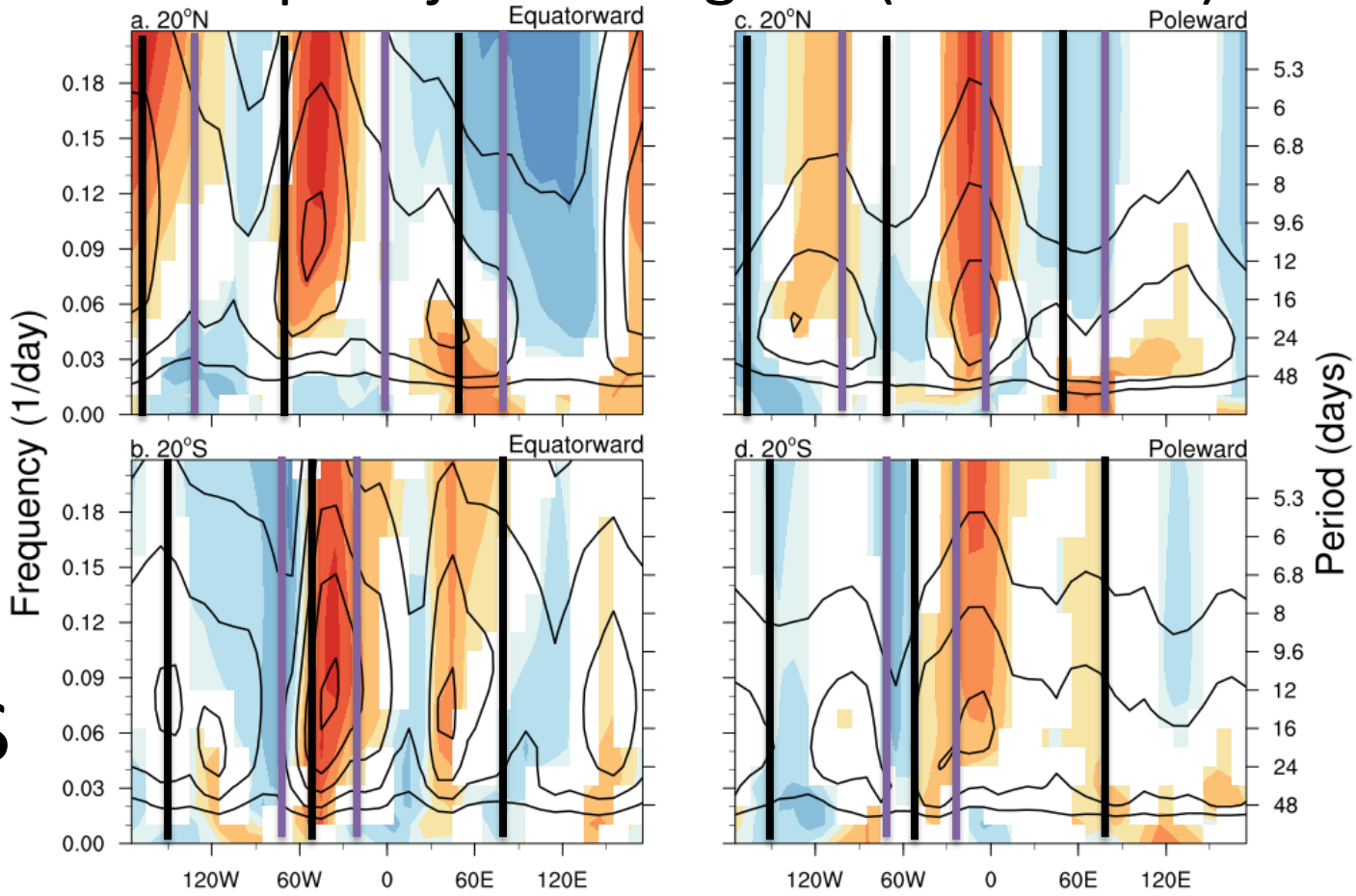

Avg. for all southward meridional scales

Avg. for all northward meridional scales

Longitude

Longitudes of increased equatorward power also tend to have equatorward background meridional wind

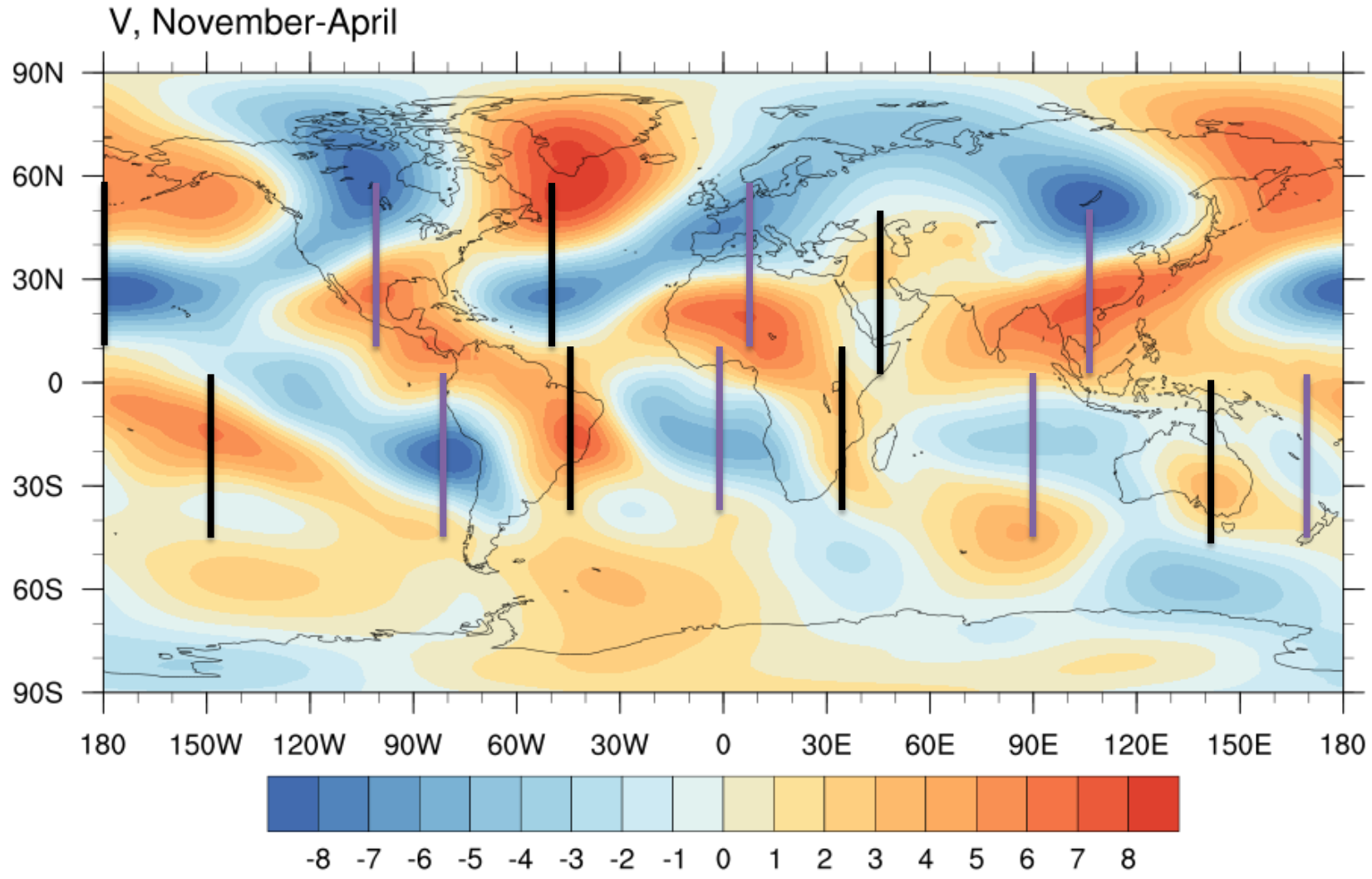

Longitudes of increased equatorward power also tend to have equatorward background meridional wind (black lines)

20° N

20° S

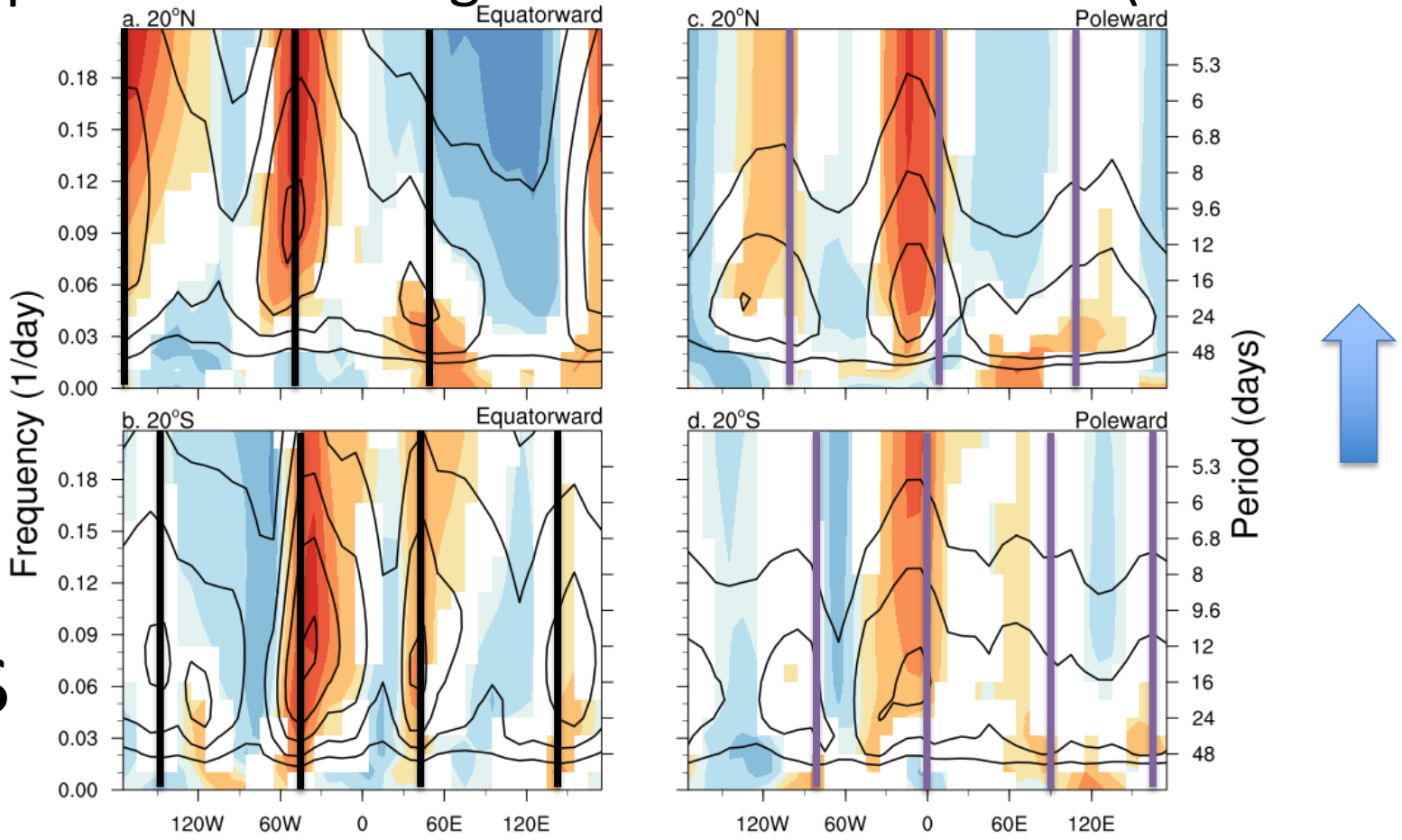

Avg. for all southward meridional scales

Avg. for all northward meridional scales

Longitude

Meridional power is increased on intraseasonal timescales near warm pool regions when RMM >1

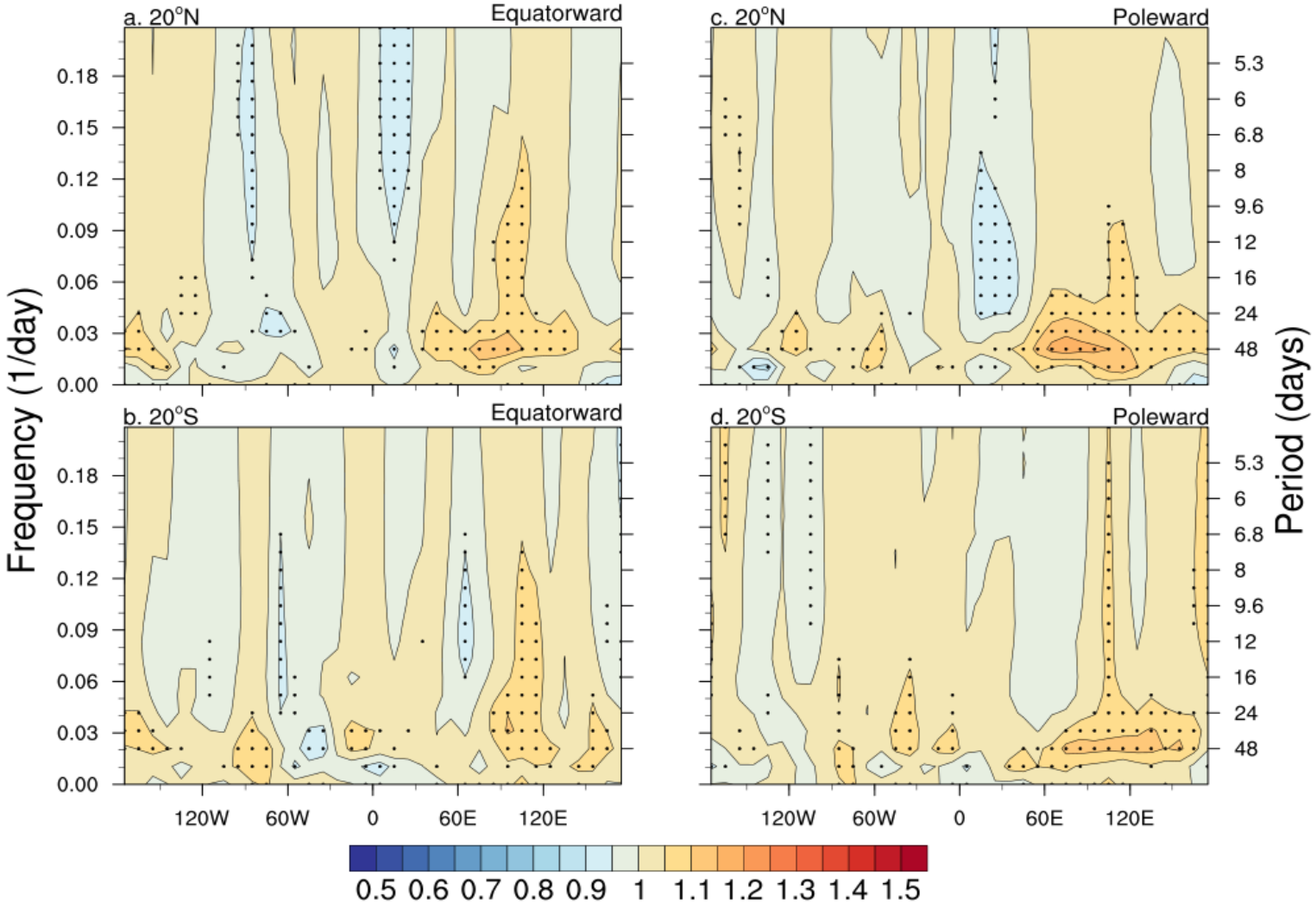

Examine relationships between the meridional power and the horizonal flow

- Normalize power by global and temporal average at that latitude
- Separate by:

Southward Northward

Periods 48-days, 32-days, 24-days, Etc.

Put 100-day lowpass horizontal flow characteristics (at each timestep and longitude range) in increasing order and

Reorder corresponding power

Bin power into 36 groups based on the values of horizontal flow characteristics

Take the average in each bin

Non-linear relationship between Zonal wind and power
-> all zonal propagation speeds are included

20° N

20° S

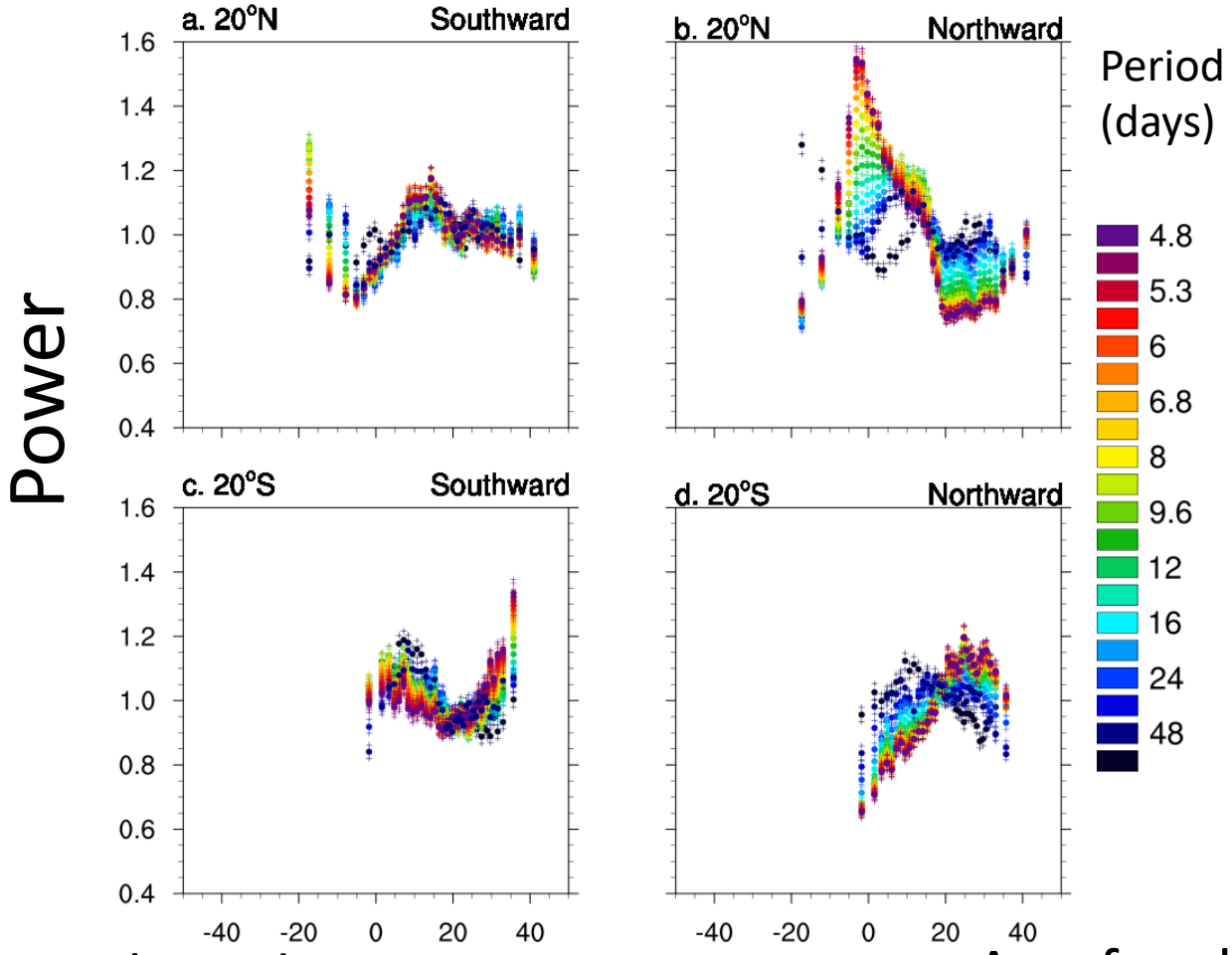

Avg. for all southward meridional scales

U (m/s)

Avg. for all northward meridional scales

Positive relationship between meridional wind and power in the same direction (especially equatorward)

20° N

20° S

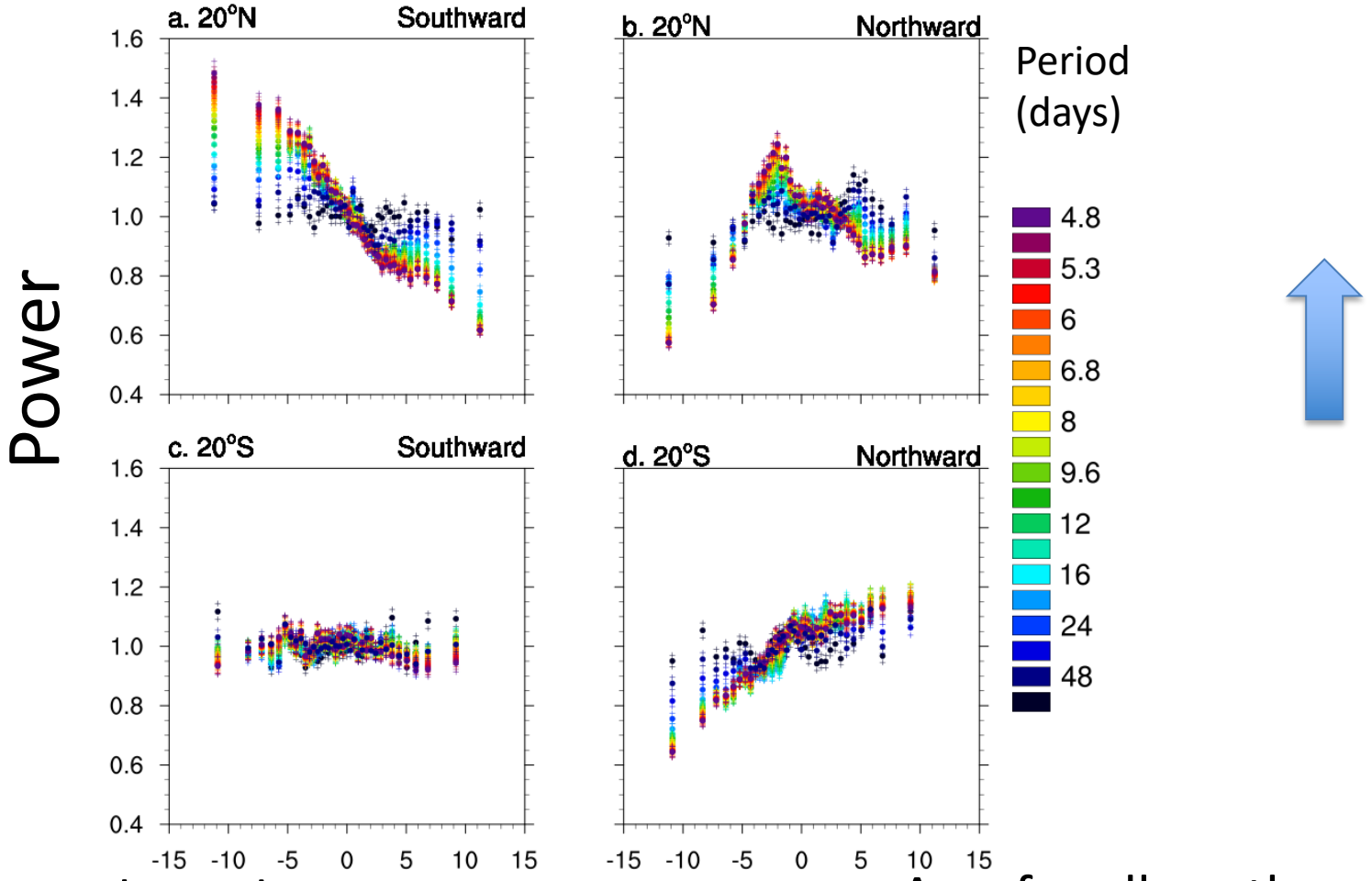

Avg. for all southward meridional scales

V (m/s)

Avg. for all northward meridional scales

Negative relationship between meridional U shear and power in NH, positive SH

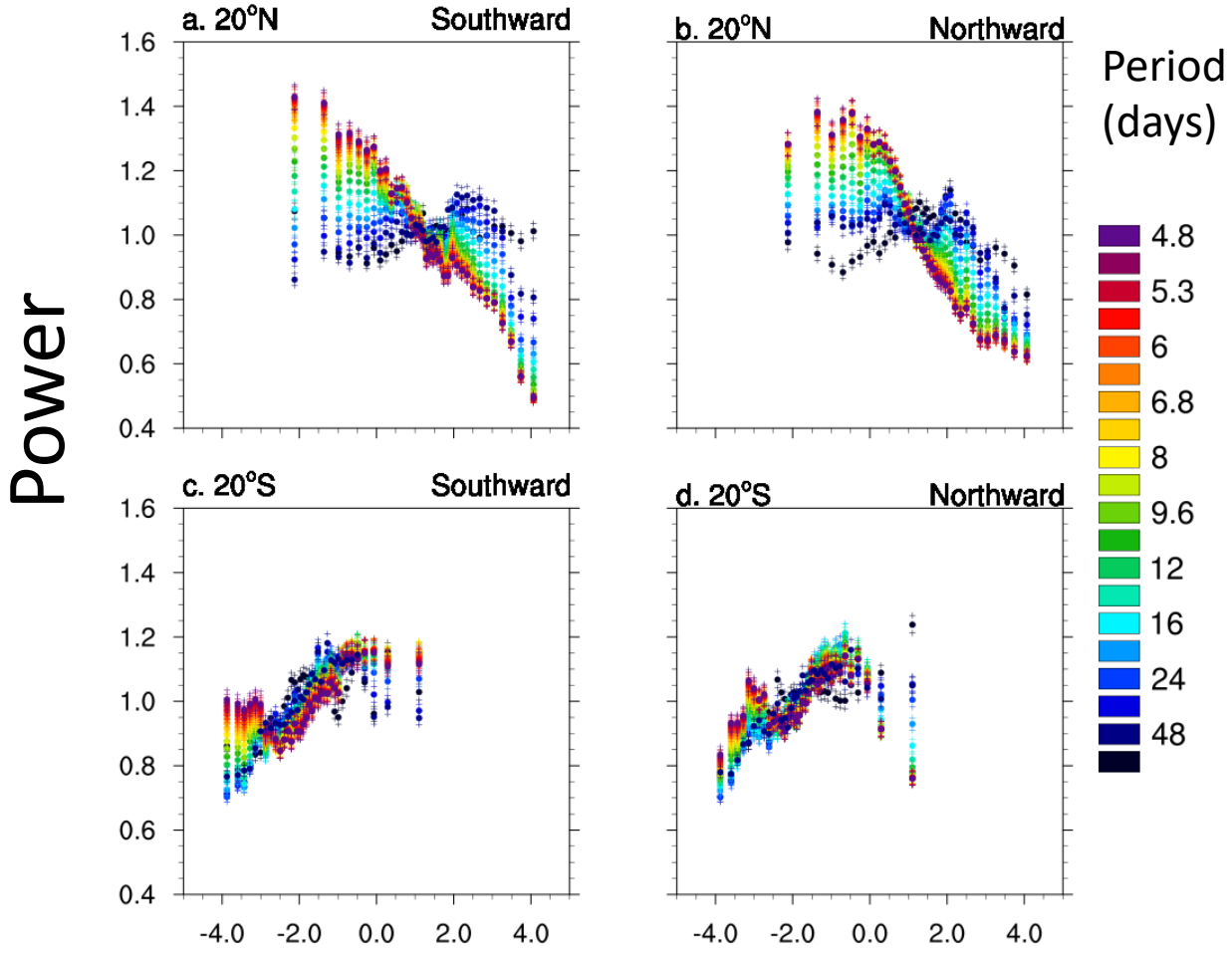

Positive relationship between zonal V shear and power in NH, negative SH

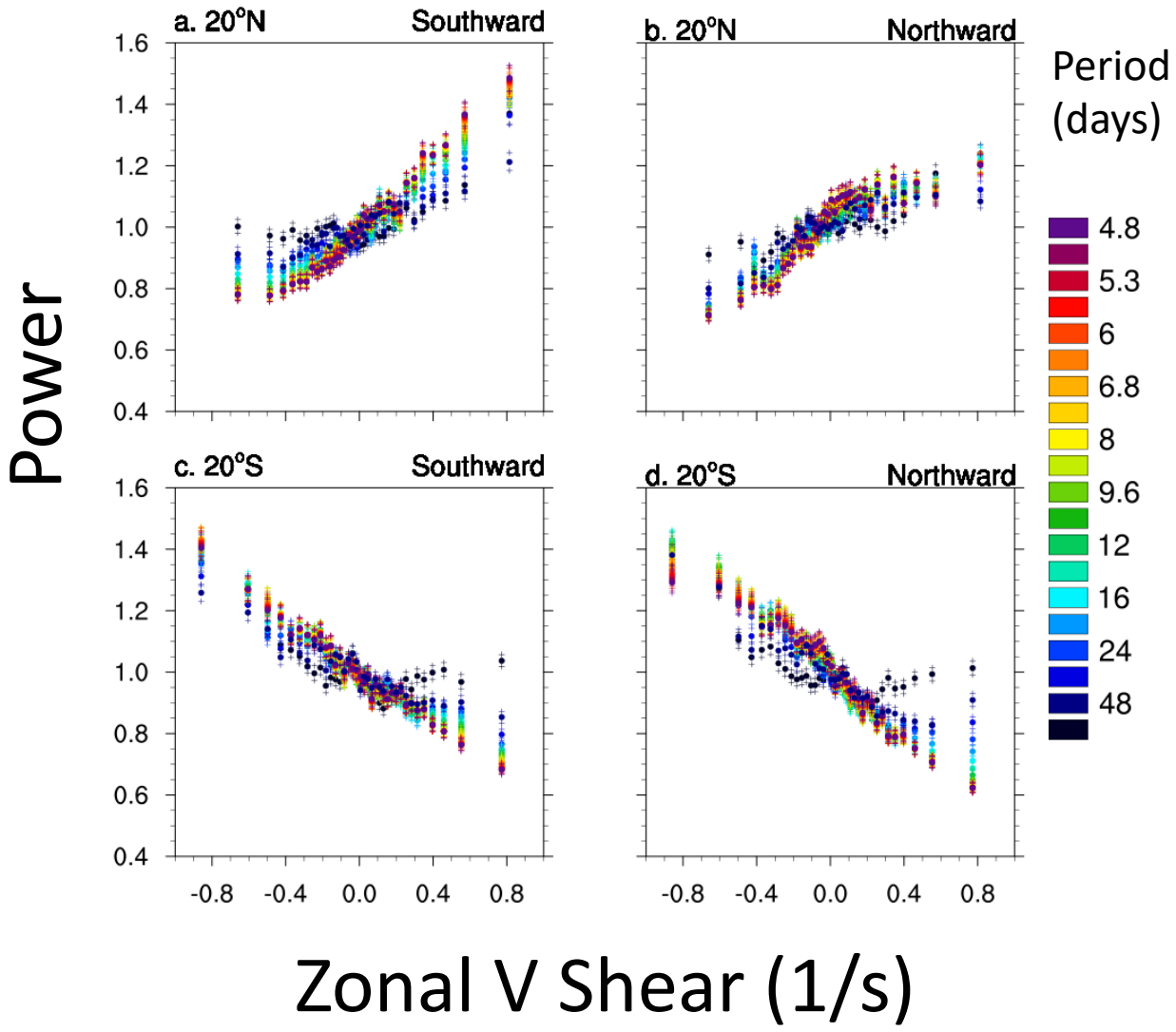

- Power for shorter periods is more heavily influenced by the horizontal flow
  - –> Different background states favor different scales of meridional wave propagation
- Directions of relationships of meridional U shear and zonal V shear with power correspond to positive relationships with Vorticity

Near the subtropics of Eastern Africa, the 200hPa background flow is equatorward

May help explain to the increased equatorward power on intraseasonal timescales in the region

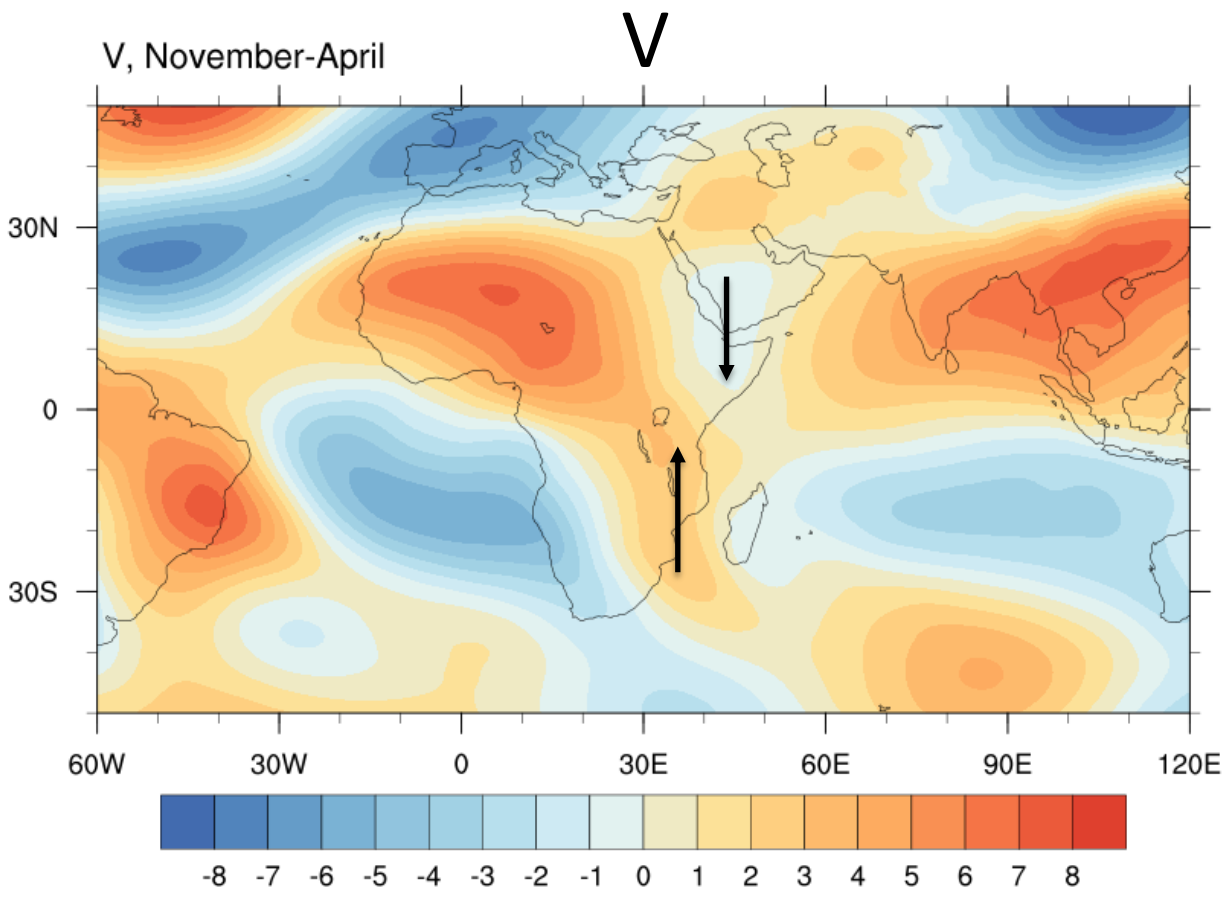

In subtropics near Eastern Africa

- Power is increased for equatorward disturbances on intraseasonal timescales during periods with strong MJO index amplitude
- Regressions against equatorward intraseasonal wavelet transforms show signals similar to those in composites leading up to MJO convective initiation

Intrusions from the extratropics may support the onset of MJO convection over the Western Indian Ocean

Upper tropospheric easterly acceleration on the west side of a region of westerlies leads to divergence which may help to provide large-scale upward motion

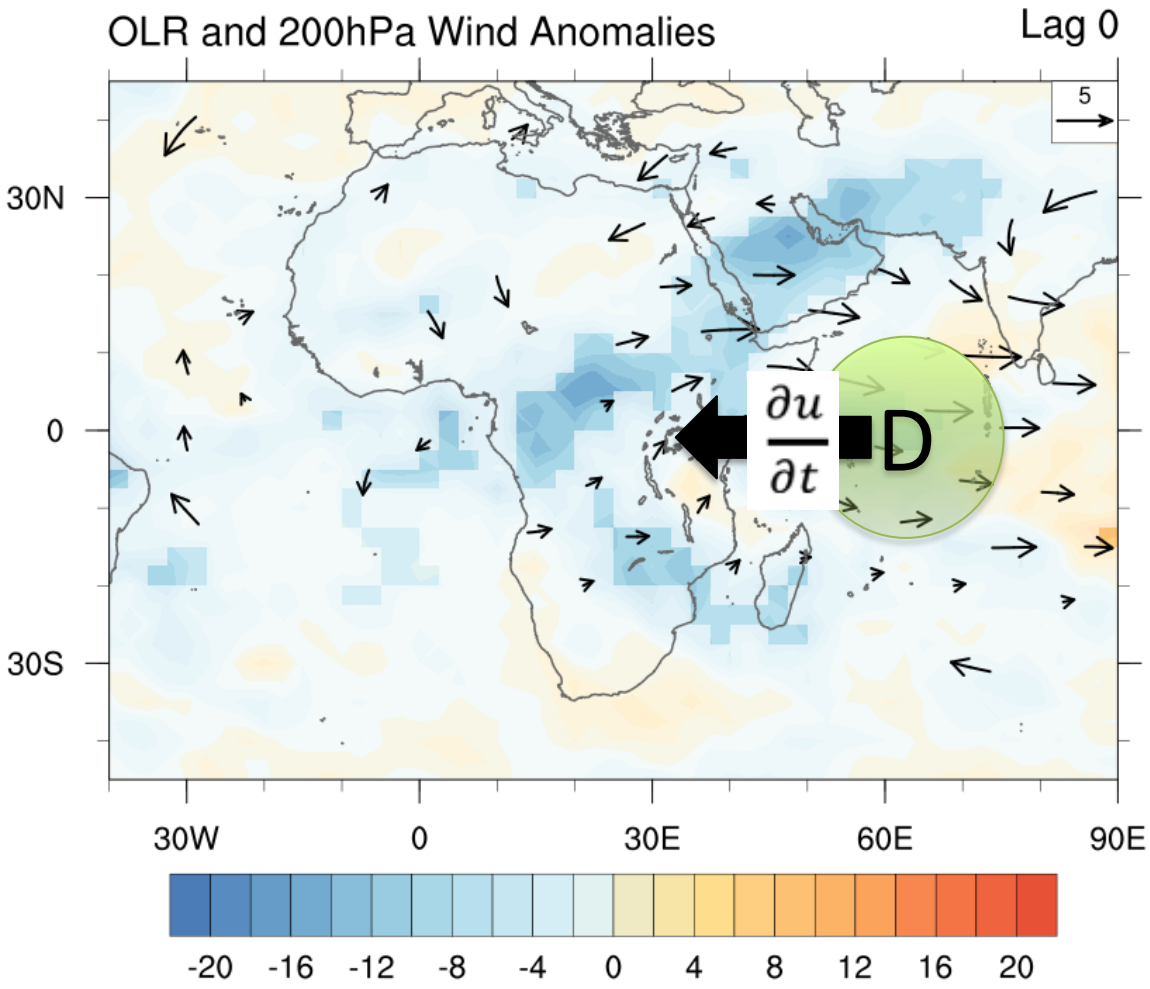

Easterly acceleration is forced by a positive zonal pressure gradient between Eastern Africa and the Western Indian Ocean for a majority of the cases

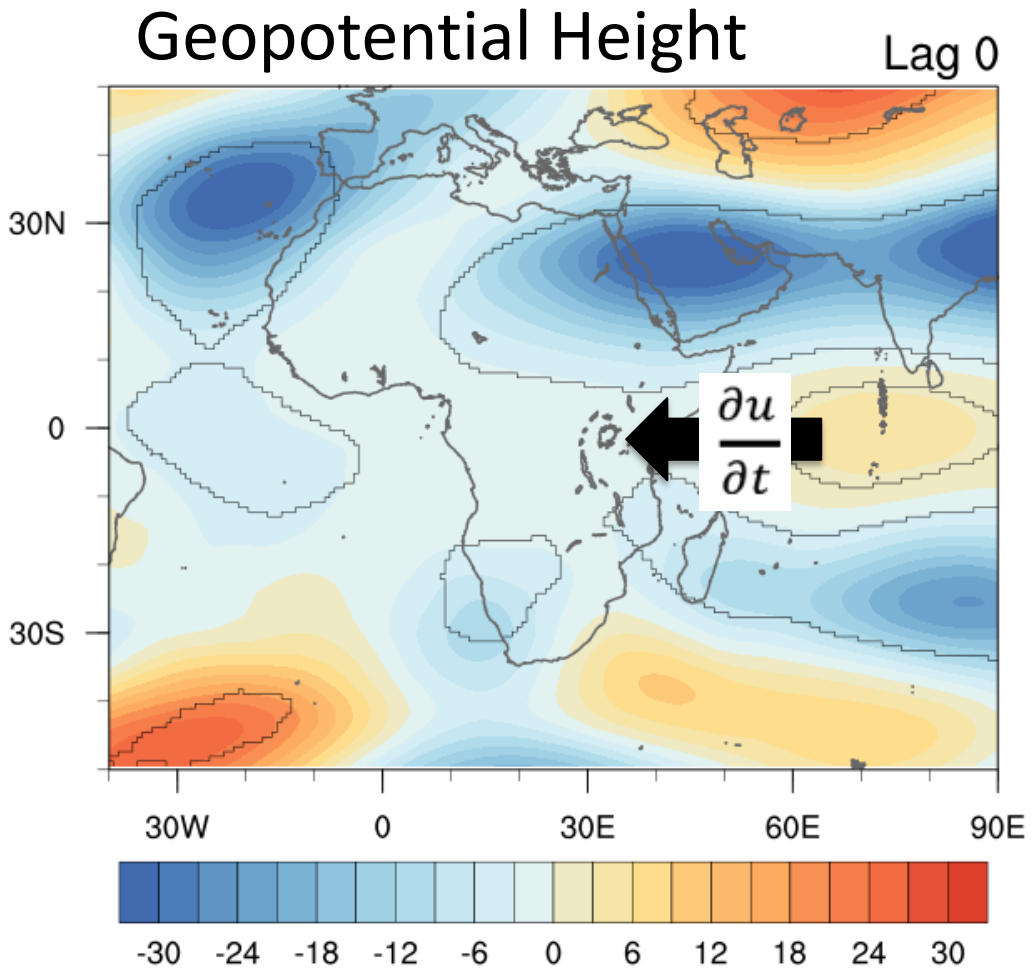

Instead of circumnavigating, the pressure gradient force intrudes from the extratropics

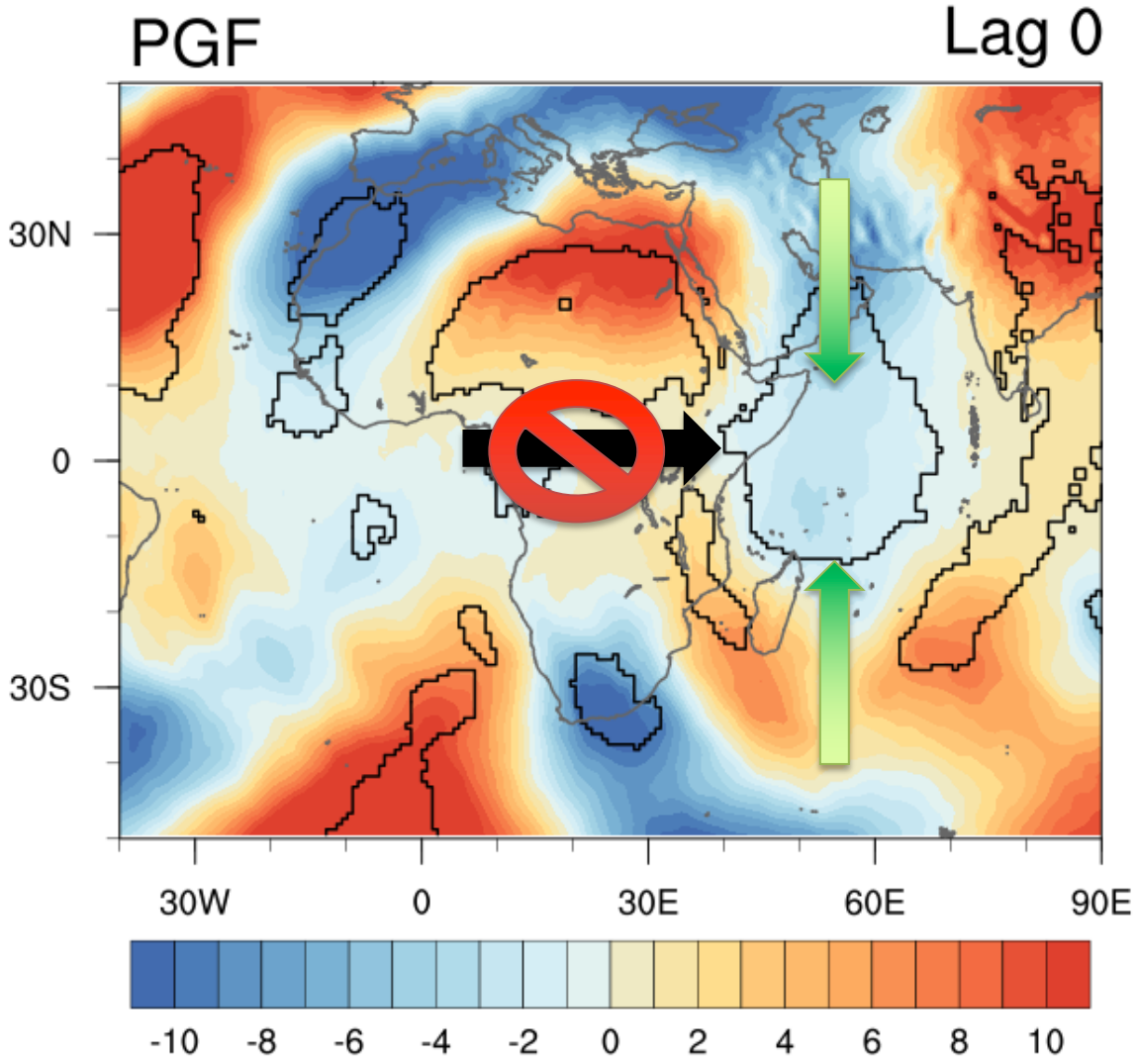

Intrusions of negative geopotential height anomalies from the extratropics may help MJO convection initiate over the Western Indian Ocean

- Supported by the background flow
- Could help to explain the timing of onset of MJO convection over the western Indian Ocean
- Circumnavigating and local features may also play a role

Seasonal cycle shows power appears to increase in the transition seasons

20° N

20° S

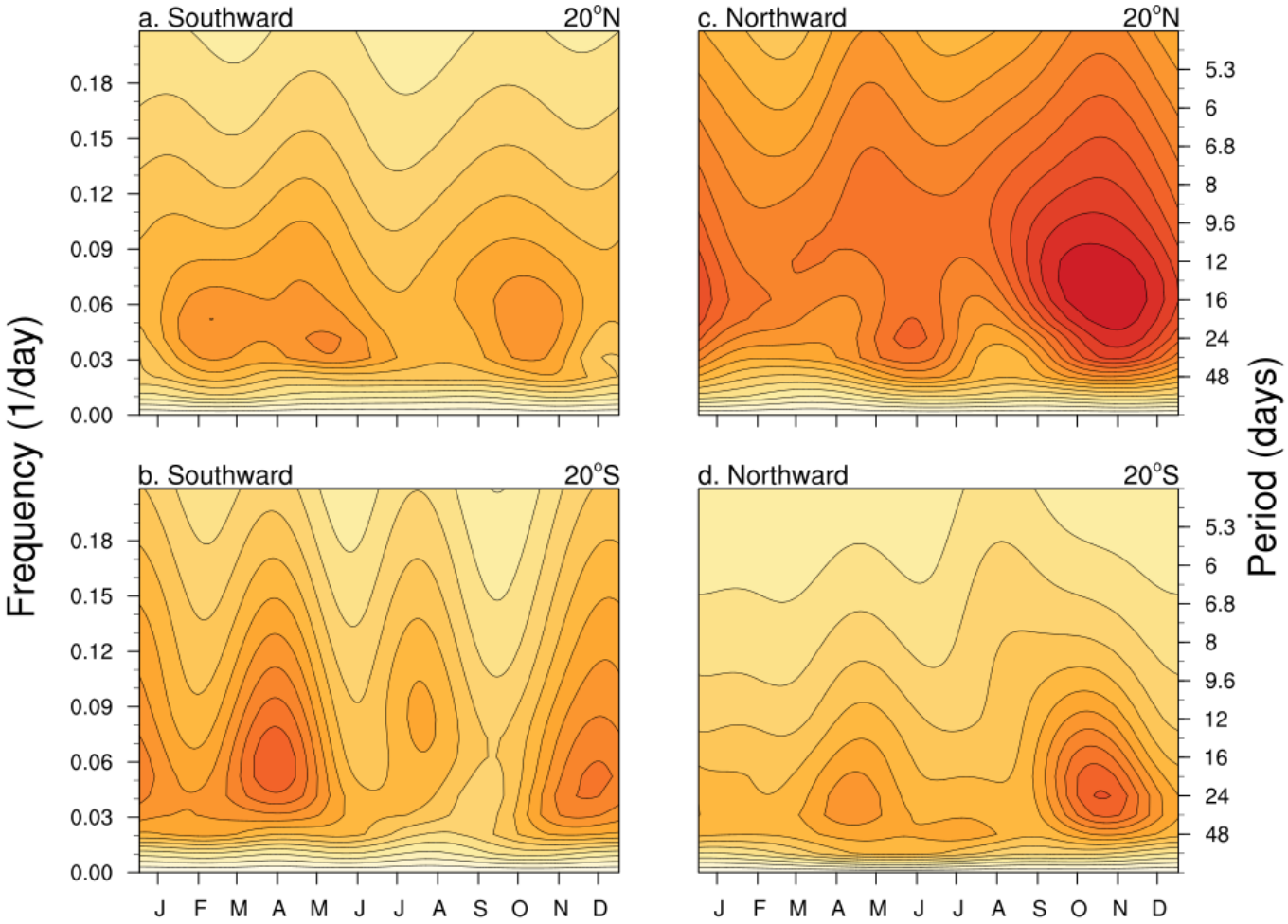

Avg. for all southward meridional scales

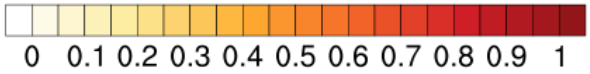

Avg. for all northward meridional scales

Global base state in the subtropics